HYTUNNEL

Draft version -Final

Deliverable D111

20 February 2009
Prepared by BRE
With contribution from partners
Final Report

EXECUTIVE SUMMARY

The HyTunnel internal project was established to contribute to the European and global activity to establish the nature of the hazard posed by hydrogen powered road vehicles in the confined space of a tunnel and its relative severity compared to that posed by traditionally powered (hydrocarbon internal combustion) vehicles.

In this project, the tunnel regulations and standards have been reviewed and identified relevant requirements and current practices in respect to the management of hazards and emergencies in the event of a fire. Of particular relevance in Europe is the recently published EU Directive on minimum safety levels now required in the main road tunnels on the trans-European Road Network (*Directive 2004/54/EC)*. Various aspects of regulations and standards that apply to road tunnels, in particular in respect of the provision of smoke control and ventilation, were identified. While much consideration has been given in recent years to escape passages, cross-bore access, refuge shelters etc for means of escape, e.g. in the new EU Directive, this is considered to be outside the context of HyTunnel.

The Phenomena Identification and Ranking Table (PIRT) exercise and the review of the related published literature helped to identify appropriate accident scenarios for further investigation, in the Hytunnel project, in respect to the vehicles involved, the hydrogen release mechanism and the tunnel environment. The scenarios identified in discussion with industry partners covered hydrogen dispersion, combustion and explosion experiments relevant to tunnels, and important physical parameters such as the variation in tunnel geometry (tunnel cross-section, gradient, obstacles), vehicle parameters (liquid, CGH2, release location and direction), and ambient and ventilation conditions

Hazard & risk assessment were performed in terms of: size of flammable gas clouds, ignition probability, exposure times of flammable gas clouds, and the resulting overpressures as a function of gas cloud size. The research of this work has led to some interesting findings.

Some findings of the dispersion study are as follows:

- Horseshoe cross section tunnel indicates lower hazard than equivalent rectangular cross-section tunnel with regards to flammable cloud volume and its longitudinal and lateral spread.
- Increasing height of the tunnel indicates safer conditions to tunnel users for buoyant releases of H2.
- Compressed gas H2 (CGH2) releases pose greater hazard than natural gas releases, but still not significant.
- Increase of ventilation velocity decreases the cloud size and hence results in lower hazard.
- The limited research work done so far has indicated 3m/s as reasonable ventilation for avoiding backlayering, but this should be supported by further research
- CFD simulation results not conclusive on the following aspects.
- Level and extent of hazard with no ventilation versus ventilation.
- Hazard posed by liquid hydrogen (LH2) versus CGH2 releases.

Some findings of the explosion study are as follows:

- Significant levels of overpressure can be generated in confined or semi-confined spaces, by the ignition of a hydrogen-air mixture filling only a small fraction, of the order of a few percent, of the space. These could be high enough to cause damage to tunnel services, e.g. ventilation ducting.
- Hydrogen explosions are more prone to produce an oscillatory pressure-time profile than hydrocarbon explosions, which may have implications for the response of structures subjected to a hydrogen explosion
- For larger percentage fills of hydrogen-air mixture, the HSL and FZK experiments have indicated that DDT is possible in principle. Ceiling design and mitigation measures are important.
- Suitable ventilation of a tunnel can significantly reduce the chance of an explosion. However, there may be the possibility that even in a well ventilated tunnel high release rate of hydrogen could produce a near homogeneous mixture at close to stoichiometric conditions, with a corresponding increased explosion hazard.

TABLE OF CONTENTS

CHAPTER 1 – BACKGROUND TO HYTUNNEL

As part of the drive towards a cleaner environment and alternative energy sources, the automotive industry is researching and developing technology to allow vehicles to run in part (hybrid) or completely on hydrogen. It has been suggested that hydrogen vehicles will emerge as a leading contender to replace today's internal combustion engine powered vehicles. Whilst in reality this vision may not materialise, or not be realised for some years, the safety issues surrounding the use of hydrogen vehicles inside tunnels need to be addressed now.

The Phenomena Identification and Ranking Table (PIRT) exercise [1] conducted at the start of the HySafe project identified that the transport of hydrogen powered road vehicles through road tunnels might present an increased hazard compared to conventionally powered (hydrocarbon internal combustion) vehicles. The PIRT exercise also identified a number of scenarios associated with the use of hydrogen vehicles inside tunnels, and provided a starting point for a HySafe internal project.

HyTunnel was established with the following objectives:

- To review tunnel regulations, standards and practice in respect to the management of hazards and emergencies.
- To identify appropriate accident scenarios for further investigation.
- To review previously published work.
- To extend our understanding of hydrogen hazards inside tunnels by means of new physical experiments and numerical modelling activities.
- To develop recommendations for the safe introduction of hydrogen powered vehicles into tunnels.

The focus of HyTunnel has been on the potential hazards associated with hydrogen passenger cars and commercial vehicles using road tunnels. The transport of hydrogen (in tankers or trucks), which could potentially present a significantly greater hazard, has not been considered in this report.

The safety and hazard mitigation features incorporated into tunnels is driven, in general, by the requirement to deal with selected design fire scenarios. From the perspective of fire and general hazard control in tunnels, it is important to understand the mitigation features related to tunnel design, ventilation and operational procedures. These are discussed in chapter 2. Various aspects of regulations and standards that apply to road tunnels, in particular in respect of the provision of smoke control and ventilation, were also identified in this chapter.

Understanding the vehicle traffic behaviour in road tunnels is a key factor in enabling the identification of realistic accident scenarios for the HyTunnel hydrogen release scenarios. The traffic characteristics in tunnels and the types and frequencies of traffic accidents are summarised in chapter 3.

Chapter 4 discusses the emerging technologies in respect to powering hydrogen vehicles.

Chapter 5 provides examples of recently published work of direct relevance to Hytunnel, particularly focusing on experimental and modelling studies of dispersion and explosion of hydrogen releases within the confined space of a tunnel.

Ventilation in tunnels is a recognised means of removing an explosive atmosphere to mitigate the consequences of a flammable gas release. It is therefore important to assess the hazards posed by

vehicles powered with hydrogen as compared to those powered with conventional hydrocarbon-based fuels. Furthermore, the destroying potential of blast waves resulting from combustion and explosion of burnable gases, in particular hydrogen-air mixtures, pose major hazard to safety. Understanding of the potential to provide conditions for high-speed deflagrations is of major importance. The potential of partially confined and unconfined configurations to support flame acceleration, onset of detonation and detonation propagation is still poorly understood. These issues are addressed in chapter 6 through experimental studies undertaken in the frame of Hytunnel project. IN particular, the chapter examines the effect of ventilation in removing an explosive atmosphere to mitigate the consequences of a flammable gas release, and compares the overpressures generated by igniting a stoichiometric hydrogen-air cloud with that by igniting a stoichiometric methane-air cloud. It also examines high-speed deflagrations in stratified hydrogen layers for determining the critical conditions defining the possibility of the self-sustained detonation in flat mixture layers.

Chapter 7 discusses the accident scenarios chosen to better understand the dispersion and explosion hazards posed by the release of hydrogen in liquid or gaseous form in the confined space of a tunnel, and assess them with the release of the conventional hydrocarbon-based fuel used in vehicles.

Chapter 8 provides main findings and recommendations from the experimental and modelling work undertaken in the project.

CHAPTER 2 – REVIEW OF TUNNEL DESIGN, VENTILATION, OPERATION AND EMERGENCY PROCEDURES

Information in this section is drawn from a variety of other sources. In particular, two recent publications, listed below, collate a wide range of useful information and provide a good summary of tunnel design, ventilation, operations and general emergency procedures:

1. *Fire and Smoke Control in Road Tunnels*, published by the World Road Association / PIARC in 1999 [2].

2. *The Handbook of Tunnel Fire Safety* [3] edited by Beard and Carvel and published by Thomas Telford in 2005 with contributions provided by experts on topics ranging from tunnel ventilation to fire and rescue operations.

Other documents such as *NFPA 502 on Standard for Road Tunnels, Bridges, and other Limited Access Highways* [4] and *BD 78/99 on Design of Road Tunnels* [5] also provide useful information.

While the focus in the above publications is on fire issues, the information is applicable also to general hazard scenarios such as hazardous gas dispersion. Furthermore, the safety and hazard mitigation features incorporated into tunnels is driven, in general, by the requirement to deal with the selected design fire scenario(s) based on existing transport loads and energy carriers .

From the perspective of fire and general hazard control, tunnel designs and operational procedures need to address one or more of the following issues:

- Construction materials. This addresses the resistance of the tunnel walls and lining materials to fire gases and radiation fluxes. Resistance of concrete to spalling has been of particular interest in recent years, and a number of developments in respect to improved performance have been reported, e.g. addition of fibres into the concrete mix. The structural integrity of tunnel construction is usually designed for and tested in terms of exposure to a specified time-temperature curve, representing the exposure conditions to be expected for the design scenario. The construction may also consider the resistance to the effects of explosion.

- Detection and surveillance. In normal operation, detection of vehicle emissions, e.g. CO, may be incorporated in the tunnel design. Additional ventilation can then be provided to alleviate conditions inside the tunnel. Heat detection is used principally to detect a fire event. Video surveillance, including in the infrared, may be used to detect the presence of smoke, and coupled with appropriate image processing technology may be able to automatically detect the onset of a fire.

- Ventilation and smoke control. This is discussed in more detail below.

- Fire suppression. There has been much debate, and controversy, over the potential benefits or disadvantages of installing water suppression systems inside tunnels. While actively pursued in some parts of the world, e.g. Australia and Japan, fixed-suppression water systems were considered unproven, and not cost-effective in others, e.g. The World Road Association [2] opposed the introduction of water suppression systems into road tunnels and earlier editions of *NFPA 502* (2004) [4a] remained cautious. It is now more widely accepted e.g. NFPA 502 (2008) [4b] that water suppression can be an important part of the overall fire safety strategy for a road tunnel, both for life safety and property protection.

  An alternative to water sprays and mists is provided by aqueous film-forming foam (AFFF), designed principally for extinguishing liquid hydrocarbon fires – see for example Cafaro et al [6].

- Egress and tunnel user behaviour. The safe evacuation of tunnel users in the event of an emergency has received much attention in recent years, prompted in part by the series of

catastrophic fires in a number of alpine road tunnels in Europe, e.g. the Mont Blanc tunnel fire in 1999. Fraser-Mitchell and Charters [7] review the current understanding of human behaviour in the event of a tunnel fire. Shields [8] reviews what happened in various recent tunnel fire incidents.

Provisions for emergency lighting, audio instruction, safe shelters, escape passages etc are all important in the overall question of *means of escape*. Shields [8] and Egger [9] review human behaviour and driving practice in road tunnels. A recent directive from the European Parliament [10] imposes strict new regulations on the minimum level of safety within the main trans-European road tunnels.

In the context of HyTunnel, the issue from the list above that arguably requires most immediate attention is tunnel ventilation, both in normal and emergency modes. It is the tunnel air distribution, both from the tunnel ventilation systems and the influence of traffic and environmental conditions that will determine the distribution of hydrogen if there is a release inside the tunnel. Other issues, in particular the possibilities to detect hydrogen releases and the effect of water suppression systems, are also of potential significance.

The next two sub-sections summarise respectively the tunnel ventilation practice and the regulations and standards that apply in various locations.

2.1 Tunnel ventilation

During normal operation road tunnels require ventilation in order to achieve a minimum level of air quality, removing the potentially harmful vehicle emissions such as CO, NO_x and diesel particulates. For tunnels above a specified length this is generally augmented by additional emergency ventilation to mitigate the effects of the smoke and heat generated in the event of a fire, initially to assist in the egress of tunnel users and then to assist fire-fighting and emergency operations.

Bendelius [11] summarises the different types of ventilation found in tunnels. This is extended by Jagger and Grant [12] who examine more closely the use of ventilation to control smoke and heat generated in the case of fire.

Ventilation is of interest in the context of HyTunnel from two aspects:

1. Following the release of hydrogen, but before any combustion or detonation, the ventilation will influence strongly how the hydrogen spreads and mixes inside the tunnel. The location of nearby vehicles and the geometry of the tunnel will also be important.

2. If there is a fire inside the tunnel (from a H_2 vehicle or otherwise), then the ventilation system (before and after any change to emergency mode of operation) will again influence the spread of hydrogen as well as determining the thermal hazard posed to H_2 vehicles not necessarily directly involved in an accident.

While much of the work that has been conducted and published in relation to emergency ventilation relates specifically to fire scenarios, this is also directly relevant to hydrogen dispersion. Due to its high buoyancy, hydrogen gas behaves in many ways like smoke from a fire.

It is worth summarising here some of the positive and negative effects that ventilation inside a tunnel may have in respect to a release of hydrogen gas or on the smoke and heat from a fire (not necessarily a H_2 vehicle):

- The supply of air may dilute the hydrogen such that it is below the flammability limit.

- The dispersed hydrogen may be transported safely out of the tunnel through either a portal or via en exhaust ventilation duct or shaft.

- The ventilation system may break down a stratified layer of flammable hydrogen gas mixture such that the resultant fully mixed gas is below the flammable limit.

- The released hydrogen may be transported such that the cloud of flammable gas mixture is extended well away from the point of release, either within the traffic space or along ventilation ducts or shafts.

- Hot smoke gases from a fire may get transported to neighbouring H_2 vehicles, exposing them to thermal hazard.

- Strong mechanical ventilation may create turbulence within the tunnel sufficient to affect the combustion regime (of hydrogen in particular) if ignition occurs.

Overall, the interaction of the ventilation system, tunnel geometry and hydrogen release is complicated, and recourse to numerical modelling is required.

The main approaches to tunnel ventilation are reviewed below:

Natural ventilation

In short tunnels ventilation is generally provided by a combination of the piston effect of the vehicles passing through and atmospheric (e.g. pressure difference across the portals). Such tunnels are often two-way, and egress and escape from the effect of smoke and heat is not considered a major concern. There may be a need to include structural fire protection to a specified level.

Natural ventilation air flow may pass one tunnel portal to the other, or ventilation shafts may be incorporated. This is illustrated in Figure 2.1, taken from Bendelius [11].

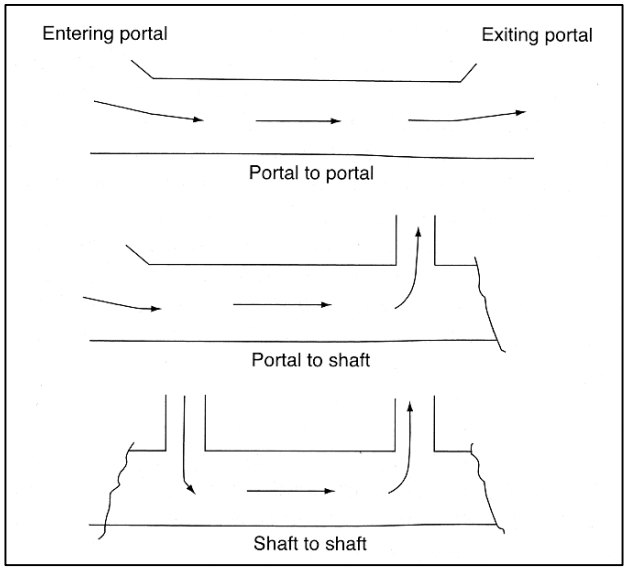

Figure 2.1 Natural (longitudinal) ventilation – taken from *The Handbook of Tunnel Fire Safety* [3]

Generally, as air passes along the tunnel the concentration of vehicle emissions contained within (and the temperature) increases. If all air enters from one portal and exits from the other there is, in the case of an even distribution of vehicle emissions along the length of the tunnel, a uniform increase in emission concentration. Adverse atmospheric conditions, which may act to reduce the longitudinal air speed, may results in an increase in emission concentrations inside the tunnel. This is illustrated in Figure 2.2, again taken from Bendelius [11].

A temperature difference between ambient air and the tunnel structure (and ventilation shafts) may act to increase or decrease the rate of air flow, and hence the level of emissions or smoke inside the tunnel.

In all but short tunnels, natural ventilation cannot generally be relied upon to provide sufficiently clean air, or in the event of fire or hazardous chemical release to provide safe conditions. Some form of

mechanical ventilation, possibly only operated when emission concentrations dictate or in an emergency, is then required. The maximum length of tunnel where natural ventilation alone will suffice depends on factors such as traffic density, for which a value ranging somewhere from a few hundred meters to about 1 km is typical.

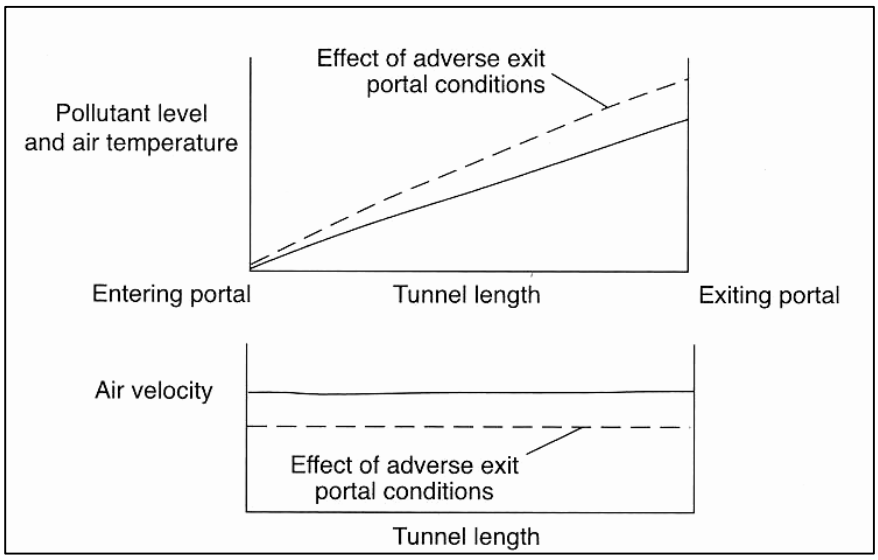

Figure 2.2 Airflow characteristics in a naturally (longitudinally) ventilated tunnel – taken from *The Handbook of Tunnel Fire Safety* [3]

Mechanical longitudinal ventilation

The simplest, and often least expensive, form of mechanical ventilation is of the longitudinal type. Air enters or leaves the tunnel from either the portals or from a limited number of ventilators located along the tunnel. The movement of air is provided either by centrally located fans, i.e. outside the traffic space whereby air is supplied or extracted via ventilation ducts and shafts, or by jet fans located within the traffic space (generally at ceiling level). In the case of centrally located fans supplying air, this is usually combined with a Scaccardo nozzle which provides a high velocity jet of air which augments the longitudinal thrust provided by the piston effect of the moving vehicles. The jet fans operate purely by providing longitudinal thrust within the traffic space.

Figure 2.3, taken from NFPA 502 [4], illustrates various arrangements of mechanical longitudinal ventilation. The airflow distribution in a mechanically ventilated longitudinal system is similar to that of a naturally ventilated tunnel. Although more resilient to the effects of adverse atmospheric conditions, the mechanical option is still subject these influences and the performance may be detrimentally effected.

Where air enters one portal and exits from the opposite one, the concentration of emissions or smoke increases along the tunnel as in the naturally ventilated case. The scheme shown in Figure 2.3 (c) illustrates an alternative approach whereby additional fresh air enters the centre of the tunnel, thus increasing the quality of air at the exit portal. And Figure 2.3 (d) illustrates a scheme whereby air enters from both portals, and a longitudinal air movement is generated from each portal towards the centrally located exhaust shaft.

A longitudinal air flow rate of 0.5 to 1.0 m s^{-1} is typically required for control of vehicle emissions. As discussed below, a higher air speed is required in order to control the movement of smoke in the event of a fire.

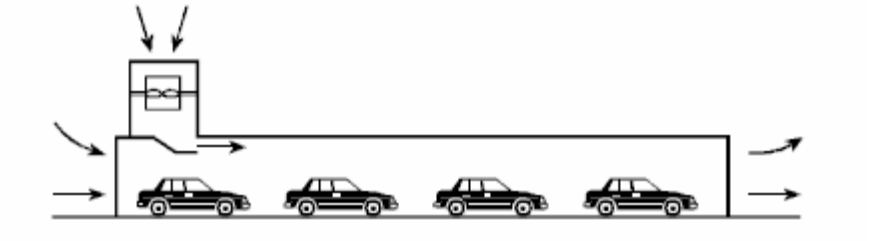

(a) Central fans (located outside traffic space) and Saccardo nozzle

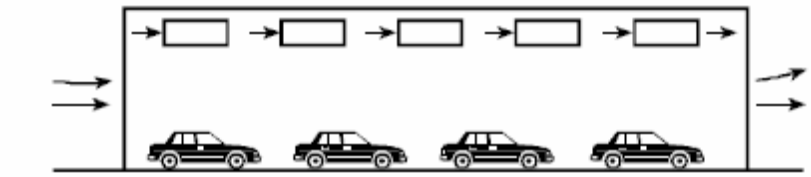

(b) Jet fans (located in traffic space)

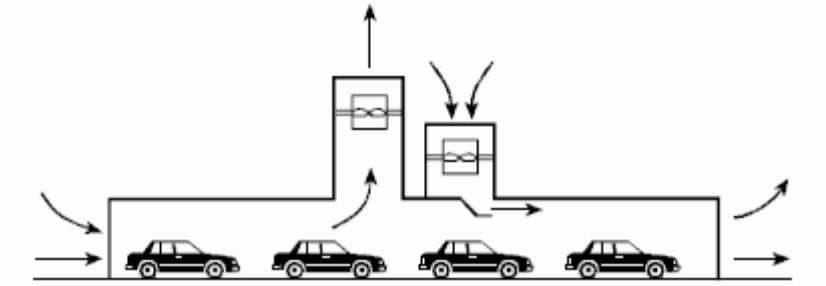

(c) Central fans with Saccardo nozzle (supply) and exhaust shaft

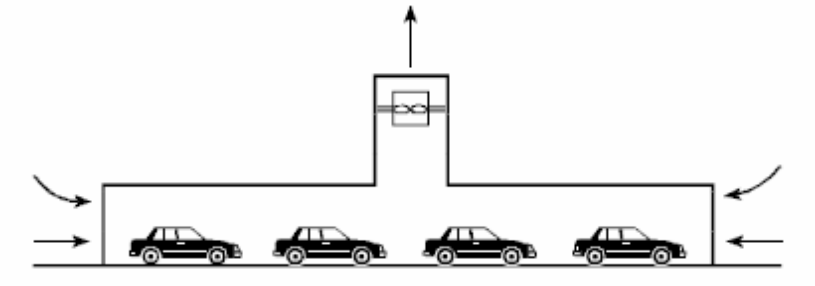

(d) Central fans with exhaust shaft only

Figure 2.3 Some examples of mechanical longitudinal ventilation (taken from *NFPA 502* [4])

In the case of longitudinal emergency ventilation, the basic design philosophy is to force all the smoke or hazardous gas in one direction from the source location to the point of extraction (the downstream portal or exhaust vents(s)). To achieve this, a minimum design air speed (the 'critical velocity') is required, which in the case of fire depends on the heat release rate of the fire and other parameters such as the tunnel cross-section and gradient.

Approximate, semi-empirical formulae are available for calculating the critical velocity for general situations. Equation 1, derived by Danziger & Kennedy [13] and widely used in design calculations, e.g. in NFPA 502, actually defines the critical velocity, V_c, as the solution of two simultaneous equations,

$$\left.\begin{aligned} V_c &= K_1 K_g \left(\frac{gHQ}{\rho C_p A T_f} \right)^{1/3} \\ T_f &= \left(\frac{Q}{\rho C_p A V_c} \right) + T \end{aligned}\right\} \qquad (2.1)$$

Here, Q is the convective heat-release rate of the fire, A the cross-sectional area of the tunnel and K_g is a gradient correction factor. More general expressions for critical velocity remains the subject of ongoing research, e.g. Hwang & Edwards [14].

Figure 2.4, taken from the World Road Association/PIARC [2], shows the calculated critical velocity using Equation (1) for an example tunnel of cross-section area 37.8 m^2 and height 4.2 m (which would correspond to a two-lane tunnel). It also compares spot values derived from computer simulation.

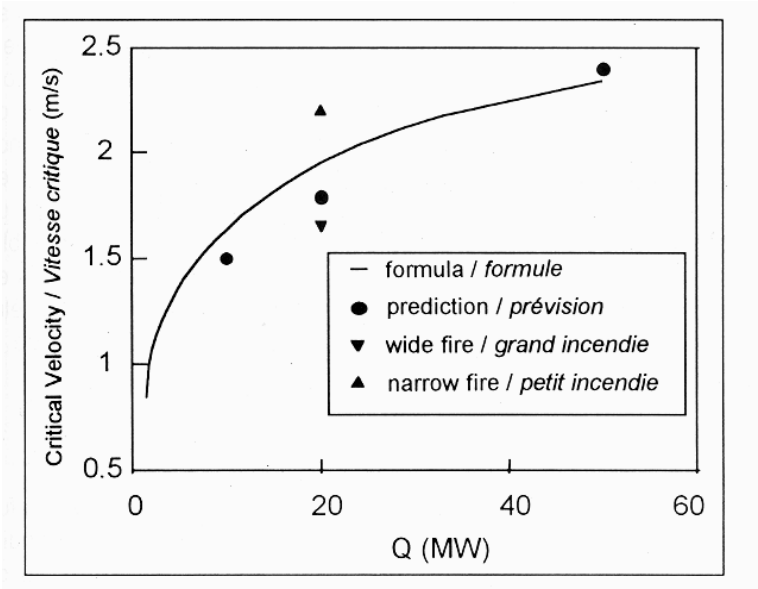

Figure 2.4 Predicted critical velocity – taken from *Fire and Smoke Control in Tunnels* (World Road Association / PIARC [2])

While previous engineering recommendations for critical velocity in the case of large (≥~ 100 MW) fires were 5 m s^{-1} or greater, that value has been generally reduced in recent years following, in part, the results from full-scale tunnel experiments involving large fires, e.g. (Lemaire [15]). There is also evidence that while the critical velocity increases according to the 1/3 power of fire heat release rate (HRR) up to a certain value of HRR (for a given geometry), it then remains at a constant value, the so-called 'super-critical velocity'. This is illustrated in Figure 2.5 (Wu & Baker [16]), which shows the variation of a non-dimensional definition of critical velocity with a non-dimensional definition of HRR – the details are beyond the scope of this report. Broadly speaking, a critical velocity of about 3.5 m s^{-1} seems sufficient for most tunnel fires, including large HGV fires in excess of 100 MW.

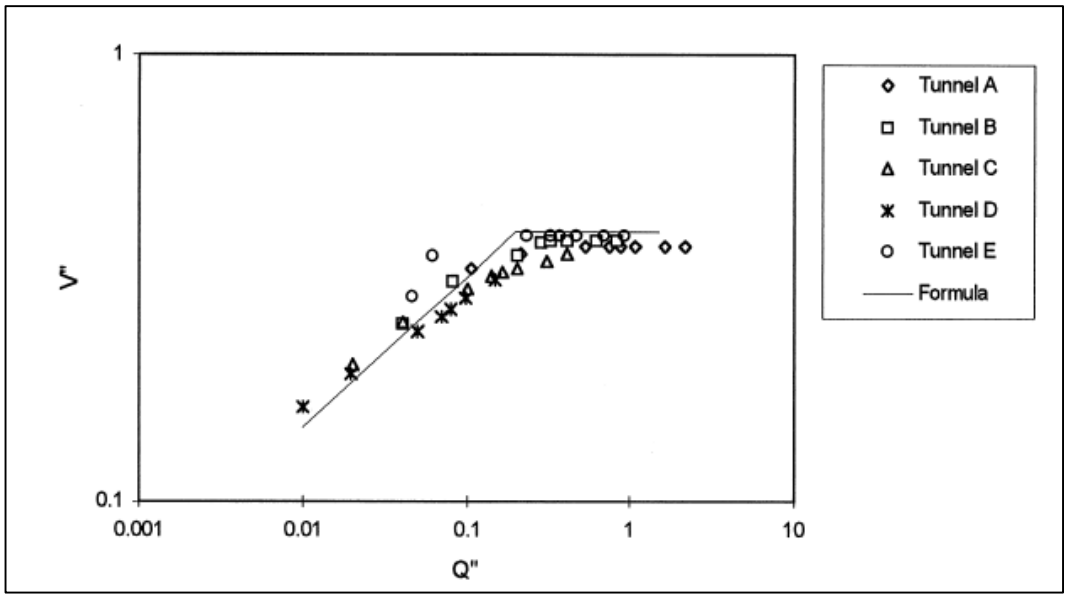

Figure 2.5 Relationship between non-dimensional critical velocity and non-dimensional heat release rate – taken from Wu & Baker [16]).

By forcing the smoke and heat in one direction, safe conditions are maintained upstream of the fire source, where stationary vehicles may be located, allowing people to make their escape and to provide fire-fighting access as required. It is assumed that downstream of the fire the vehicles are able to drive out of the tunnel ahead of the hazardous conditions. For this reason, longitudinal emergency ventilation is not ideally suited to two-way tunnel bores or where traffic jams may be encountered inside the tunnel. Where it is important to maintain clear conditions on both sides of the fire source the alternative method of transverse or semi-transverse ventilation will generally be preferable.

Figure 2.6, taken from Jagger & Grant [12], illustrates the problem that may be associated with longitudinal emergency ventilation. It shows the effect of portal-to-portal and shaft-to-shaft longitudinal ventilation on the transport of smoke. Note that in the latter case while the vehicles immediately downstream of the fire source are still immersed in smoke, those beyond the downstream exhaust shaft are in good conditions.

In addition to a minimum (critical) velocity, adherence to the maximum longitudinal air speed is required, so that conditions are amenable to means of escape. The Swedish and Norwegian regulations quote a maximum allowed air speed in the range of 7 to 10 m s^{-1}. NFPA 502 quotes a maximum value of 11 m s^{-1}. Higher values may cause problems to persons walking to safety.

Mechanical (full) transverse ventilation

Transverse ventilation systems are characterised by a uniform distribution of supply air and/or uniform distribution of extraction points. The concept was developed originally for the Holland Tunnel in New York.

In normal operation, a full transverse system supplies and extracts equal volumes of air from the tunnel through ducts that generally run parallel to the traffic space, illustrated in Figure 2.7. Often air is supplied at road level and extracted at ceiling level – though this is not always the case.

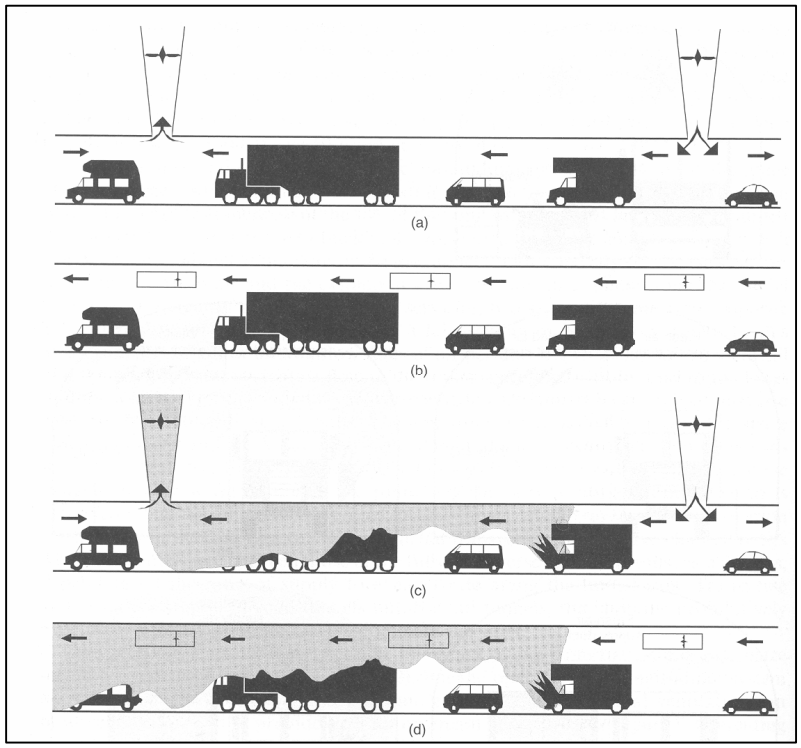

Figure 2.6 Influence if alternative forms of longitudinal ventilation on smoke transport– taken from *The Handbook of Tunnel Fire Safety* (Thomas Telford 2005)

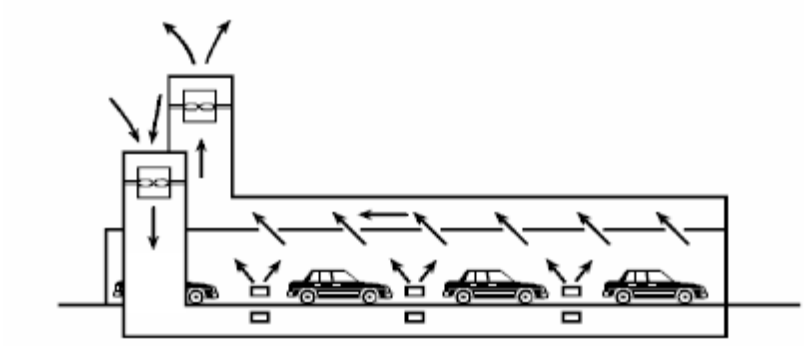

Figure 2.7 Example of mechanical (full) transverse ventilation (taken from NFPA 502)

Unlike in a longitudinally ventilated tunnel, air is supplied at right angles to the direction of the traffic flow. However, this is perturbed by the influence of traffic flow and atmospheric conditions to create a net longitudinal air flow. Furthermore, the direction and magnitude of the net longitudinal flow is difficult to control. Some control of the longitudinal flow can be achieved by dividing the tunnel into sections where air supply and/or extraction is operated separately.

A key difference compared to longitudinal ventilation (mechanical or natural) is that, to a first approximation, pollutant concentration is uniform along the length of the tunnel. This is an advantage for long tunnels – where in the case of longitudinal ventilation the pollutant concentration at the exit portal may become high (see Figure 2.2 above). However, the required rate of air flow along the supply and extract ducts may become excessively high, and this is another reason (see note above about control of resultant longitudinal velocity) for the supply and extract to be divided over a number or ducts, each servicing a section of tunnel. Typically air speeds in the range 15 to 25 m s^{-1} will be generated inside the ventilation ducts when operating at full power (World Road Association /PIARC [2]).

In case of fire the recommended procedure is, where possible, to turn the extraction to maximum in the vicinity of the fire and to adjust the ventilation settings in neighbouring sections of tunnel to control the smoke. Smoke control here can imply reducing the longitudinal air speed as close to zero at the fire source, or moving it on one direction or other to facilitate evacuation or fire-fighting operations. In the latter case, the system can be considered to be operating in a quasi-longitudinal emergency ventilation mode, and the issues raised above then hold.

Ideally, smoke is extracted through vents in the vicinity of the fire, thus eliminating the hazard in the far-field. This can be achieved by focussing the extraction capacity at those vents close to the fire (in contrast to distributing the extraction along the entire tunnel (or sub-section of). Vents located at the ceiling are obviously beneficial in respect to smoke (or other buoyant gas) extraction.

Other issues associated with transverse ventilation (including semi-transverse ventilation – discussed next) operating in an emergency (fire) mode are listed below:

- The (transverse) air supply (in the region of the fire at least) should be reduced to minimise the de-stratification of the smoke layer (should it exist). The World Road Association /PIARC [2]) recommends reducing the supply air rate to 1/2 - 1/3 of full capacity. Recall that a stratified smoke layer assists means of escape for those persons below.
- Again, to minimise the de-stratification of a smoke layer, the size of the longitudinal air speed should be minimised (unless there is no requirement to maintain safe conditions downstream). A longitudinal air speed of 2 m s^{-1} or greater is likely to de-stratify a smoke layer. Furthermore, a high rate of air supply may increase the growth rate of the fire.
- Where, in normal operation, air is supplied through ceiling vents, this should ether be stopped in a fire emergency, or the vents set to extract rather than supply.

Mechanical semi-transverse ventilation

Semi-transverse ventilation differs from full transverse ventilation in that the supply (or exhaust) air enters (or exits) via the portals. Figure 2.8 illustrates the concepts of semi-transverse supply and semi-transverse exhaust ventilation.

There are some important differences between supply and exhaust semi-transverse ventilation. Notably, whereas in the supply mode the level of pollutant concentration is nominally uniform along the length of the tunnel (as in the case of full transverse ventilation), in the case of exhaust case ventilation the level of pollution increases towards the exit portal(s) (as in a longitudinally ventilated tunnel).

Some further issues in relation to smoke management for semi-transversely ventilated tunnels are listed below:

- While, in normal operation, a supply semi-transverse system will dilute the smoke generated in the event of a fire, it is recommended however (e.g. World Road Association / PIARC [2]) to reverse the airflow such that fresh air enters via the portals. This can assist egress and fire-fighting activities. It is important for the changeover to take place as quickly as possible, in particular if the vents are located at ceiling level since as long as air is being supplied it will disturb the smoke layer and act to drag smoke to floor level.
- An alternative strategy is to construct a separate smoke extraction duct for use in the event of a fire emergency (with the vents located at ceiling level). This was the system employed in the original Mont Blanc tunnel prior to refurbishment following the 1999 fire (note: the extraction duct was actually used in supply mode during normal operation to augment the supply of fresh air, and indeed was partly operated in supply mode during the fire itself).
- In a fire emergency, the extraction duct of an exhaust semi-transverse system should be set to maximum (preferably with the extraction capacity located at the fire). It is unlikely, however, that the system will be able to control the effects of a large fire.

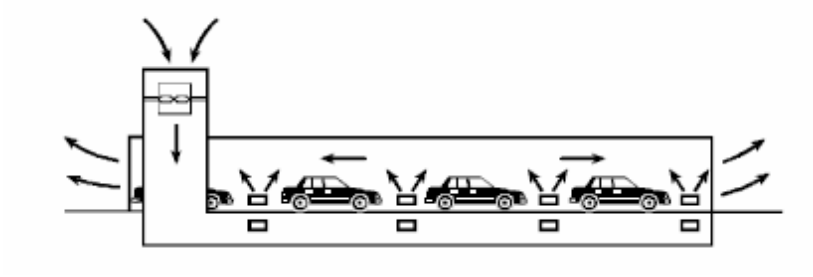

(a) Semi-transverse supply ventilation

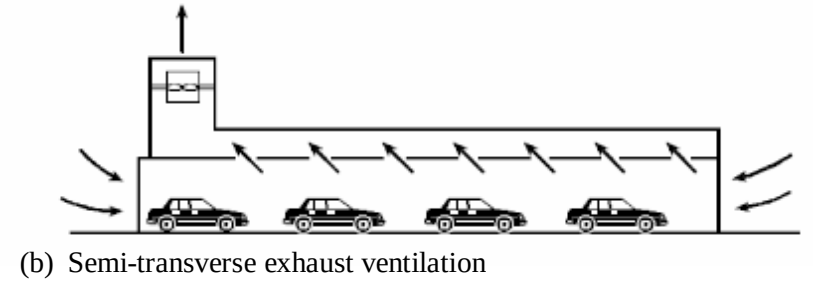

(b) Semi-transverse exhaust ventilation

Figure 2.8 Examples of mechanical semi-transverse ventilation (taken from *NFPA 502[4]*)

While longitudinal ventilation is often characterised in terms of a design critical velocity, for full and semi-transverse systems it is the exhaust ventilation capacity that is generally cited. For a given design fire (and associated smoke generation rate), and a distance over which the smoke is to be restricted (the fire zone), the capacity of the smoke ventilation system is specified in terms of volume of air extracted per unit length of tunnel (in the fire zone). In Europe this is often specified in terms of $m^3 s^{-1}$ extraction per km of tunnel.

French regulations (Centre d'Etudes des Tunnels [17]), for example, specify that smoke should be contained within a 400 m zone in an urban tunnel and a 600 m zone in a non-urban tunnel. Ceiling extraction vents should ideally be placed approximately 50 m apart, and no more than 100 m. In terms of extraction capacity, the World Road Association /PIARC [2]) refers to a value of 80 $m^3 s^{-1}$ per km, but also acknowledges that this value is probably too low for a HGV fire. The French regulations specify an extraction capacity between 110 and 155 $m^3 s^{-1}$ per km, depending on various factors.

While tunnel ventilation systems have above been grouped into distinct classifications, in practice a particular system may be a hybrid of these. Indeed, some of the most sophisticated emergency ventilation systems use a combination of jet fans (to control the longitudinal movement of air and smoke) and transverse smoke extraction through ceiling vents. The refurbished Mont Blanc tunnel employs such a system whereby jet fans act to restrict the longitudinal spread of smoke to a short region of a few hundred metres, from which the smoke is extracted through ceiling vents (Vuilleumier [18]).

2.2 Summary of regulations and standards

Of particular relevance in Europe is the recently published EU Directive on minimum safety levels now required in the main road tunnels on the trans-European Road Network (*Directive 2004/54/EC [10]).*

Internationally, NFPA 502 [4] and the World Road Association / PIARC [2]) are both widely cited and used. Two further publications from the World Road Association /PIARC [19,20] (Report 05.11.B *Cross Section Design for Uni-Directional Road Tunnels* and Report 05.12.B *Cross Section Design for Bi-Directional Road Tunnels*) provide useful summaries of tunnel requirements in selected countries.

Various aspects of regulations and standards that apply to road tunnels, in particular in respect of the provision of smoke control and ventilation, were identified in the preceding section. While not intending to provide a complete review of regulations and standards applying to road tunnels, some of the main issues are summarised below. While much consideration has been given in recent years to escape passages, cross-bore access, refuge shelters etc for means of escape, e.g. in the new EU Directive, this is considered to be outside the context of HyTunnel.

- Maximum length of tunnel where only natural ventilation is provided.

  The maximum length of tunnel that requires no form of mechanical ventilation varies from about 200 to 800 m, depending on country, traffic density, tunnel gradient, urban or rural location etc. The new EU Directive (2004) specifies that 'mechanical ventilation system shall be installed in all tunnels longer than 1 000 m with a traffic volume higher than 2 000 vehicles per lane'. A typical ('broad brush') value of 400 m is suggested by the author.

- Restrictions on longitudinal ventilation

  Longitudinal ventilation (given the tunnel is mechanically ventilated) is either discouraged or forbidden in two-way or congested tunnels, and if accepted in these cases is generally the subject of a risk analysis. Transverse or semi-transverse ventilation is, however, the preferred option for two-way or high traffic volume (subject to congestion) tunnels.

  For rural, one-way tunnels, longitudinal ventilation is now generally accepted in tunnels of any length. Obviously this is subject to engineering limitations, e.g. the pollution levels remain acceptable at the exit portal where they will be highest (unless intermediate ventilation shafts are included).

- Other restrictions on ventilation

  As discussed above, there is generally a maximum allowed air speed within a tunnel. Where quoted, values are broadly in the range of 7 to 11 m s^{-1} in respect to means of escape. However, lower values (say 2 ms-1) may be specified in the case of emergency fire ventilation, if the aim is to maintain stratification of the smoke layer for as long as possible (applies more to transverse ventilation).

- Traffic space cross-section

  The traffic space of a road tunnels is generally either of a rectangular or an arch profile ('horse-shoe') section. Regulations and guidelines may stipulate minimum clearance distances and bore widths (which depends on the number of lanes). Provision for sidewalks (often elevated) may also be included. Figures 2.9 and 2.10, taken from BD 78/99 [5]), show examples or rectangular and arch profile cross-sections respectively.

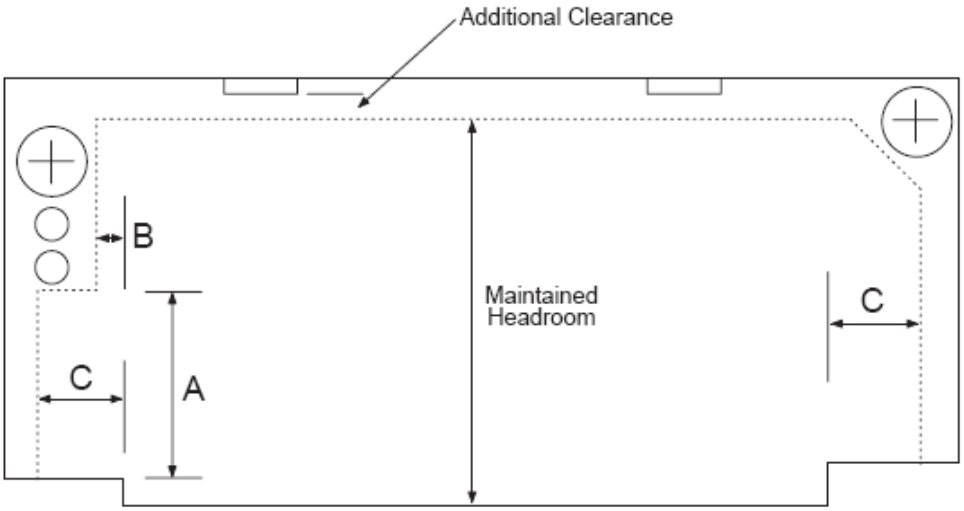

Figure 2.9 Example of rectangular tunnel cross-section(taken from *BD 78/99: Design of Road Tunnels*, UK highways Agency [5])

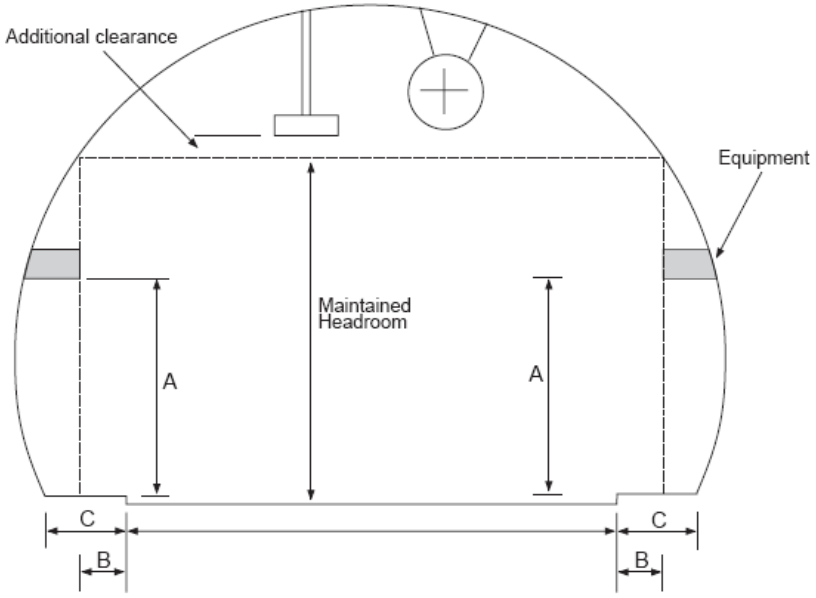

Figure 2.10 Example of arch profile cross-section(taken from *BD 78/99: Design of Road Tunnels*, UK highways Agency [5])

Table 2.1 Minimum dimensions for Figure 2.9 and 2.10 (from (UK) *BD 78/99 [5]*)

Dimension	Description	Box Profile	Arch Profile
A	Walkway headroom	2300mm	2300mm
B	Width of verge with full headroom	600mm	600mm
C	Width of verge	1000mm	1000mm

While continuous emergency lanes are uncommon, the provision for emergency lay-byes is often required.

- Road surface construction and drainage

  Road surfaces are typically either exposed concrete, or have an asphalt/bituminous covering. However, regulations may not allow asphalt/ bituminous coverings, e.g. Spain, as it is considered that they may contribute to fire spread, or they may be discouraged.

  Drainage of water, fuel or other spills is included in the tunnel design by including a transverse gradient (i.e. downwards towards the side of the tunnel bore). Typically values between 0.5 and 2.5 % may be specified. Provision for prevention of the spreading of hazardous spills is generally required where hazardous cargoes are allowed to use the tunnel. This may be in the form of gutters or other measures, and there is likely to be a requirement for liquid sumps.

- Max gradients

  The maximum tunnel gradient is generally specified in national guidelines, and may vary depending on traffic density and means of ventilation. Typical maximum gradients are 5 to 6 %.

- Traffic control

  Hazardous cargoes are generally controlled, e.g. escorted in groups. For general vehicle use, there may be recommended minimum separation distances, e.g. the distance covered in 2 s is stated in the new EU Directive [10]. Overtaking is generally prohibited, especially in two-way tunnel bores. Stopping (except in emergency or due to congestion) and turning/reversing is also prohibited. Drivers may be recommended to turn their radios on so that emergency information can be relayed.

  Additional speed limits may be applied in tunnels if deemed necessary, e.g. where the lanes narrow inside the tunnel. It is generally accepted, however, that on main highways to impose additional restrictions on speed serves no benefit and may unnecessarily disrupt the flow of traffic (i.e. the tunnel should be built appropriately to serve the highway where it is located).

  In the event if a vehicle fire starting, it is recommended, where possible, for the driver to drive the vehicle out of the tunnel.

CHAPTER 3 – REVIEW OF VEHICULAR TRAFFIC AND ACCIDENT STATISTICS IN ROAD TUNNELS

Understanding vehicle traffic behaviour in road tunnels is a key factor in enabling the identification of realistic accident scenarios for the HyTunnel hydrogen release scenarios. This chapter discusses traffic characteristics in tunnels and the types and frequencies of traffic accidents.

3.1 Traffic mix

When considering hydrogen releases in tunnels one factor that may influence the resulting dispersion and possible combustion of the released hydrogen is the traffic mix in the tunnel, i.e. the proportion of commercial vehicles. The traffic mix may affect the release scenario due to:

- the effect of commercial vehicles on air velocity in tunnels while traffic is flowing,
- commercial vehicles causing significant obstructions in tunnels which could influence the combustion regime depending on the proportion of the tunnel cross-section and total tunnel volume that they account for.

For the purposes of this report commercial vehicles are considered to be a combination of trucks heavier than 3.5 tonnes and buses/coaches, the former corresponding to a typical definition of a “heavy goods vehicle”.

As heavy goods vehicle predominate in the commercial vehicle category, it is proposed that the notional commercial vehicle is approximated by the following dimensions:
Length = 15m, Width = 2.55m, Height = 4.0m

The traffic mix is influenced by many factors and national average values will vary substantially when compared with specific roads because of the type of road, and the strategic value of the road in terms of freight transport or particular local conditions such as significant industrial concentrations.

Based on a variety of road traffic statistics, the proportion of commercial vehicles averages 7% in the EU increasing to 9% on major roads and increasing further to approximately 15% if only motorways are considered. However, specific roads can have proportions of commercial vehicles as high as 25-30% [21, 22].

Minimum EC safety requirements for Trans-European Road Network tunnels assume a baseline traffic mix including 15% heavy goods vehicles [23]. In some countries, e.g. Hong Kong, the percentage of commercial vehicles in the overall traffic flow can be significantly higher reaching as much as 55-60% of the total vehicle traffic [24].

On the basis of the above it is proposed that generalised modelling should allow for 15% of the vehicles in the tunnel being commercial vehicles, i.e. approximately 1 commercial vehicle in every 7 vehicles, with randomly generated positioning of the commercial vehicles within the overall traffic flow.

3.2 Effects of commercial vehicles on air flow velocities in tunnels

A study on the dispersion of natural gas releases in naturally ventilated tunnels conducted in the US [25] provides limited information on the effects of commercial vehicles on air movements in naturally ventilated tunnels. Traffic mix details are not provided for any of the tunnels considered in the study. However, for one of the tunnels an indication of the effects of commercial vehicles on air velocities is provided. The effects of commercial vehicles were considered to be significant for an individual 10 second velocity measurement but much less significant when individual 10 second measurements are averaged over the 80-100 second measurement period used. It was considered that the traffic mix could have a significant effect on the overall air flow. Individual air velocities are not provided in the report to allow the effect of commercial vehicles to be identified.

Clearly any effect of commercial vehicles on the overall air flow would be related to the proportion of commercial vehicles in the traffic flow and could be significant for key routes with 25-30% commercial vehicles.

3.3 Traffic accidents

Typically road traffic accidents (RTA) are the result of a chain of events caused by failures, i.e. deviation from the intended, in any or all of the principle elements of the road traffic environment; driver, vehicle, road and surroundings. The road layout and interactions between users have a significant effect on the accident rate. In the UK, 60% of personal injury accidents involving road users occur at or within 20m of junctions, and 84% of those accidents at or near junctions occur within built-up areas [26]. Road traffic accidents are basically of three types:

i) Vehicle-vehicle conflicts,
ii) Vehicle - hard object conflicts, e.g. bridge piers,
iii) Vehicle - soft object conflicts, e.g. people.

Factors influencing the degree of damage include the type, size, weight and construction of the vehicles and objects involved, the relative velocities of the vehicle(s) involved and the angle of impact. In tunnels, the factors influencing safety are indicated in Figure 3.1 [27].

Many road users consider road tunnels to be special elements of the road infrastructure that generate feelings of concern for their personal safety [28], in others words they perceive a higher risk. The perception of increased risk is in part due to entering a darker confined space, but also due to well known tunnel accidents such as the relatively recent Mont Blanc Tunnel fire in 1999, Tauern Tunnel fire in 1999 and Gotthard Tunnel fire in 2001. In terms of traffic accident frequencies, studies indicate that tunnels are either at least as safe as, if not noticeably safer than, comparable stretches of open road. Nonetheless if accidents do occur in road tunnels, the potential exists for more severe consequences than on the open road.

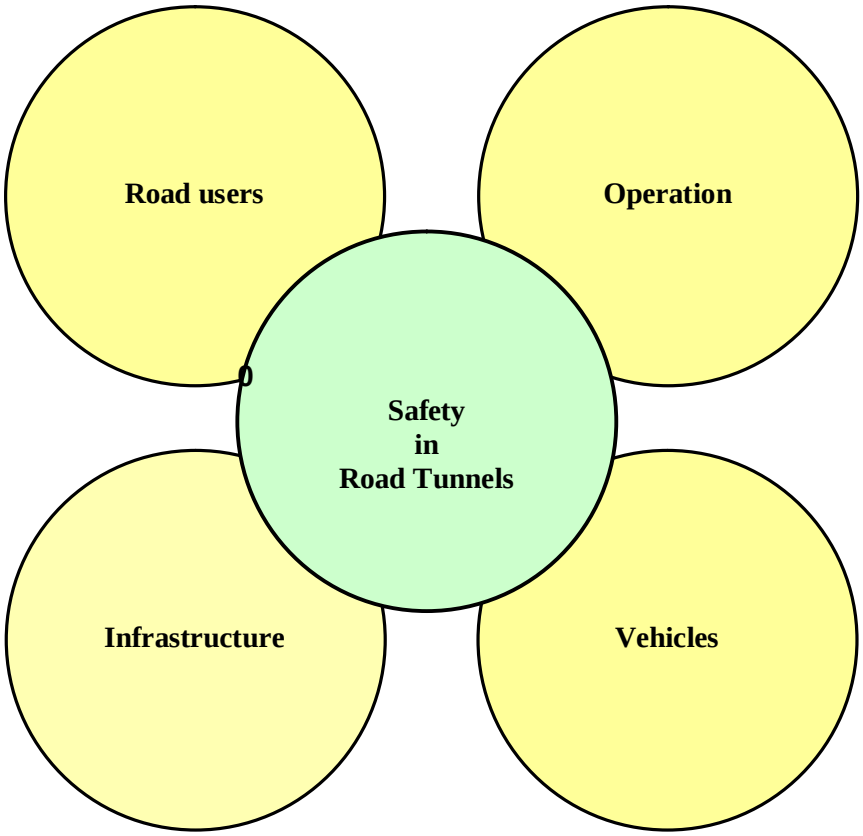

Figure 3.1: Factors Influencing Safety in Road Tunnels [27]

Tunnel characteristics affecting traffic accidents

Many of the factors that contribute to traffic accidents on open roads are absent or of reduced significance in tunnels including:

i) Traffic in tunnels is not exposed to adverse weather conditions, e.g. rain, wind, snow, ice,
ii) Tunnels often have reduced speed limits,
iii) Steady lighting conditions,
iv) Restricted overtaking either by physically separate traffic flows or by regulation,
v) Normal absence of junctions or reduced occurrence of merging/diverging traffic flows in the majority of tunnels,
vi) No stopping,
vii) Normal absence of pedestrians or bicycles,
viii) More concentrated drivers due to unusual surroundings/perception of danger,
ix) Often high standard road alignments (less severe curves and shallower inclines – except for water crossings).
x) This reduction in hazard exposure increases in longer tunnels.

However, some additional hazards may exist in tunnels including:

i) A fire in a tunnel may have more severe consequences than an equivalent fire in the open,
ii) Confinement if a vehicle leaves the carriageway,
iii) Confinement causing traffic jams (blocking the carriageway) in the event of a vehicle break down,
iv) Poor visibility due to build up of vehicle emissions,
v) Poor lighting transitions between the tunnel and open road including blinding sunlight at the tunnel exit,
vi) Hypnotic lighting in long tunnels,
vii) Inadequate lighting.

Additionally longitudinal gradients greater than 2.5% increases the frequency of breakdowns by up to 5 times [27] with a related increase in the risk of further incidents.

Some possible scenarios that could result in a traffic accident in a tunnel include:

i) Vehicle related incidents:
   - Fire in tunnel
   - Accidents
   - Breakdowns
   - Debris on road
   - Overheight vehicles.

ii) Non vehicle related incidents:
   - Lighting failure
   - Ventilation failure
   - Pumping failure
   - Emergency telephones out of order
   - Pedestrians in the tunnel
   - Animals in the tunnel
   - Vandalism
   - Terrorist attack.

iii) Traffic queues:
   - Traffic queues due to other causes, e.g. volume of traffic.

iv) Vehicle loadings:
   - Hazardous loads
   - Slow moving loads
   - Wide loads
   - Abnormal Indivisible Loads.

v) Weather hazards:

Fog
Rapid, air vapour condensation on windscreen, mirrors, etc
High winds
Ice
Snow
Flood
Dazzle from the sun (particularly east to west tunnel alignments)

vi) Planned maintenance:

Lane closures
Carriageway closures
Tunnel bore closures
Total closure
Contraflow operation
Temporary signing.

Accident statistics

As with most publicly available road traffic accident (RTA) statistics most of the available data is based on police reports of personal injury accidents (PIA) resulting in personal injury or death, and including at least one moving vehicle. The available statistics are often very wide ranging and detailed, however, they have a number of limitations and the following accidents may not be included:

i) Damage-only accidents with no human casualties,
ii) Accidents not reported to the police or not reported within a given time limit,
iii) Reported accidents that are not recorded.

In order to use PIA data to estimate the probability of a release of hydrogen following a traffic accident, it has to be assumed that personal injury relates to vehicle damage, i.e. intrusion into the vehicle structure. Such assumptions are misleading for three important reasons:

i) PIA statistics do not describe the degree of damage incurred by the vehicles involved in the accident,
ii) PIA statistics do not indicate which part of the vehicle was damaged, e.g. front, rear or side,
iii) There is not a clear relationship between the severity of personal injuries and vehicle damage,
iv) Under-reporting of accidents is a significant problem, as not all accidents are reported to the police regardless of any legal requirement to do so. The degree of under reporting varies inversely to the severity of the accident. Very few, if any, accidents resulting in a fatality do not become known to the police, however, a significant proportion of non-fatal injury accidents are not reported to the police. A regional study in the UK estimated that 36% of RTA casualties were involved in accidents that had not been reported to the police [29]. In Sweden official estimates suggest that only 40% of the actual number of PIA are reported [30].
v) Nonetheless PIA statistics do give a reasonable basis for comparing the relative frequency of accidents in tunnels.

The only sources of publicly available RTA statistics for tunnels that were identified are from a number of studies focussing primarily on Norway but also including German, Hong Kong and Swiss data [24, 27, 28, 31-35]. The available statistics do not differentiate between types of vehicles, i.e. cars, etc. and commercial vehicles.

Accident frequencies

In terms of RTA frequencies, studies generally indicate that accidents in tunnels are significantly less frequent than on comparable stretches of open road.

An analysis of accidents on Switzerland's national road network between 1992 and 1999 reveals that the average accident rate in tunnels is 0.35 per million vehicle-km compared to 0.47 on open roads [33] (the type of accidents, i.e. PIA or property damage, is not stated). In Norway a similar analysis shows that the PIA frequency in tunnels is slightly less than the average for national roads in sparsely populated areas (on which many of the longest tunnels are situated) but is half of the average road

accident frequency at 0.15 per million vehicle-km [28 and 34], see Figure 3.2. It is not clear if the Norwegian and Swiss figures are directly comparable in terms of the scope of accidents considered. A German study [34] suggests that accident frequency in German road tunnels is at most approximately 50% of that for open roads. However, most German road tunnels have a speed limit of 80km/hr which is low in comparison to the open road which will also influence the RTA frequencies.
Other Norwegian reports [31 and 32] are less clear on the reduced accident frequency in tunnels compared to open roads. One report [31] suggests comparable tunnel and open road accident rates of 0.52 and 0.50 accidents per million vehicle -.km respectively, however, this is based on 25 year old data. Comparison of tunnel accident rates with open road rates must be undertaken for the same years as in most countries there has been a general reduction in accident frequency due to vehicle and infrastructure improvements. Between 1990 and 2000 road traffic increased by approximately 20% in terms of person kilometres and freight transport increased by 50% in terms of tonne-kilometres over the same period, while road fatalities decreased by approximately 56000 to 27% [33].

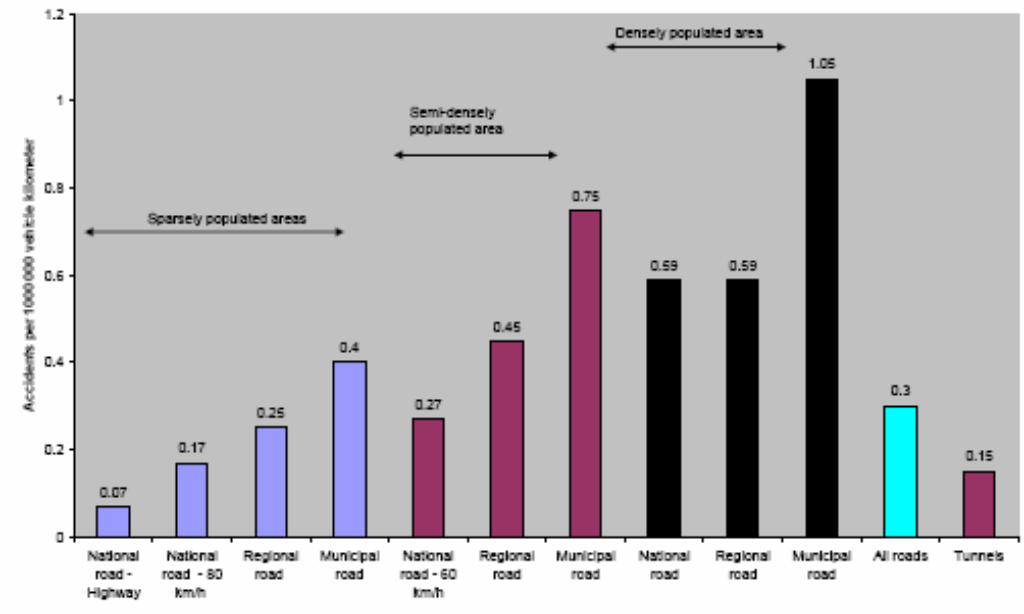

Source: [33]

Figure 3.2: No. of accidents per annum per million vehicle kilometres in Norway

Table 3.1: German RTA Rates (1993-1997)

Type Of Road	Personal Injury (Accidents/million veh.km)	Property Damage (Accidents/million veh.km)
Motorways with hard shoulders	0.074 (0.147)	0.328 (0.619)
Motorways without hard shoulders	0.130 (0.202)	0.354 (0.923)
Regional 2-way roads	0.141 (0.315)	0.249 (0.983)

Notes:
1. Main figures refer to tunnels
2. Figures in brackets refer to open roads

Source: [14]

The Norwegian studies [28 and 31] also investigate the variation of accident frequency in different parts of tunnels, e.g. entrance, mid-section, etc. The studies identify significant variations between the different sections, see Table 3.2.

Table 3.2: Accident Rate In Different Tunnel Zones

Tunnel Zone	Description	Accident Rate (Accidents per million veh.km)
1	*50m in front of tunnel openings*	*0.30*
2	First 50m inside the tunnel openings	0.23
3	Next 100m inside the tunnel	0.16
4	Mid-zone (remainder of the tunnel)	0.10
2 - 4	Tunnel	0.13

Source: [28]

Tunnels shorter than 100m only have zones 1 & 2, while tunnels shorter than 300m do not include Zone 4. A study of the effect of tunnel length on the accident rate [28] shows that the accident rate decreases as the tunnel length increases, see Tables 3.2 and Table 3.3.

A similar relationship was found for traffic flow [28], with the accident rate decreasing with increasing traffic volume, although this could also be influenced by increased design standards for roads with higher traffic flows.

A recent Swiss study [35], however, contradicts the previous finding:

i) An increase in traffic density increases the risk of collisions and the risk that persons will be injured since the gaps between vehicles are shorter,

ii) In longer tunnels, the risk of suffering an accident or being injured is reduced per unit of length as opposed to shorter tunnels (increased attention paid by motorists when driving through long tunnels),

iii) Compared with single tunnels with bi-directional traffic, twin tunnels have half the risk of accidents and casualties,

iv) An increase in the proportion of heavy goods vehicles in ADT also increases the risk of accidents in a tunnel (the rigid bodywork and large bulk of heavy goods vehicles represents a greater risk of danger since little energy is absorbed in an accident).

v) Wide road shoulders reduce the probability of an accident (in narrow tunnels with limited shoulder widths, motorists tend to drive down the middle of the road, which increases the risk of collisions).

A UNECE survey in 2001 [36] provided the following data for the Netherlands which has a number of relatively short (300 to 1500 m) immersed tunnels with steep ramps (4.5%). The PIA rate varies from 0.07 to 0.25 per million vehicle kilometers. The average for open motorways in the Netherlands is 0.05 per million vehicle kilometers.

A Hong Kong study [34] indicated that the probability of a PIA occuring in a tunnel (0.69 accidents per million vehicle kilometres) is 50% that of a PIA occurring on the open road based on data for five Hong Kong tunnels. However, of more interest the Hong Kong study provides the number of non-injury accidents with an accident rate of 4.12 per million vehicle kilometres, i.e. six times greater than the PIA rate (though the severity is not known).

Table 3.3: Accident Rate In Different Tunnel Zones

Tunnel Length (m)	Accident Rate (Accidents per million veh.km)
0-100	0.35
101-500	0.21
501-1000	0.15
1001-3000	0.11
>3000	0.05
Average	0.13

Source: [28]

Accident density

One of the Norwegian reports [28] gives a very useful measure of accidents for the HyTunnel work, that is, the accident density. The accident density was defined as the annual number of accidents per road km, giving an average annual tunnel value of 0.16 accidents per km. If the different zones are considered, the variation in the accident density figures can clearly be seen in Table 3.4.

Accident types

For the HyTunnel work the type of RTA is also of interest and some of the studies identified provide useful statistics. The type of accident is greatly influenced by the type of tunnel, e.g. uni- or bi-directional, and whether the tunnel contains junctions or merging/diverging links. Clearly there is a lower probability of head-on accidents in a one-way tunnel than in a bi-directional tunnel. Table 3.5 shows the proportion of different accident types from a Norwegian study [28] and limited results from a German study [34].

Accident severity

A Norwegian study [28] provides details of RTA severity based on personal injury reports. However, as indicated earlier, accidents that may result in significant vehicle damage or fires that could cause a hydrogen release may not result in personal injuries and vice versa. The RTA severity data is not considered appropriate for the HyTunnel project.

Table 3.4: Accident Density In Different Tunnel Zones

Tunnel Zone	Description	Accident Density (Annual accidents per road km)
1	50m in front of tunnel openings	0.43
2	First 50m inside the tunnel openings	0.35
3	Next 100m inside the tunnel	0.24
4	Mid-zone (remainder of the tunnel)	0.11
2 - 4	Tunnel	0.16

Source: [28]

Table 3.5: Accident type

Accident Type	1-Way Traffic Tunnel (%)	2-Way Traffic Tunnel (%)	National Roads (%)
Single vehicle	23	34	26
Frontal (opposing direction)	4	21	14
Rear end (same direction)	62 (69)	33 (34)	22
Crossing & turning	2	4	24
Pedestrian involved	3	2	9
Other	6	6	5

Source: [28] except (xx) [34]

Summary

Table 3.6 summarises the results from the various studies.

Table 6: Summary of traffic accident studies

Factor	Switzerland	Norway	German PIA	German Property
Tunnel accident rate (per million veh.km)	0.35	0.15	0.074 – 0.141	0.328 – 0.249
Open road accident rate (per million veh.km)	0.47	0.30	0.147 – 0.315	0.619 – 0.983
Tunnel rate as % of open road rate	75	50	50-45	53 – 25
Effect on accident rate				
Increasing tunnel length	Decrease	Decrease		
Increasing traffic flow	Increase	Decrease		
1-way traffic compared to 2-way traffic	Decrease	Decrease (0.12 for 1-way, though noticeably smaller in tunnel entrance)		
Increasing % HGV	Increase	-		
Additional width (hard-shoulders/lane width)	Decrease	Decrease		

3.3 Vehicle fires

Fire is perhaps the worst scenario in a tunnel due to both thermal effects and the toxic gases that are released. Minor incidents or technical failures that would have relatively minor consequences on the open road may have severe consequences in a tunnel. Vehicle fires in tunnels can occur due to a variety of reasons:

i) Traffic accident,
ii) Technical failure,
iii) Behavioural, e.g. smoking.

Vehicle fires can be initiated by various sources including

i) Fuel system,
ii) Electrical system,
iii) Accidental, e.g. smoking related.

Vehicle fire statistics - general

General vehicle fire statistics were collected for a safety study undertaken by Volvo in EIHP (http://eihp.org/eihp1/index.html). The results are presented in Table 3.7 which gives the estimated car fire frequency from the various sources identified. A German study [34] quotes general statistics for roads in central Europe having a rate of 0.02 fires per million vehicle km.

Vehicle fire statistics – tunnels

A German study [34] provides data for the Elbe Tunnel in Hamburg indicating the over-proportional involvement of heavy goods vehicles (HGV) in fires in the tunnel. HGV account for 15% of the tunnel traffic but were involved in 25% of vehicle fires between 1990 and 1999. The same study also provides data from the Gotthard Tunnel in Switzerland. In 1998, 4 fires occurred out of 55 accidents. Between 1992 and 1998, 42 vehicle fires occurred of which 21 involved cars, 14 HGV and 7 buses; HGV account for approximately 15% of the traffic but were involved in 33% of the fires. Other Gotthard statistics give 0.04 fires per million vehicle km for all vehicles and 0.06 fires per million vehicle km for HGV. In comparison the same study quotes general statistics for roads in central Europe having a rate of 0.02 fires per million vehicle km.

Table 3.7: Frequency Of Car Fires On All Roads

Data Source	Estimated Car Fire Frequency (per million veh.km)	Estimated Car **Petrol** Fire Frequency (per million veh.km)	Estimated Car **Petrol Fire** Frequency **Due To Traffic Accidents** (per million veh.km)
Swedish Rescue Services Agency [37]	0.0617	0.0284	-
US EPA [38]	0.2429	0.0874	-
Vägverket [39]	-	-	0.0012
Michigan [40]	-	-	0.0232

Statistics from a Hong Kong study [24] give a fire rate of 0.05 fires per million vehicle km.

A UN ECE report [26] quotes results of a PIARC study:

i) Average fire frequency = 0.25 fires per million vehicle km,
ii) Fire frequency is higher in urban tunnels than in other tunnels,
iii) 40% of tunnels have not had a fire,
iv) In certain tunnels the frequency of fires involving HGV is much higher than for cars.

A Norwegian study [41] quotes unreferenced UK and German studies indicating that fires caused by traffic accidents represent only 1-5% of the total number of vehicle fires, however, the Norwegian study finds the comparable Norwegian figure closer to 10%. The results of the studies are summarised in Table 3.7.

Table 3.7: Fires caused by traffic accidents as a fraction of total vehicle fires

Source	Fire rate per million vehicle km
Gotthard – all vehicles [34]	0.04
Gotthard – HGV [34]	0.06
Hong Kong [24]	0.05
UN ECE/PIARC [27]	<0.25

Hazardous material tanker truck fires

A US DoT report [42] provides a method for estimating hazardous material tanker truck fires.

3.4 Risk analysis

Documents published by the Swedish National Roads Administration (Vägverket) [43] and the World Road Association /PIARC [19 - 20] include risk assessment methodologies that may be of use for HyTunnel.

CHAPTER 4 – REVIEW OF HYDROGEN POWERED VEHICLES

A vehicle fuelled with hydrogen emits no pollutants, only water and heat. Two technologies have emerged in respect to powering hydrogen vehicles, described briefly below.

- Hydrogen fuel cell vehicles

  In a hydrogen fuel-cell the stored hydrogen reacts with oxygen (from the air) to produce water and electricity, the latter of which is used to power the electric motor. Hydrogen is stored as a compressed gas in cylinders under high pressure, typically at 35 or 70MPa, in order to provide sufficient range and packaging opportunities.

  The fuel cell approach is being more widely pursued compared to that of the hydrogen internal combustion engine. A number of motor manufacturers are developing hydrogen fuel cell cars. Fuel cell buses are also being developed, and have been introduced in various cities around the world.

  It has been suggested that hydrogen vehicles will emerge as a leading contender to replace today's internal combustion engine powered vehicles. Whilst in reality this vision may not materialise, or not be realised for some years, the safety issues surrounding the use of hydrogen vehicles and all alternative fuel vehicles inside tunnels need to be addressed now.

- Hydrogen internal combustion vehicles

  Here the hydrogen is burned in an internal combustion engine in basically the same way as traditional gasoline fuelled cars. Whilst the idea has bee around for a long time, the technology is currently being pursued only to a limited degree compared to fuel cell vehicles (see below). BMW has recently launched a limited number of its Hydrogen 7 car which is a bi-fuel vehicle can switch between hydrogen and gasoline. When in hydrogen mode, hydrogen is injected directly into the car's air intake manifold.

  In the BMW example, hydrogen is stored as liquid rather than as compressed gas. To remain as a liquid, the hydrogen must be super-cooled to cryogenic temperatures of at least −253°C.

As an illustration, this chapter discusses, in more detail, the compressed gaseous hydrogen (CGH_2) system used by Volvo and liquid hydrogen (LH_2) system used by BMW.

4.1 Description of Volvo's CGH2-storage system [44]

In the medium term typical hydrogen powered vehicles will be applications that can exploit the potential efficiency gains of fuel cell drivetrains such as passenger cars, city buses and distribution trucks.

For city buses hydrogen is currently being used by a variety of OEMs with fuel cell based drivetrains and to a lesser extent internal combustion engines (ICE). For a typical full size city bus the maximum quantity of hydrogen required is in the order of 40-50kg, typically stored in 35MPa compressed gaseous hydrogen (CGH_2) systems as storage space is not as critical as for other applications. The maximum storage pressure could also be 25MPa or 70MPa depending on the application and storage requirements. For city buses CGH_2 storage systems are usually roof mounted, with the fuel cells either mounted on the roof or at the back of the vehicle, with both locations offering good ventilation that maximises the use of the strong buoyancy characteristics of hydrogen in the event of leaks. Roof mounted systems are also outside of the impact zones of most traffic accidents.

For cars hydrogen is currently being used by many OEMs with fuel cell based drivetrains and to a much lesser extent internal combustion engines (ICE). For a typical car the maximum quantity of hydrogen required is in the order of 3-10kg depending on the size and characteristics of the car. Until recently, CGH_2 systems for cars typically used 35MPa CGH_2 systems, however, 70MPa systems are now available and are likely to become the norm due to the range and packaging demands of cars. For cars CGH_2 storage systems are usually mounted underneath the car near the rear axle as this position offers the best protection in the event of an accident, with the fuel cells mounted in the "engine" compartment or also underneath the car. In many prototype vehicles, the CGH_2 system has been located in the boot or luggage area.

CGH_2 systems (see Figure 4.1) usually have a maximum storage pressure of 35 or 70MPa. For hydrogen applications by far the most common types of container are known as Types 3 and 4 (see Figure 4.2). Type 3 containers have a metallic liner to contain the hydrogen with carbon fibre overwrap providing the structural strength. Type 4 containers have a non-metallic (plastic) liner to contain the hydrogen with carbon fibre overwrap providing the structural strength. Other types of fibre may be used, though carbon fibre is the current industry standard for automotive hydrogen containers due to its excellent structural properties. Draft legal requirements and standards demand that the containers are 100% leak tight, however, hydrogen permeates through the plastic liner of Type 4 containers and limits are placed on the allowable permeation rate. For other components a very small nominal leak rate is permitted in some draft legal requirements as it is very difficult to achieve 100% leak tightness with hydrogen in components where many seals and connections are required.

Source: Dynetek

Figure 4.1: Typical CGH_2 storage system

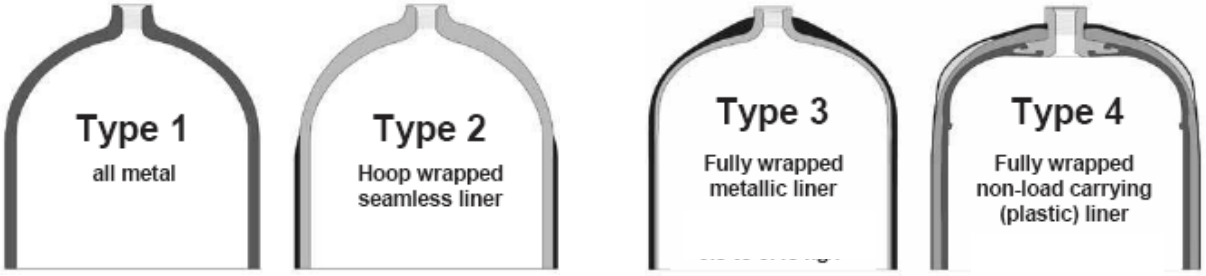

Source: Dynetek

Figure 4.2: Types of CGH_2 container construction

In tunnels there are two significant failure modes to consider, rupture of the container and a hydrogen line break. Rupture can occur due to internal pressures exceeding the strength of the container, or by factors reducing the strength of the container. Mitigation against the first case is achieved by designing and testing the containers to pressures significantly in excess of the working pressure. ISO and SAE standards for the refilling interface prevent refilling stations from connecting to vehicles with a lower working pressure than that of the refilling station. A further possibility is that the internal pressure in the container can exceed the design strength of the container through excessive heat transfer into the hydrogen, most likely when the container is exposed to fire. Increased heat transfer into the container

causes the pressure to rise as the gas expands. This latter case is particularly important and it could occur as a result of a traffic accident or other potential fire sources. This type of failure is mitigated by the use of a temperature triggered, non-reclosing pressure relief device. When the temperature reaches a set value (around 105^0C) the PRD opens and vents the contents of the container to atmosphere. The subsequent potential effects are considered to be less hazardous than a container rupture. There are also potential causes of rupture below the working pressure of the container if its structural integrity is impaired, by for example, chemical exposure or mechanical damage. These cases are dealt with by a rigorous testing regime. Increased work on localised fire effects is being undertaken, however, as a minimum the drafts usually require consideration of the orientation of PRD vent lines relative to other containers.

Hydrogen line breaks are controlled by excess flow systems that detect a line break and react to it by isolating the container, thus limiting the quantity of gas released from the system. Systems may incorporate, for example, excess flow limiters or automatic shut-off valves leaked to a hydrogen detection system.

4.2 Description of BMW's Hydrogen 7 with LH2-storage system [45- 49]

The BMW Hydrogen 7 is the world's first premium sedan with a bi-fuelled internal combustion engine concept that has undergone the series development process. This car also displays the BMW typical driving pleasure. During development, the features of the hydrogen energy source were emphasized. Engine, tank system and vehicle electronics were especially developed as integral parts of the vehicle for use with hydrogen.

The internal combustion engine is designed to burn either hydrogen or petrol in its cylinders. While driving, the engine can be switched from hydrogen fuel to conventional operation on petrol without any noticeable delay. Operating on hydrogen, the range before refuelling is more than 200 kilometres, to which a further 500 kilometres can be added when running on petrol. Bi-fuelled operation is an important option, particularly during the transition period in which the H_2 filling station network is still sparse.

Figure 4.3: Bi-fuel internal combustion engine

The bi-fuel power train concept calls for two separate fuel storage systems to be integrated into the car. As well as the 74-litre petrol tank, there is a LH_2 tank capable of holding about 8 kilograms of liquefied hydrogen (Fig. 4.4). BMW has adopted hydrogen in liquefied form, because LH_2 storage systems have the highest volumetric and gravimetric energy densities compared to gaseous hydrogen, which is stored at high pressure [46]. This increases the range for a given storage volume. The tank system is a major challenge, because hydrogen liquefies only at the extremely low temperature of -253°C, and this low

temperature must be maintained in the tank for as long as possible. In order to achieve this, the double-walled tank is equipped with vacuum super insulation.

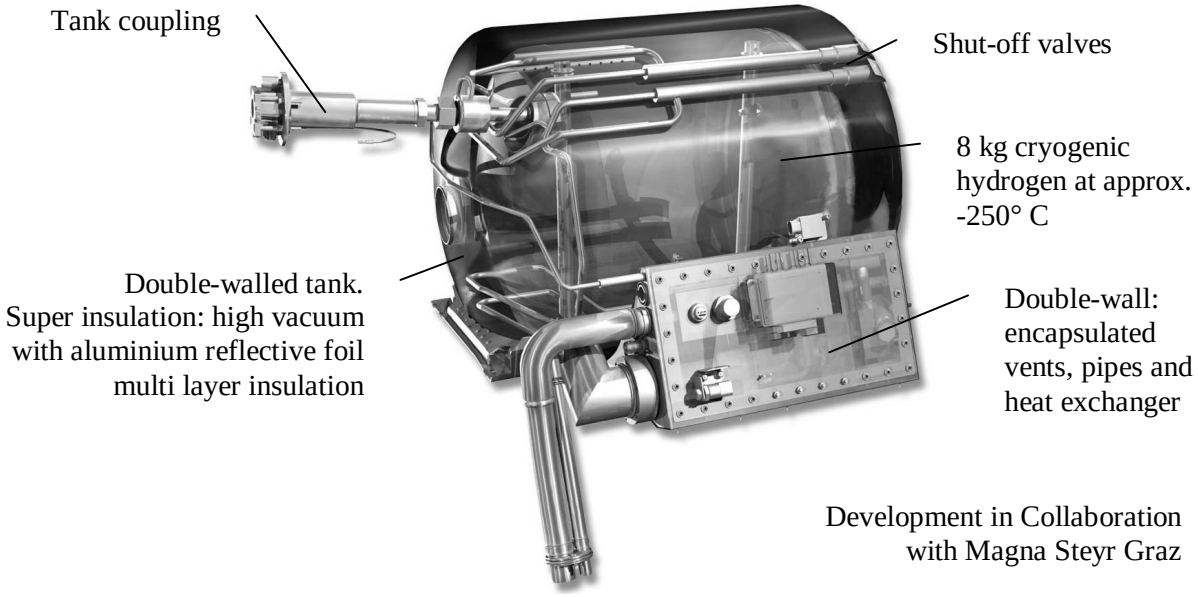

Figure 4.4: LH_2-fuel storage with filling pipe

Despite this excellent tank insulation, it is impossible to prevent a slight amount of heat from reaching the tank. As a result, a small proportion of the hydrogen evaporates ('boil-off'). The Hydrogen 7's fuel system can keep back boil-off gas for about 17 hours if no gas is consumed, after which it is supplied to a boil-off management system, where the gaseous hydrogen is mixed with air and oxidized in a catalytic converter to yield water.

4.2.1 Safety concept for vehicles with LH2-storage

Special attention was devoted to safety against the background of the specific properties of hydrogen during the vehicle development process. In addition to passive safety, the operating safety of the hydrogen system had to be taken into close consideration.

The basis for the safety system ratings is functional safety as laid down in IEC 61508; which specifies processes for the design and validation of electrical/electronic systems. For the BMW Hydrogen 7, these requirements were interpreted with respect to vehicle operation in its environment, and extended as necessary and appropriate. As a result, safe operation has been confirmed by both internal and external experts for all the relevant functions and components. Furthermore, the vehicle and filling station safety concepts have been coordinated, and special situations, for example in repair shops, were evaluated in terms of technical safety [47].

4.2.2 Tests for vehicles with LH2-storage

The safety-oriented development process established additional strict hydrogen-specific standards for the Hydrogen 7. The fulfilment of these standards were demonstrated in a comprehensive experimentation and testing program, which included all required tests and a large number of additional hydrogen-specific crash tests, such as side impacts to the tank coupling system, or rear impacts. Furthermore the behaviour of the hydrogen tank was tested under extreme conditions, for instance in flames and after strong degradation of the insulation. Testing included over 1.7 million km of driving; and all tests were passed successfully, proving the intrinsic safety of the vehicle and also confirming the success of the safety-oriented development process, which is to be continued during future vehicle development.

Even crash tests in extreme conditions, such as simulation of a rear-end collision involving a truck or the LH2 tank coupling striking a pole, confirmed that these demanding requirements had been fulfilled.

Fig. 4.5: Crash test simulating a rear-end collision

4.2.3 Hydrogen release scenarios for vehicles with LH2-storage

Although the LH2 storage system has very well proven that even heavy crash loads do not result in the uncontrolled release of the stored hydrogen, there are some possible scenarios where hydrogen release can not be excluded:

a) Failure release

The single failure release rate, for example when a fault of the boil off management system occurs, is defined with max. 60 g/h H2. Due to the low release value, this case is more relevant for garage parking issues and less interesting for tunnel safety requirements.

b) PRD release

If the tank loses its vacuum, for example in an extremely heavy rear- end crash, a safety valve reacts at a defined internal pressure of the inner tank. The safety valve blows off the gaseous hydrogen into the air through safety lines on the vehicle's roof. In that case a maximum PRD release of 8 kg H2 (100% filling) in the space of 30 minutes can occur.

In an extra test, a break of the vacuum-tank was simulated, and the exhaust hydrogen was ignited deliberately by 3 ignition plugs in order to examine this situation in detail. The flames burnt upwards, but the roofline in the passenger compartment did not start to burn until after about 5 minutes, enough time for occupants to leave the vehicle or to be rescued by helpers.

c) Instantaneous release (max. 8 kg H2)

An accident thus disastrous that the liquid hydrogen vessel itself breaks apart or the vacuum is lost and the PRDs are inoperable and the total amount of hydrogen is released instantaneous and uncontrolled is extremely unlikely to happen. However, for the reason of understanding the borderline case, this scenario can also be analysed.

CHAPTER 5 – REVIEW OF PUBLISHED WORK ON MODELLING METHOLOGIES AND THEIR APPLICATION TO HYDROGEN DISPERSION, COMBUSTION AND EXPLOSIONS

5.1 Modelling methodologies

Before reviewing the published work, an introduction to the relevant experimental and computer modelling approaches is given.

As full-scale experiments can be very costly, the well established technique of physical, reduced-scale modelling has been used for many years to study the engineering application of fluid dynamics. The basic principle of reduced-scale modelling is to build a scale model of the geometry and undertake experiments such that various dimensionless numbers, or groups, are preserved at reduced- and full-scales so that the results at reduced-scale can be extrapolated to full-scale. It has found widespread application in wind tunnel studies of the build environment and for vehicle aerodynamics, as well as other application such as air and smoke movement, including inside tunnels.

Computer modelling has been used increasingly over the past decades to investigate the movement of air and the control of fire and hazardous releases inside tunnels. A brief summary of the different modelling approaches is given below.

- Network (one-dimensional) models

  Much of the early work involved using a computer to solve sets of aerodynamic and thermodynamic equations. At this time, a number of software packages were developed to assist in the design of tunnel ventilation systems. The most widely used example is the Subway Environment Simulation (SES) Computer Program (Kennedy et al. [50]), which evolved from a relatively limited tool for analysing metro lines to a much more comprehensive tool for designing ventilation for road and rail tunnels, taking into account the full range of ventilation methods, the influence of vehicle movement and an approximate treatment for fires.

- Zone models

  Zone models represent the next level of sophistication after network models. More commonly used in building fire studies, these models predict the evolution of hot smoke layers inside enclosures and the transport of smoke, heat and fresh air through openings (windows, doors etc), either to the outside environment or to neighbouring enclosures. Central to most zone models is the concept of an upper, hot layer of smoke and a layer of cooler air below. While this provides a reasonable description for many compartment fire scenarios, it may not be applicable to more general situations. In addition to the main, gas phase zones (layers), empirical and semi-empirical sub-models are included for plume entrainment, boundary heat losses, radiative heat transfer etc.

  CFAST (Jones et al. [51]) is one of the most widely used zone models for building/compartment applications, available from NIST (USA) (Jones et al. 2000). By considering a tunnel or metro station area to be 'artificially' composed of a number of connecting compartments, CFAST has been used in its multi-room configuration to predict the transport of smoke within the tunnel or station. This approach has been reported by a few authors, see for example (Chow [52]) and (Yang et al. [53]).

  FASIT (Charters et al. [54]) is a zone model developed specifically for tunnel applications. It extends the two-layer zone concept for compartments into a three-layer zone concept more suited to smoke layers under tunnel ceilings. The three layers represent the lower (cool) air, the upper (smoke) layer and an intermediate 'mixing' layer. The tunnel length is then divided into 'segments', each with its own three-layer construct. FASIT has been applied to safety assessments for a number of rail projects including the Channel Tunnel and the Jubilee Line

Extension in the UK. The model has proven to be a useful component in a wider quantified risk assessment process, see (Charters et al. [55]) and (Salisbury et al.[56]).

- CFD models

  Computational Fluid Dynamics (CFD) models [57 – 60] represent in many respects a generalisation of network models to two- and, more generally, three-dimensions. Furthermore, they provide a more sophisticated approach than zone models, relying far less on empirical modelling assumptions. The basic idea behind a CFD model is to solve the underlying conservation equations describing the fluid and heat transfer processes within each of a large number of control volumes (grid cells), typically numbering anywhere from about 10,000 to a million or more, thus providing a very detailed solution.

  CFD models take as their starting point the system of coupled partial differential equations that describe the conservation of mass, momentum, energy and chemical species. These equations, known as the Navier-Stokes equations (momentum and mass conservation) and the related general advection-diffusion transport equation (energy and species conservation), describe both laminar and turbulent fluid flow. A solution, in time and space, is obtained by integrating and discretising the equation set over a spatial and temporal grid, and then solving the resultant set of algebraic equations by an appropriate numerical method. This yields a discrete set of solution values for velocity, temperature etc at each spatial grid point (each one corresponding to one control volume) at each time step.

  However, to resolve precisely the turbulent structures characteristic of fire induced flow would require reasonably fine spatial and temporal grids for practical solution. Thus is due to the small time and length-scales of the smallest turbulent eddies. An approximate form of the conservation equations must therefore be solved, and the influence of turbulence incorporated in some appropriate manner. There are two turbulence-modelling approaches available that are currently being used for practical fire applications, described briefly below.

  Solution of the Reynolds-averaged Navier-Stokes (RANS) equations. This has been the approach adopted in most CFD models for practical engineering applications. Here, the dependent variables are written as a sum of a time-averaged component and a fluctuating component, where the latter represents the effect of turbulence. Unfortunately, this renders the set of differential equations more complicated, with the introduction of extra terms referred to as the Reynolds stresses and the turbulent scalar fluxes. These terms have to be solved for, or modelled in some manner, in addition to the time-averaged components. Instead of solving for the Reynolds stresses individually, the eddy-viscosity approach has often been employed, which accounts for the effect of turbulence on the flow field as an increased viscosity. Commonly this involves the solution of two extra equations for the turbulent kinetic energy (k) and its dissipation rate (ε). Despite known limitations, the k-ε class of turbulence model has proven to be reliable for many engineering applications, including gas dispersion and fire modelling.

  Large eddy simulation (LES). This represents a more 'fundamental' approach. Here the larger time- and length-scales of turbulence are modelled explicitly, i.e. simulated directly from the solved equation set, and the influence of the smaller eddies is then incorporated via a sub-grid scale (SGS) sub-model. However, it is important when using an LES model to ensure that the spatial grid is sufficiently fine to be able to resolve the eddies that are not modelled by the SGS sub-model. Furthermore, a small time-step (significantly less than 1 second) is required for numerical stability and accuracy. Until recently, for most engineering applications LES remained a computationally prohibitive option. However, with the advent of cheaper computers and the wider availability of parallel processing, LES may now be considered more often as a viable option.

  Other than the treatment of turbulence, the main feature that differentiates the available CFD models is the numerical mesh (grid) that is constructed to solve the system of equations. The

main options that have been adopted include Cartesian, curvilinear block-structures and unstructured meshes.

For further information on numerical meshes and CFD in general the reader is referred to textbook references, e.g. (Versteeg and Malalasekera [61]) and (Ferziger and Perić [62]).

5.2 Conference proceedings and research publications

General publications on tunnel hazards and fire safety are numerous, and are not explicitly referenced here. The following series of conference proceedings are noted, however, as a useful source of information on hazard management and fire safety in tunnels generally:

- *Aerodynamics and Ventilation of Vehicle Tunnels [63]*. BHR Group Conference Series (most recent being the 12th International Symposium, held in Portoroz, Slovenia from 11-13 July 2006).
- *Tunnel Fires[64]*. Tunnel Management International (most recent being the 5th International Conference, held in London, UK from 25-27 October 2004).

The on-going series *International Conference on Hydrogen Safety[65]*, organised in conjunction with HySafe, is a useful source of current information on all aspects of hydrogen safety including vehicles and tunnels. The most recent conference was held at San Sabastian, Spain, from 11-13 September 2007.

Examples of recently published work of direct relevance to HyTunnel are summarised below. This supplements the previous HySafe report (Venetsanos [66]), which looked at material for hydrogen releases within confined spaces generally, focussing here specifically on tunnels. We consider here full- and reduced-scale experiments as well as computational studies (primarily CFD).

- European Integrated Hydrogen Project (EIHP) Phase 1 and 2 (Venetsanos [66, 67])

The European Integrated Hydrogen Project Phase 1 (EIHP-1) and Phase 2 (EIHP-2), supported by the European Commission, were undertaken to facilitate the approval of hydrogen vehicles in Europe. This involved, for example, identifying issues impeding the harmonisation of guidelines and regulations and of coordinating initiatives to help standardise these areas.
In EIHP-1, proposals for harmonised draft regulations for the approval of hydrogen vehicles were developed. In EIHP-2, the work was extended to look at the specifics of refuelling stations and to continue the work on vehicles. Two publishable final reports summarise the work (EIHP 2000 and EIHP 2004).

To support the central activities of the EIHP work, a CFD investigation into the explosion hazards associated with releases of compressed gaseous hydrogen from single deck city buses in urban and tunnel environments was conducted. A key aspect of the study were comparative releases from compressed natural gas systems were compared. This study provided the starting point for the HyTunnel CFD activity reported later.

The accident scenario was that the gas release occurred due to the operation (e.g. due to a fire) or failure of thermally activated pressure relief device(s) (PRD), without immediate ignition of the gas. The scenario was chosen as a worst case event to compare basic layouts and modelling. Working pressures of 20, 35 and 70 MPa were considered for the hydrogen and 20 MPa for the natural gas. The gas was housed in eight cylinders, each containing either 5 kg hydrogen or 21 kg natural gas.
Three gas release configurations were studied. In Case 1 the content of only one cylinder was released, through a vertical vent above the roof. In Case 2 the total content (8 cylinders) was released through the same vertical vent and in Case 3 the total content was released through four vertical vents above the roof. Ignition of the gas cloud was assumed to occur at the same time as the mass of flammable gas was reached its maximum against a worst case assumption.

When comparing the consequence of a hydrogen release inside a tunnel to that in the outside (urban) environment, it was determined to be significantly more severe and the energy available in the flammable cloud was greater and remained for a longer period.

Case 3 was more hazardous than Case 1 or Case 2. Furthermore, while the consequence of a release from a 20 MPa natural gas system was comparable to that from a 20 MPa hydrogen system, for consequence of a similar release from a higher pressure hydrogen system was significantly more severe, in particular with respect to predicted overpressures. The significant difference in the explosion hazard associated with the 20 and 35MPa release, despite a similar energy, was attributed to the different distribution of hydrogen mass within the flammable clouds formed.

The CFD study also highlighted that the ignition point inside the dispersed gas cloud significantly affects the combustion regime. Based on the predicted overpressures, typical effects could be damaged vehicle windows or tunnel lighting units. However, the results also indicated that fast deflagrations, or even detonations, could be produced by the most severe hydrogen releases and ignition timing from the worst case events.

It was concluded that hydrogen storage systems should be designed to avoid simultaneous opening of all PRDs. Mitigating measures should be developed to avoid Case 3 occurring in a tunnel.
A recommendation for further research was made to gain a better understanding of the release and ignition conditions that could result in fast deflagrations or detonations. The influence of ventilation, the tunnel characteristics and the blockage ratio due to the presence of vehicles in the tunnel are all likely to be important.

It was noted that a detailed risk analysis would be necessary before any detailed recommendations could be made. Such an analysis would need to balance the risks associated with venting the gas as quickly as possible against those associated with restricting the energy flow from the storage system, so that the explosion risk is reduced, but with an increased risk of an uncontrolled release from a fire damaged tank.

- CFD study of Mukai et al [68]

A CFD study into the explosion risks associated with hydrogen releases from vehicles in two road tunnels has been published by Mukai et al [68]. The influence of tunnel cross-section shape and ventilation velocity was investigated for a release of 60m^3 of hydrogen, stored at a pressure of 35 MPa, through a PRD leakage vent hole of 5.5mm diameter. The release lasted 52 seconds.

The hydrogen was vented downwards, from the underside of the vehicle, which is in contrast to the scenarios investigated in the EIHP work.

The STAR-CD RANS CFD code was employed. The calculations were conducted in two stages. Firstly, the high pressure release was modelled over a small region located underneath the vehicle. The outflow from this small region then provided the inlet boundary condition for the tunnel CFD simulation.

For the scenarios investigated, it was concluded that the released hydrogen either vented naturally due to its buoyancy, or else was dispersed rapidly due to the tunnel ventilation. A potential risk due to a hydrogen-air mixture above the lower flammability limit (4% volume) at the exhaust fan was concluded to be minimal.

- CFD studies of Wu [69,70]

In the paper presented by Wu at the 12th Symposium of Aerodynamics & Ventilation of Vehicle Tunnels [69] and the Second International Conference on Hydrogen Safety [70] the potential hazards associated with high pressure hydrogen jets released inside a longitudinally ventilated tunnel are explored. In contrast to the EIHP studies [66, 67] and the work of Mukai et al [68], the subject of this work is the consequence of an ignited fuel release, generating a hydrogen jet flame.

Two hydrogen release mechanisms are investigated for a car containing 3kg of compressed gas hydrogen. In one case the hydrogen is vented at $0.1 kgs^{-1}$ and an exit velocity of $10 ms^{-1}$ (resulting in a 6MW jet fire lasting 10 minutes) while in the second case it is vented at $0.5 kgs^{-1}$ and an exit velocity of $50 ms^{-1}$ (resulting in a 30MW jet fire lasting a shorter duration).

CFD simulations of the above hydrogen jet fires inside a 5m by 5m cross-section tunnel have been performed using the Fluent code. The k-ε (RANS) turbulence model is employed. An emergency longitudinal ventilation velocity of $2.5 ms^{-1}$ is imposed 40m upstream, representing the critical velocity to control 'conventional' fire incidents for this cross-section, i.e. to eliminate 'back layering' of heat and fire gases in the upstream tunnel direction.

The simulations showed that whereas the $2.5 ms^{-1}$ longitudinal ventilation was able to eliminate back layering for the smaller (6MW) hydrogen jet fire, in the case of the larger (30MW) fire there was some back layering, extending three tunnel heights upstream.

More significant perhaps than the presence of some back layering, the papers raise a concern regarding the length of the downstream flaming region in the case of the larger hydrogen release. At 45m (9 tunnel heights) it is argued that the extent of the ignited hydrogen ceiling jet poses a significant hazard compared to other (hydrocarbon) fuels. The papers do not, however, take into consideration the contribution of the vehicle and any carried goods, which is likely to more important than the actual fuel. The rapid development of an ignited hydrogen ceiling jet, extending some distance along the tunnel, does however warrant further investigation.

- Risk and modelling studies of Hansen and Middha [72]

The work reported at the Second International Conference on Hydrogen Safety by Hansen and Middha [72] forms part of the HyTunnel activities covered later in this report, and only brief mention is made here.

The paper includes a CFD modelling study to provide insight into the risk posed by hydrogen vehicles in road tunnels, and examines different tunnel geometries and hydrogen release scenarios, including cars and buses. The maximum released fuel load considered was 20kg of hydrogen stored at a pressure of 35 MPa. As for the EIHP work, comparisons to natural gas vehicles are included.
CFD calculations of the dispersion of gas following activation of one or more PRDs are made using the FLACS consequence analysis computer model. The maximum possible pressure load predicted by the simulations was in the range 0.1-0.3 barg, which represents a limited human fatality risk due to direct injuries. It is noted that that local overpressures due to reflections from the sidewalls and/or the vehicles can be expected to be higher than those calculated in the study.

The study assumed a smooth tunnel ceiling with no obstructions near the ceiling. It is noted that the presence of blockage elements, e.g. light armatures or fans, could add some turbulence to flame propagation and make explosions more severe. This awaits further study.

The study utilises the concept of an equivalent stoichiometric gas cloud, from which the explosion pressure can be estimated more speedily than if the actual (computed) dispersed gas cloud is used. While it is reported that this approach has been found to work reasonably well for various risk assessment studies for natural gas systems, some doubt has been expressed about its suitability for HyTunnel scenarios.

- Reduced-scale experiments and CFD study of hydrogen explosions (Groethe et al. [73])

A series of experiments inside a reduced-scale tunnel geometry have been conducted by Groethe et al [73] to examine the effects of hydrogen release deflagrations in a reduced-scale vehicle tunnel. The tests showed that the confinement of the hydrogen by the tunnel significantly raises the explosion hazard.

Tunnel ventilation was shown to reduce the hazard dramatically, and suggested that suitable ventilation of a tunnel can significantly reduce the chance of an explosion. Further work is required, however, to examine higher release rates of hydrogen than those studies so far. There may be the possibility that even in a well ventilated tunnel a high release rate of hydrogen could produce a near homogeneous mixture at close to stoichiometric conditions, with a correspondingly increased explosion hazard.

A computational study, based on the above experiments performed in a reduced-scale tunnel has been conducted by Groethe et al. [73] using CFD. The model employs an LES treatment for turbulence, using an LES sub-model developed by the authors within the framework of the FLUENT commercial CFD code. Predicted explosion pressures were in good agreement with the experimental data, covering both obstructed and unobstructed tunnel arrangements.

The work has demonstrated the usefulness of CFD in extending the findings obtained from experiments alone, e.g. in examining explosion pressure effects in the locality of obstructions. Furthermore, it represents an important step in extending the validation of a model that has previously been calibrated for hydrogen-air explosions in the open. It is recommended that further work is conducted to investigate more realistic hydrogen gas distributions, and to examine the mechanisms that could lead to deflagration to detonation transition.

- LES of hydrogen-air deflagrations in a 78.5-m tunnel (Molkov et al. [74])

Hydrogen-air deflagrations in confined spaces present more severe hazards and associated risk than those in the open atmosphere. Molkov et al [74] applied the LES model, calibrated previously to predict the dynamics of large-scale hydrogen-air deflagrations in the open atmosphere, to validate it against the experiments on hydrogen-air deflagrations in the confined environment of a 78.5 m long tunnel. They included deflagrations in both an unobstructed tunnel and tunnel with obstacles.

The LES model enables the transient modelling of deflagration dynamics with a laminar flame burning velocity which alters with mixture composition, pressure, and temperature. The turbulent burning velocity is computed by using the Yakhot's formula [75] for turbulent pre-mixed combustion, which accounts for both the transitional phenomenon of turbulence generated by the flame front itself, and fractal structure of the flame surface on the unresolved sub-grid scale.

The numerical simulations were shown to reproduce the experimentally measured deflagrations for both 20% and 30% hydrogen-air mixtures in the unobstructed as well as the obstructed tunnel. The simulation gave insight into the dynamics of flame propagation and the pressure build up within and outside of the tunnel.

The simulations confirmed experimental observations that obstacles with a blockage ratio of 0.03m, as per tested configuration, have no significant effect on maximum explosion overpressure in the tunnel beyond the immediate vicinity of the obstacles. Both experiment and numerical simulations small variance in maximum pressure along the tunnel. Based on the LES analysis, it was demonstrated that side-on obstacle overpressure can increase significantly due to reflection of the shock wave formed in the tunnel during the deflagration.

The authors have suggested that the validated LES model can be used to assess the consequences of more realistic releases of hydrogen in real scale tunnels. However, firstly a worst case scenario of a near stoichiometric hydrogen-air deflagration of 40kg of hydrogen released from a bus in a real scale tunnel has to be studied. The possibility of shock to detonation transition should be estimated to assess the potential risk associated with an accident involving hydrogen powered vehicle in a tunnel. Following this, a scenario of deflagration of non-uniform mixture, created by the realistic hydrogen release and dispersion, should be considered to assess realistic consequences and risks posed by the non-uniform hydrogen-air mixtures in a tunnel.

CHAPTER 6 – HYTUNNEL RESEARCH ON EXPERIMENTAL WORK

Many tunnels are equipped with ventilation and it is a recognised means of removing an explosive atmosphere to mitigate the consequences of a flammable gas release. The experiments with hydrogen are part of the investigation of ventilation as a control strategy in vehicle tunnels. The use of hydrogen is complementary to the previous work using methane.

The destroying potential of blast waves resulting from combustion and explosion of burnable gases, in particular hydrogen-air mixtures, pose major hazard to safety. Understanding of the potential to provide conditions for high-speed deflagrations is of major importance. The potential of partially confined and unconfined configurations to support flame acceleration, onset of detonation and detonation propagation is still poorly understood.

This chapter focuses on the experimental work, performed in the frame of the internal project HyTunnel, to examine the effect of ventilation in removing an explosive atmosphere to mitigate the consequences of a flammable gas release, and to examine high-speed deflagrations in stratified hydrogen layers under a tunnel ceiling

6.1 HSL experiments [76]

The objectives of the HSL experiments were:

- to provide a means of comparing the over-pressures generated by igniting a stoichiometric hydrogen-air cloud with that generated by a stoichiometric methane-air cloud released into the congested volume of an enclosure,
- to investigate the effects the ventilation may have on the over-pressure,
- to provide guidance in the design of more realistic scenarios, where the over-pressure should be lower than in the worst-case scenario.

The work is split into two parts, ignited steady state tests and quiescent explosion tests. In the steady state tests hydrogen is released into the congested volume of an enclosure. This is equivalent to a hydrogen leak into a tunnel from a pressure relief valve or damaged pipe work on a vehicle. In the quiescent tests the congested volume is filled with a flammable hydrogen-air mixture and would be equivalent to a hydrogen build up within a small confined and congested area. A congested volume is used to create turbulence and allow this effect of on explosion behaviour to be investigated.

For the experimental programme a 93.1 m^3 rectangular vessel was used. This was used in two forms, firstly as a ventilated enclosure and secondly as a totally enclosed vessel. As a ventilated enclosure the ventilation rate could be varied and a critical flow orifice plate was used to create different hydrogen leakage rates into the enclosure. In the totally enclosed mode small quiescent volumes of stoichiometric hydrogen/air mixture (up to 1% of the enclosure volume) were created. In all of the tests the resulting hydrogen cloud was ignited and the pressure generated in the enclosure measured.

6.1.1 Experimental set-up

Figure 6.1 shows an enclosure made up of one module, with approximate dimensions of 2.5 by 2.5 by 2.5 m. In principles, up to total of 12 modules can be combined to give a total enclosure length of 30 m, corresponding to an enclosure volume of 188 m^3. In the present study, six modules were combined to give a total enclosure length (internal dimension) of 14.9 m, corresponding to an enclosure volume of 93.1 m^3.

Ventilation of the enclosure is achieved through suction, using a variable speed fan attached to one end of the enclosure (can be seen on the left of Figure 6.1). The modules have pressure relief panels on the top to ensure venting so that the enclosure is not damaged by too powerful deflagrations.

The module is placed at the inlet of the geometry to try to reduce the effect of the ambient wind field. A further measure to try to create a homogeneous flow through the enclosure was the use of an end plate

with 324 circular holes, each with a diameter of 0.05 m (see Figure 6.2), for the air inlet ports. For the air outlet ports there are 16 square holes in the fan end of the enclosure. This arrangement allows air to be sucked through the enclosure.

Figure 6.1 The small enclosure, with a volume of approx 14.7 m^3

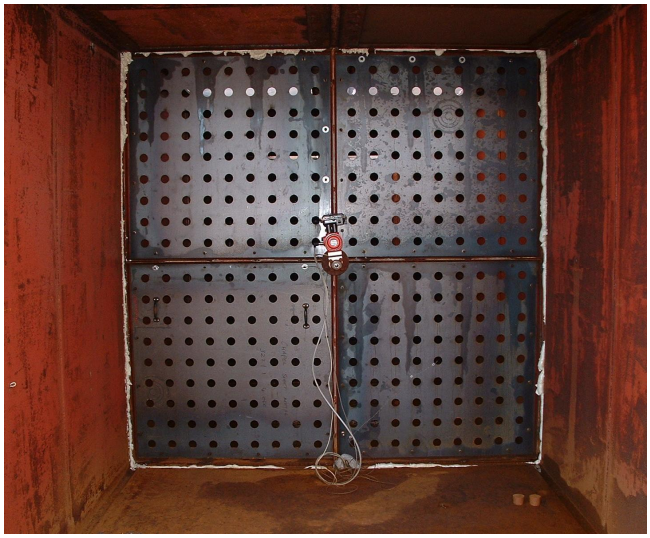

Figure 6.2 Inlet plate with 324 circular holes with 0.05 m diameter

Congestion is provided by means of a cube-shaped cage with a number of small pipes. The cage is constructed from angle iron and has a solid back plate (see Figure 6.3). There are four different cage sizes, see Table 6.1, with the intention of creating fuel-air mixtures with volumes corresponding to 0.1 %, 0.5 % and 1.0 % of the total enclosure volume. The pipes of different diameters are made of PVC or metal and are attached to the cage by metal brackets. The ends are sealed to ensure that no flammable gas mixture can enter the pipes. The pipe diameter scales with the cage size. The pipes are arranged in rows, which are perpendicular to each other and are also offset with respect to every other row. Figure 6.4 shows a plan view of the cage with obstacles.

Table 6.1 Available cage sizes

Cage No.	**Side length [m]**
1	0.25
2	0.45
3	0.8
4	1.0

Two types of test were undertaken. Quiescent tests in which the cage was filled with a homogenous fuel-air mixture (polythene sheets were used to contain the fuel-air mixture in the cage during these tests) and with no air flow through the enclosure. The ignition source (an electric match head) was located in the centre of the back plate. Steady-state tests in which a jet of fuel was directed into the cage (cage sides open) and with an air flow through the enclosure. The resulting fuel cloud was ignited when steady-state conditions were achieved in the cage. For these tests, with a flowing fuel-air mixture, a more powerful ignition source, a chemical ignitor, had to be used.

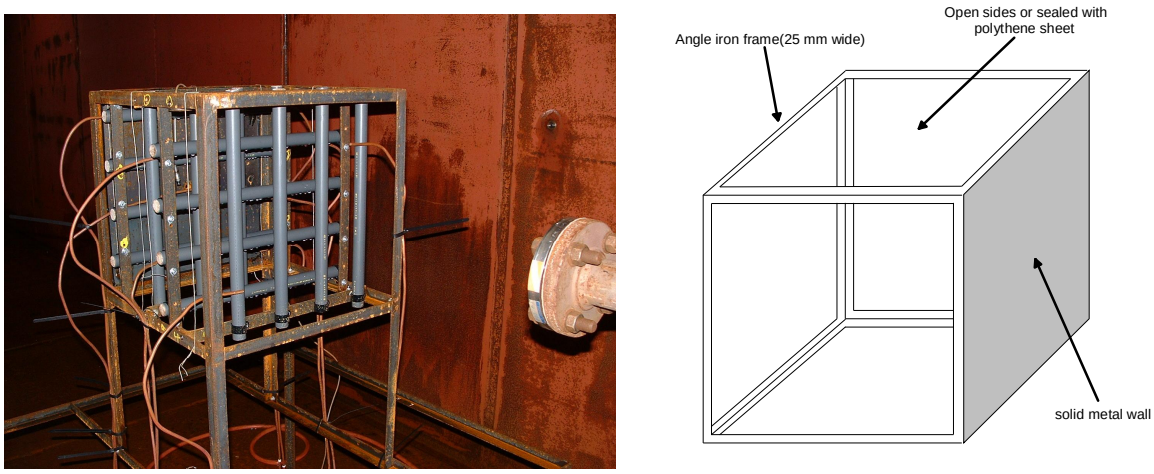

Figure 6.3 Photograph showing the cage (with 0.5 m side) and drawing showing the cage layout

The nozzle used for the steady-state tests is a critical flow venturi type (see Figure6.5 for more details of the type of nozzle used for the methane work). It might be advantageous to manufacture a new orifice plate with smaller diameter in order to be able to operate at high pressures.

Table 6.2 Available pipe dimensions

Pipe No.	***Diameter [m]***
1	0.0125
2	0.025
3	0.05

6.1.2 The test matrix

In all a total of 23 tests were carried out, 5 quiescent tests and 18 steady state.
Ignition tests were carried out in a 93.1 m^3 enclosure with congested volumes of quiescent stoichiometric hydrogen/air mixture at 0.1% and 0.5% of the total enclosure volume. The tests covered two different obstacle arrangements, with different levels of congestion and for comparison tests with no obstacles. Table 6.3 outlines the experimental test matrix. The only experiment not listed in Table 6.3 is the quiescent test, where the cage is wrapped in polythene, filled with a stoichiometric hydrogen-air mixture and the ignited. Tests could be carried out for a range of congestion levels within the cage (by changing the pipe spacing), the enclosure ventilation rate and hydrogen injection rate (steady-state tests only).

Table6.6 Experimental test matrix

		Ventilation Velocity		
		1 m s^{-1}	***2 m s^{-1}***	***4 m s^{-1}***
Mass flow rate kg s^{-1}	1.5e-03	x	x	x
	2.0e-03	x	x	x
	4.0e-03	x	x	x

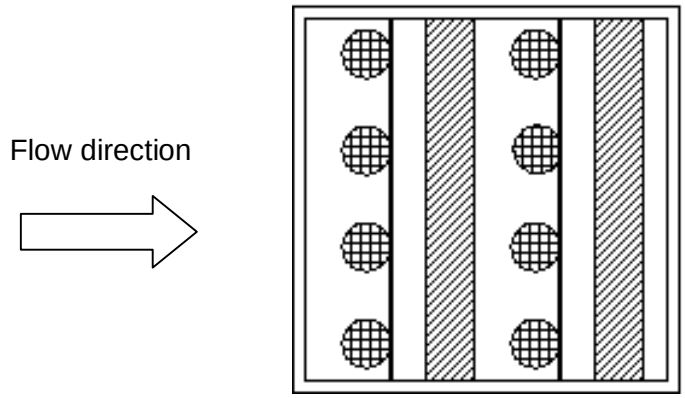

Figure 6.4 Plan view of the cage with obstacles and supports

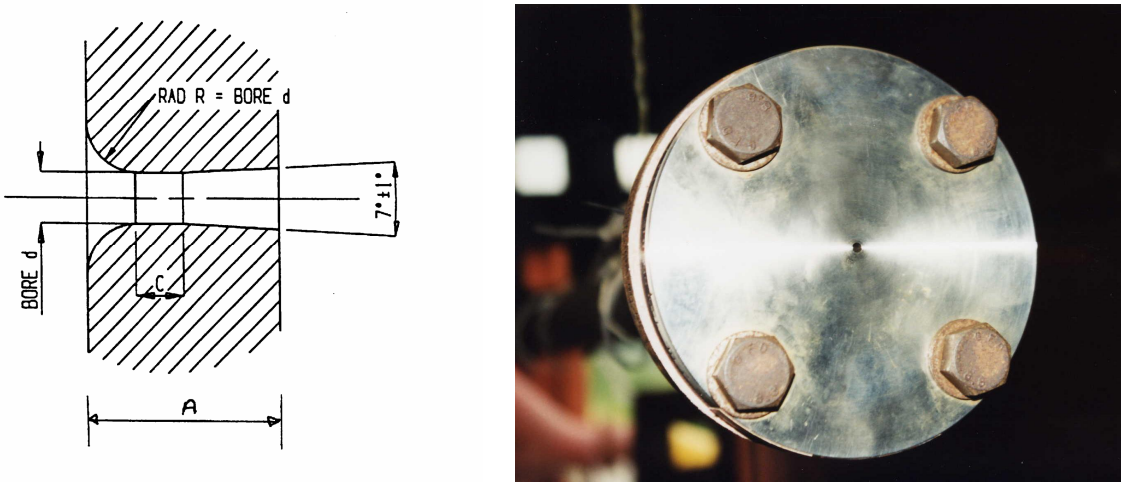

Figure 6.5 Details of the critical flow venturi nozzle, a) schematic drawing of the nozzle with A = 19.1 mm, C = 3 mm and d = 3 mm, b) photograph of the nozzle in-situ

6.1.3 Data output (quantities measured)

Pressure transducers, mounted in the walls of the enclosure, were used to provide measurements of the explosion overpressures generated in the enclosure. Some limited gas concentration measurements inside the cage were also undertaken, by the use of fixed sample probes and oxygen deficiency analysers or fast response electronic sensors. Use of the latter would reduce the length of time the steady-state experiments would have to run.

Note that the hydrogen mass flow rate should be chosen so as to resemble the methane mass flow rate used in the previous set of experiments. This could be 5.5 g s^{-1} to match the number of moles of CH_4 released in the methane tests. The smaller mass flow rates in Table 6.3 roughly corresponds to the mass flow rates that would result from the scenarios identified in the HyTunnel project, but scaled to take

into account that the HSL enclosure is somewhere between 1/3-scale and 1/2-scale of a real tunnel. The exact scale depends on what criterion is used to determine the scale factor. The exact mass flow rates are yet to be determined.

6.1.4 Results summary

For all the 23 tests, 5 quiescent tests and 18 steady state, the pressure-time plots have been processed to give gauge pressure. The time of ignition is 0.164 s from zero time.

Quiescent tests
Tests were undertaken with congested volumes of 0.098%, 0.55% and 1.07% of the total enclosure volume. For each size of congested volume three obstacle arrangements were used, arrangements A and B and also with no obstacles, giving a total of nine different test conditions. However tests with obstacle arrangement B in the 0.55% congested volume caused damage to the enclosure. The damage was repaired but the risk of damage from further explosions was considered to be to high to continue. Table 6.4 gives the peak explosion pressures for three congested volume sizes, and examine the influence of obstacle arrangements A and B with the no obstacle case.

Table 6.4: Peak Explosion Pressures

Congested Volume Size (%)	Obstacle Arrangement	Test No	Maximum Pressure (mbar)				
			Pt097	Pt102	Pt136	Pt137	Pt139
0.098	None	HT002	23.85	28.18	30.3	51.06	24.72
	B	HT003	39.4	37.21	41.84	88.71	41.97
	A	HT004	25.63	27.39	27.75	55.46	24.18
0.55	None	HT005	Over-range	Over-range	110.21	148.57	85.02
	B	HT006	Over-range	Over-range	144.65	224.29	114.59

Steady state tests
The steady-state tests undertaken in the enclosure were limited to a congested volume of 0.098% (0.45 m obstacle cage) of the total enclosure volume with only two obstacle arrangements. To minimise the number of test variables three hydrogen flow rates and three fan speeds were used.

Peak explosion pressures
Tables 6.5 and 6.6 give the peak explosion pressures from each test with obstacle arrangements A and B respectively.

Table 6.5: Peak Explosion Pressures with Obstacle Arrangement A

Hydrogen release rate		Test Number and Peak Explosion Pressure at					
	Air velocity	1 $m.s^{-1}$		2 $m.s^{-1}$		4 $m.s^{-1}$	
	Transducer	No.	mbar	No.	mbar	No.	mbar
1.5 $g.s^{-1}$	Pt097	23	34.5	24	10.3	25	8.7
	Pt102	23	28.2	24	13.6	25	12.1
	Pt103	23	124.2	24	66.6	25	39.5
	Pt136	23	35.3	24	16.1	25	10.9
	Pt139	23	63.5	24	12.6	25	10.5
2.0 $g.s^{-1}$	Pt097	26	35.4	27	23.5	28	10.5
	Pt102	26	32.4	27	23.2	28	14.1
	Pt103	26	123.3	27	117.7	28	53.6
	Pt136	26	42.1	27	28.7	28	13.6
	Pt139	26	55.4	27	39.6	28	14.7
4.0 $g.s^{-1}$	Pt097	29	53.3	30	35.8	31	23.6
	Pt102	29	48.9	30	37.3	31	26.0
	Pt103	29	255.8	30	222.5	31	160.4
	Pt136	29	56.2	30	42.1	31	37.0
	Pt139	29	71.2	30	66	31	39.2

Table 6.6: Peak Explosion Pressures with Obstacle Arrangement B

Hydrogen release rate		Test Number and Peak Explosion Pressure at					
	Air velocity	1 $m.s^{-1}$		2 $m.s^{-1}$		4 $m.s^{-1}$	
	Transducer	No.	mbar	No.	mbar	No.	mbar
1.5 $g.s^{-1}$	Pt097	14	13.6	15	6.3	16	4.4
	Pt102	14	16.2	15	8.8	16	6.0
	Pt103	14	63.4	15	20.6	16	13.1
	Pt136	14	18.1	15	8.3	16	6.0
	Pt139	14	19.6	15	7.5	16	5.0
2.0 $g.s^{-1}$	Pt097	17	30.9	18	24.2	19	13.9
	Pt102	17	27.5	18	25.7	19	20.9
	Pt103	17	106.0	18	66.3	19	39.4
	Pt136	17	33.6	18	27.6	19	21.1
	Pt139	17	46.6	18	46.6	19	25.4
4.0 $g.s^{-1}$	Pt097	20	50.1	21	53.9	22	35.5
	Pt102	20	48.5	21	48.1	22	28.9
	Pt103	20	136.9	21	196.4	22	126.2
	Pt136	20	56.0	21	56.4	22	31.6
	Pt139	20	91.7	21	85.8	22	51.2

Hydrogen concentration measurements

Hydrogen concentrations were measured at four locations within the cage for each obstacle configuration. The samples lines were colour coded red, green, blue and yellow and the numbers in tables 6.7 and 6.8 have corresponding colours.

Table 6.7: Hydrogen concentrations with obstacle arrangement A

Hydrogen release rate	Hydrogen concentration % at					
	1 m.s^{-1}		2 m.s^{-1}		4 m.s^{-1}	
1.5 g.s^{-1}	22.9	23.3	17.0	13.6	12.6	11.2
	24.3	24.3	11.7	16.6	8.6	13.1
2.0 g.s^{-1}	29.7	23.8	19.0	15.1	18.0	13.1
	27.2	27.2	19.9	18.0	13.6	15.6
4.0 g.s^{-1}	44.2	39.9	31.6	26.3	24.8	18.5
	39.9	37.9	28.7	36.4	24.8	22.4

Table 6.8: Hydrogen concentrations with obstacle arrangement B

Hydrogen release rate	Hydrogen concentration % at					
	1 m.s^{-1}		2 m.s^{-1}		4 m.s^{-1}	
1.5 g.s^{-1}	24.3	19.4	18.0	13.1	11.2	9.2
	18.0	22.4	9.7	13.1	5.8	11.2
2.0 g.s^{-1}	31.6	28.3	16.0	15.1	15.6	11.2
	25.8	21.9	13.1	19.4	10.7	13.1
4.0 g.s^{-1}	37.4	29.2	28.7	22.4	22.8	19.4
	33.1	36.5	21.4	23.8	16.5	21.4

6.1.4 The main findings

- In contrast to the results obtained for the quiescent tests with methane, the ignitions with hydrogen generated a non-uniform pressure field throughout the enclosure. Increasing the volume of hydrogen/air mixture increased the maximum explosion pressure, but, unlike the results obtained with methane, increasing the level of congestion did not result in increasing explosion pressures. An initial increase in the congestion level increased the maximum explosion pressures, but a further increase in congestion resulted in a reduction in pressure.

- Maximum explosion pressures for hydrogen in the quiescent ignition tests were of the order of four times higher than the pressures obtained for methane under identical conditions. In addition the pressure traces for hydrogen exhibited marked oscillatory behaviour in contrast to the relatively smooth traces obtained in the methane tests. Full frequency analysis of these oscillations has not been carried out, but the fundamental frequency found in the pressure-time waveform is related to the length of the chamber.

- Ignition tests have been carried out within a ventilated 93.1 m^3 enclosure with a steady state hydrogen leak into a congested volume that is 0.1% of the total enclosure volume. Hydrogen leakage rates of up to 4 g.s^{-1} and ventilation rates of up 1500 m^3.min^{-1} were used. Explosion pressures were measured at the same locations as in the quiescent tests. The obstacle arrangements used were the same as those used in the quiescent ignition tests.

- In the steady state ignition tests the maximum explosion pressures increased with increasing leakage rate and decreased with increasing ventilation rate. Explosion pressures were similar in magnitude to those obtained in the quiescent tests and were also non-uniform throughout the enclosure.

- The trend in maximum explosion pressure with the level of congestion depended on hydrogen leakage rate. At the lowest leakage rate the more congested configuration gave the highest explosion pressures. While for the highest leakage rate the less congested configuration, except at the lowest ventilation rate, gave the highest explosion pressures.

- Hydrogen concentration measurements have been made within the congested volume under the same conditions as the steady state ignition tests. These measurements have shown the expected trend. Increasing leakage rate leads to increased hydrogen concentration. While increasing the ventilation rate reduces the hydrogen concentration. Increasing the level of congestion also increases the hydrogen concentration.

The above findings of the HSL experiments have following implications to the safety of hydrogen powered vehicles in tunnels:

- Significant levels of overpressure can be generated in confined or semi-confined spaces, by the ignition of a hydrogen-air mixture filling only a small fraction, of the order of a few percent, of the space. These could be high enough to cause damage to tunnel services, e.g. ventilation ducting.

- For larger percentage fills of hydrogen-air mixture, the possibility of DDT cannot be ruled out.

- Hydrogen explosions are more prone to produce an oscillatory pressure-time profile than hydrocarbon explosions, which may have implications for the response of structures subjected to a hydrogen explosion

6.2 FZK experiments [77]

The objective of FZK experiments were:

- to examine high-speed deflagrations in stratified hydrogen layers, akin to that which might be found under a tunnel ceiling, and
- to obtain critical conditions defining the possibility of the self-sustained detonation in flat mixture layers.

6.2.1 Description of Experiments

In the work presented here, two series of experiments with high-speed deflagrations in flat hydrogen-air mixture layers are described, a summary of them follows next.

Preliminary experiments

In total nine preliminary experiments were performed in a small scale facility having the dimensions of 1.5 m x 0.5 m x 0.4 m (L x W x H). The first two preliminary experiments were conducted without any channel obstructions while in the later experiments an acceleration section, consisting of a large number of thin metal grids piled up in longitudinal direction, was installed close to the ignition end of the channel. Table 6.9 summarises the initial conditions for hydrogen concentrations for all the preliminary experiments. The first two preliminary experiments without hydrogen were performed to check the experimental procedure and the triggering of the data acquisition system. In all these experiments, a commercially available spark plug was used to ignite the mixtures.

Main experiments

In total ten main experiments were performed in a wide large rectangular channel having the dimensions of 5.7 m x 1.6 m x 0.6 m, using layer heights of 0.15, 0.3 and 0.6 m and hydrogen concentrations in the range of 15 to 25 Vol.-% H_2. Figure 6.6 shows the main experimental facility used, where the rectangular channel was opened from below. One additional experiment was conducted in advance to check the experimental procedure with the destruction of the film and the subsequent ignition, as well as the triggering of the data acquisition system. The test matrix used for the main experiments is shown in Table 6.10.

Table 6.9: Test matrix for the preliminary experiments.

Experiment Number	c(H_2) [Vol.-%]	Acceleration section
HT01	0	-
HT02	0	-
HT03	15	-
HT04	15	-
HT05	20	-
HT06	25	-
HT07	15	+
HT08	20	+
HT09	25	+

The main experiments were either performed in the unobstructed channel or with the channel being equipped with an acceleration section and further obstacles with an effective blockage ratio equal to 60%. Both presented series included variations of the hydrogen concentration in H_2-air mixtures, whereas only in the main experiments additionally the layer thickness was altered. A high frequency spark generator was used to ignite the mixture inside the large scale facility. Hydrogen concentration was maintained uniform throughout the facilities at the level of non-uniformity not more than 1 Vol.-% H_2. The experiments were equipped with pressure transducers (only main experiments), ion probes, light sensors, and high-speed photography. The sequence of frames obtained from high-speed photography was processed using 'background-oriented schlieren' method with the aim to provide visualization assistance of the flame propagation process.

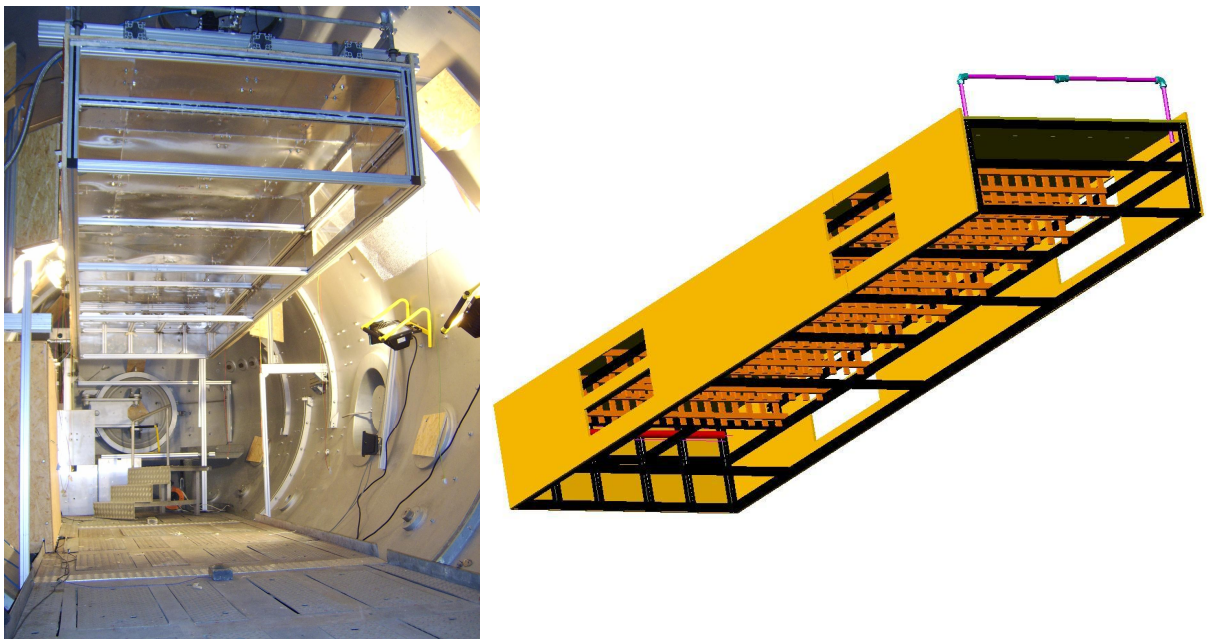

Fig. 6.6: Photograph and sketch (with obstacles) of the main experimental facility.

6.2.2 Summary of Results

All experiments in the unobstructed channel led to slow flame propagation regimes, with a maximum flame velocity of approx. 33 m/s. In the experiments with the obstructed channel three different combustion regimes could be distinguished according to the records of the sensors installed to the facility. The results are summarised in Table 6.11.

Two fields in the matrix above could not be covered by experiments since the facility was destroyed in experiment HLT10 with a layer height of 0.3 m and a hydrogen concentration of 25 Vol.-% H_2. But following the trend detected during the experiments one can assume that for a layer height of 0.6 m and a hydrogen concentration of 20 Vol.-% H_2 a fast Deflagration and for a layer height of 0.6 m and a hydrogen concentration of 25 Vol.-% H_2 a detonation would have been observed.

Preliminary assessments gave a value for the critical layer thickness for a DDT (Deflagration-to-Detonation-Transition) event in the range of 7 - 20 detonation cell widths. With the results obtained from the experiments in the facility described, this value can be identified in the closer range from 7.5 to 15 times the detonation cell width.

The results of the full scale FZK experiments have highlighted the hazard posed by the explosion of hydrogen-air mixture in a tunnel. The results have indicated that DDT is, in principle, possible in the confined space of a tunnel. Consequently, ceiling design and mitigation measures may be important. Note that the obstructions in the tunnel ceiling could add some turbulence to flame propagation and make explosions more severe.

Table 6.10: Test matrix for the main experiments.

Experiment Number	Height of layer □ [m]	c(H_2) [Vol.-%]	Obstruction BR [%]
HLT00		0	-
HLT01	0.30	15	-
HLT02	0.30	17.5	-
HLT03	0.30	25	-
HLT04	0.30	15	60
HLT05	0.30	20	60
HLT06	0.60	15	60
HLT07	0.15	15	60
HLT08	0.15	20	60
HLT09	0.15	25	60
HLT10	0.30	25	60

Table 6.11: Summary of the experimental results conducted in the obstructed experimental facilities.

Small scale				Large scale				
		Layer height □ [m]				Layer height □ [m]		
		0.40				0.15	0.30	0.60
c(H_2) [Vol.-%]	15	**slow Deflagration**		c(H_2) [Vol.-%]	15	**slow Deflagration**	**slow Deflagration**	**fast Deflagration**
	20	**fast Deflagration**			20	**fast Deflagration**	**fast Deflagration**	***(fast Deflagration)***
	25	**Detonation**			25	**decaying Detonation**	**Detonation**	***(Detonation)***

CHAPTER 7 – HYTUNNEL COMPUTER MODELLING WORK

7.1 Introduction

A computer modelling activity, using Computational Fluid Dynamics (CFD), has been conducted in support of the HyTunnel internal project. Simulations have been performed by GEXCON [72], WUT [78] and UU [79,80], using as a starting point the tunnel accident scenario description developed by the HyTunnel partners in the first phase of the project and presented below in Section 7.2. An additional 'bridge scenario', representative of an urban underpass with exposed beams at ceiling level, has been examined also, and is discussed in Sections 7.3 and 7.4.

The aim of the computer modelling activity was to extend our understanding of the consequences of accidents inside road tunnels resulting in the release of hydrogen from hydrogen powered (H2) vehicles. This addressed two aspects of the problem; Firstly, the dispersion of the released hydrogen within the tunnel, as a result of the activation of a pressure release device (PRD), and secondly the result of an explosion involving the dispersed hydrogen. Other aspects of the problem, arguably as important as those investigated, have not been addressed in the HyTunnel computer modelling activity. These include, for example, the consequence of an ignited high pressure jet of hydrogen, which may promote fire spread between vehicles as the jet flame propagates along the tunnel.

Sections 7.4 to 7.6 summarise the individual contributions of the three organisations that have presented results of their CFD modelling activities for the main tunnel scenarios. Section 7.4 (GEXCON) also includes results from the simulations for the 'bridge scenario', and discusses limitations of the Q9 methodology for the risk analysis. Section 7.7 summarises the collective findings from the CFD modelling work.

It is important to emphasise that results from the numerical modelling have not be used in isolation. Rather, they have been fed into a probabilistic risk assessment looking at the wider picture, and taking into account the probabilities of the various events.

7.2 Description of the Tunnel Accident Scenarios selected for CFD Analysis

A provisional description the proposed set of traffic/accident scenarios and tunnel geometry/ventilation arrangements to be investigated by computer modelling was presented in HySafe Deliverable 62. This was revised further prior to the CFD and associated probabilistic risk analysis by GEXCON, and is presented below.

The scenarios included were not intended to represent an exhaustive set of possible accidents, but instead to allow an attempt to quantify the hazard that may be posed by the release of hydrogen from H2 powered vehicles inside natural and longitudinally ventilated tunnels. The hazard is from the ignition (and possible explosion) of a dispersed cloud of hydrogen following its accidental release (or designed release following an accident, e.g. due to a PRD operating).

The CFD study has focussed on two-lane, single bore tunnels with cross-section in the range 50 to 60m^2. Furthermore, it has been assumed that traffic flow is unidirectional. It is assumed that following an incident, all the vehicles remain upright and in the direction of travel, and the spacing between all vehicles is maintained.

Longitudinal ventilation along the tunnel, in the direction of traffic flow, has been considered (with no ventilation as a limiting case). This is a common method of ventilation in road tunnels, especially urban tunnels and where unidirectional traffic flow is present (as reported in HySafe Deliverable 49). While transverse and semi-transverse ventilation is also found in road tunnels, it should be noted that in this case the air flow locally is often predominantly longitudinal in nature. Furthermore, the 'piston effect' of the traffic or the influence of external atmospheric conditions may generate a longitudinal air flow. The tunnel walls and ceiling are assumed to be smooth with no obstructions present. Ambient conditions of 1 bar pressure and a temperature of 20°C were assumed.

The hydrogen release is assumed to be due to the activation of a PRD resulting in the emission of the entire contents of the cylinder/tank (or group of cylinders/tanks). The activation could be as a result of thermal conditions (e.g. as a consequence of a fire), as a consequence of an impact or due to a component failure.

Tunnel geometries

Two geometry cross-sections were considered:

a) "Horseshoe" (arched) tunnel with radius 5.1 m and circular cross-section of approximate area 60 m^2 as shown in Figure 7.2.1a.

b) "Rectangular tunnel", using a simple box profile and rectangular cross-section area of approximately 50m^2 (10 m wide and 5 m high) as shown in Figure 7.2.1b.

In both cases the length of the tunnel was 500m, with the hydrogen release located mid-way along the tunnel.

Vehicle parameters

Three hydrogen powered vehicles were considered; a compressed hydrogen gas (CGH_2) fuel cell city bus, a CGH_2 fuel cell car and a liquid hydrogen (LH_2) internal combustion engine car. These technologies are described in Chapter 4. Specific details for the modelling study are provided below. Comparative simulations for the release of compressed natural gas (CNG) from a car and a city bus have been conducted.

a) **CGH_2 city bus**. The description was taken from the work of the EIHP-2 project, i.e. a representative city bus with roof mounted compressed gas fuel tanks housing a total 40 kg of hydrogen in 8 cylinders (in two sets of four cylinders) – 5 kg per cylinder at a storage pressure of 350 bar. The hydrogen storage arrangement is shown in Figure 7.2.2. The length and width of the bus were 12.0 m and 2.55 m respectively and its height 2.9 m, with the distance to the top of the tanks being 3.1 m. The bus specification was similar to the one used in the CUTE project The vehicle was approximated in the CFD modelling as a rectangular block of dimensions 12.0 m by 2.55 m by 2.9 m as shown in Figure 7.2.3. The hydrogen release location was similar to the one used in the EIHP-2 project, illustrated in Figure 7.2.4.

b) **CGH_2 (fuel cell) car.** An inventory of 5 kg hydrogen is stored in one cylinder at a pressure of 700 bar. The car was approximated as a simple rectangular block (5.0 m $\times$ 1.9 m $\times$ 1.5m) located 0.3 m above the ground.

c) **LH_2 (internal combustion engine) car**. An inventory of 10 kg of liquid hydrogen was assumed.

Both the cars were approximated as shown in Figure 7.2.5. For each car, the release of hydrogen was from a height above ground of 1 m at the rear corner of the vehicle.

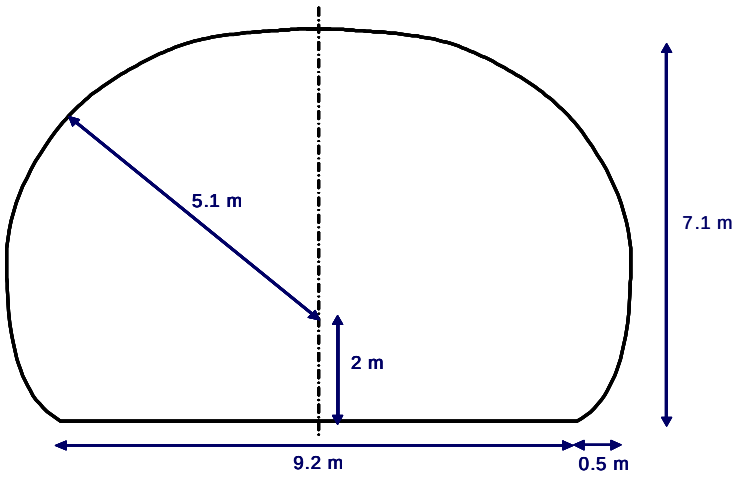

(a) Horseshoe cross-section tunnel (Cross-section area = 60 m^2)

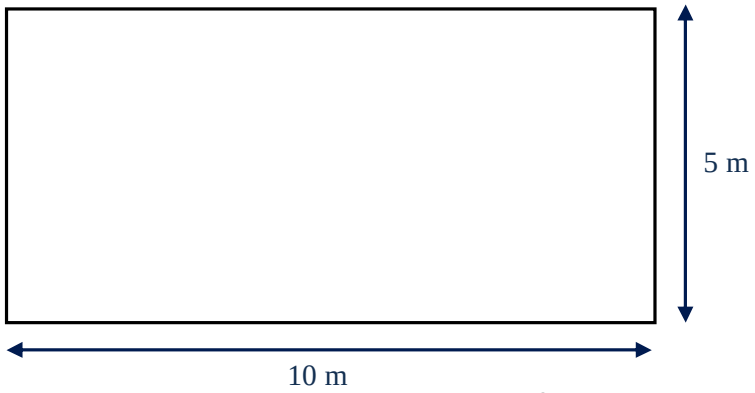

(b) Rectangular cross-section tunnel (Cross-section area = 50 m^2)

Figure 7.2.1 Tunnel cross-sections

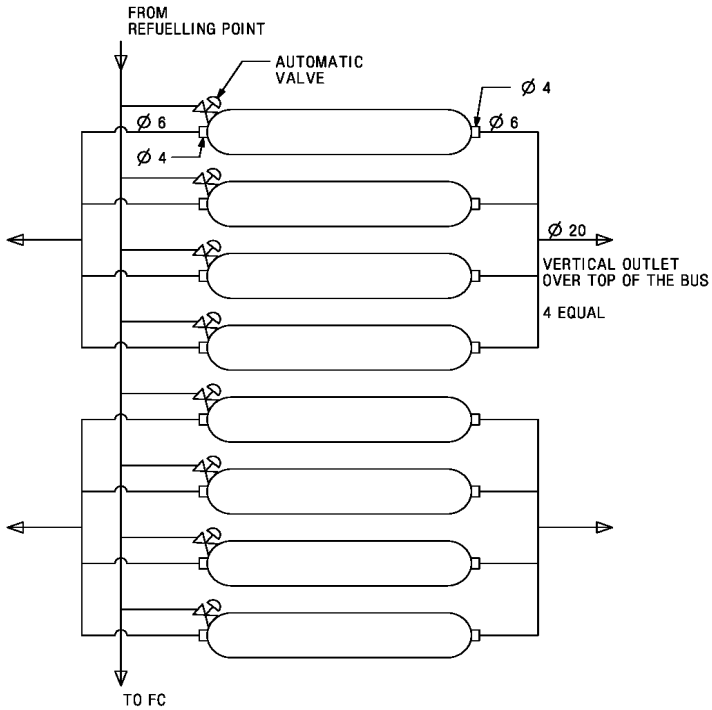

Figure 7.2.2 CGH_2 storage arrangement for city bus

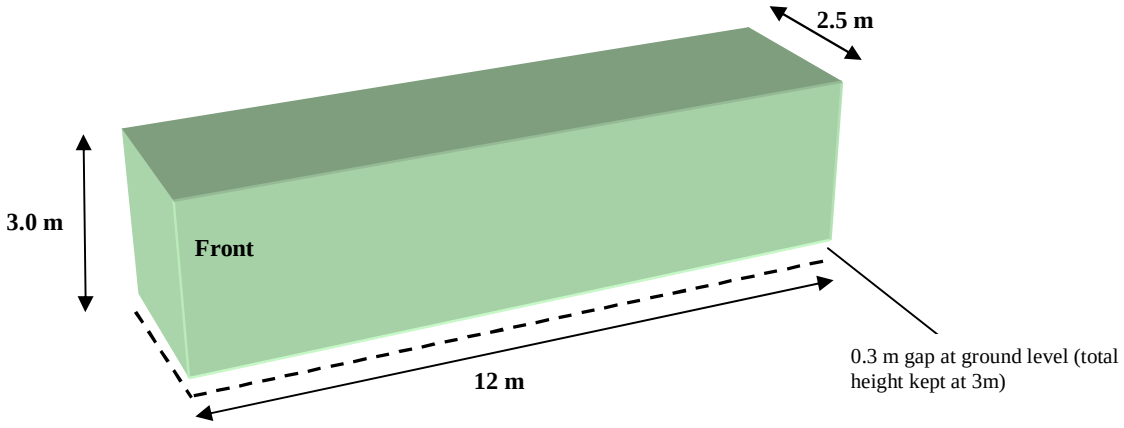

Figure 7.2.3 Schematic of CGH_2 Bus

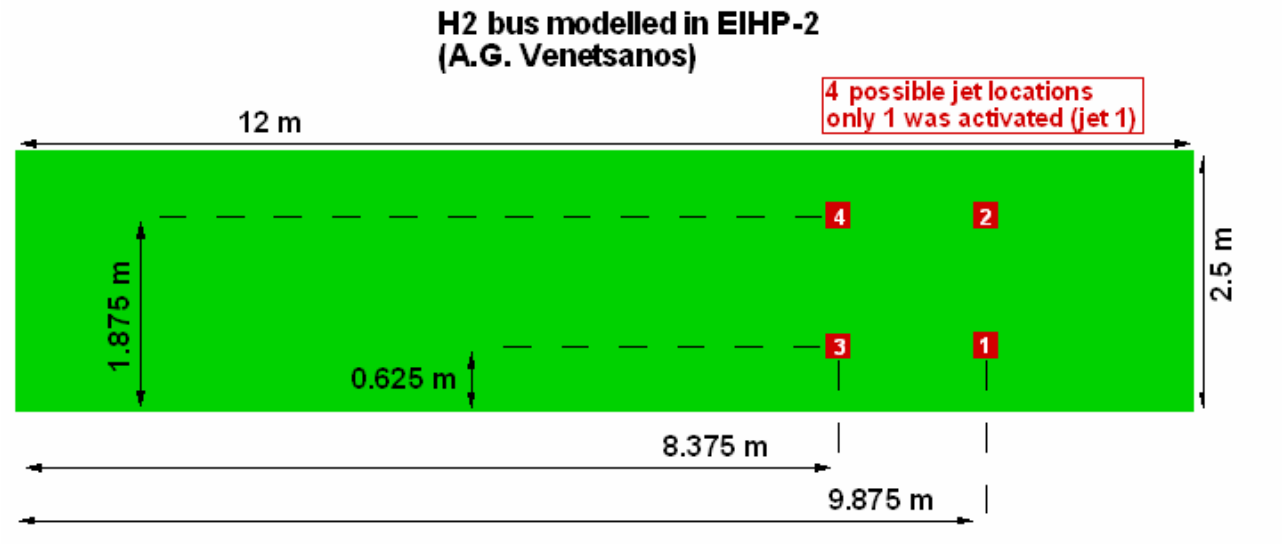

Figure 7.2.4 Hydrogen release location for city bus

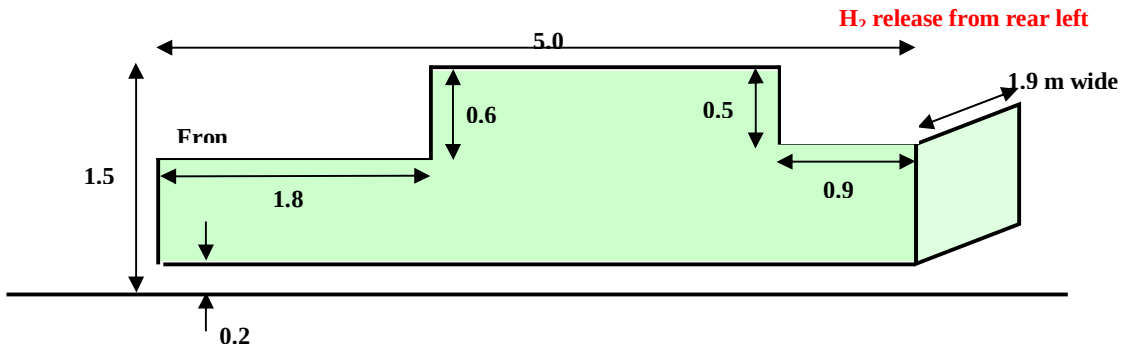

Figure 7.2.5 Simplified geometrical representation of CGH_2 and LH_2 car

For comparative purposes the following CNG vehicles have been considered (assuming the same geometry as the hydrogen car and bus):

a) City bus where 104 kg of natural gas stored at a pressure of 200 bar is released. It is assumed that the release occurs from a set of four cylinders with, each containing 26 kg.

b) Car where 26 kg of natural gas stored at a pressure of 200 bar is released.

Traffic parameters

A dual-lane tunnel with traffic running in a single direction was assumed. Both lanes were assumed to be fully filled by a regular pattern of buses and cars spaced 1.5m apart, with six cars for each commercial vehicle. The pattern was such that there was a bus in the middle of the tunnel in one direction, and a car in the middle of the tunnel in the other direction. The incident location was assumed to be in the centre of the tunnel.

Figure 7.2.6 and Figure 7.2.7 show the traffic (stationary) arrangements (plan view) for the car and bus release scenarios.

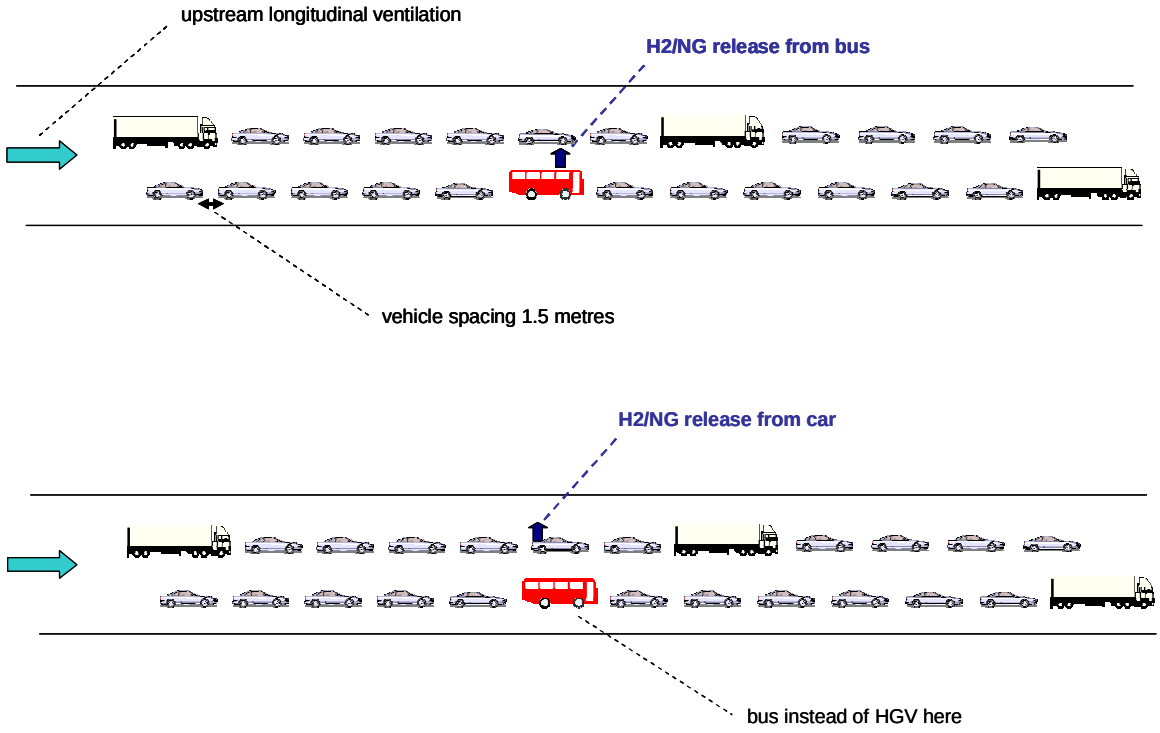

Figure 7.2.6 Traffic arrangements (schematic diagram)

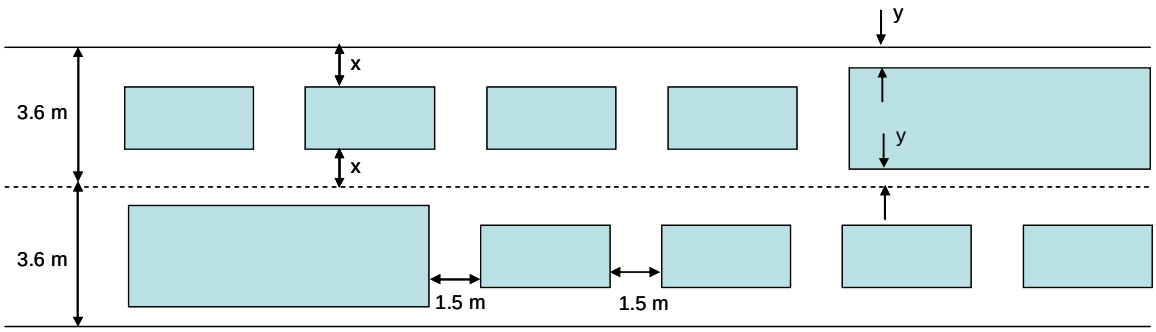

Figure 7.2.7 Traffic arrangements across tunnel (not to scale)

Release and dispersion

The release scenarios included in the study are listed in Table 7.1. All releases were taken to be from the centre of the tunnel, with a release height of 3 m for the bus and 1 m for the cars (upward and downward cases).

For the LH_2 car the 10 kg of hydrogen is released through a 20 mm nozzle during a period of 15 minutes.

For the compressed gas releases a sonic release velocity was assumed. Release profiles were calculated for a 100 litre (700 bar) or 200 litre (200 bar or 350 bar) gas bottle with a 4 mm opening for hydrogen and 6 mm for natural gas. In both cases a discharge coefficient of 0.8 was assumed (at a temperature of 10°C). These are presented in Figure 7.2.8. Note that the worst-case scenario considered has a hydrogen release rate four times higher than the release rate shown from a 350 bar tank due to the simultaneous release from four bottles. Also, to be conservative, it has been assumed that the cylinders are full when the incident occurs. The release profiles are used as a boundary condition for dispersion simulations. It must be pointed out that the durations for hydrogen releases in the table below are based on the time it takes for the release rate to drop below 1 g/s. It can be seen that the release rates are significantly over-predicted if an ideal gas model is considered for high-pressure hydrogen releases.

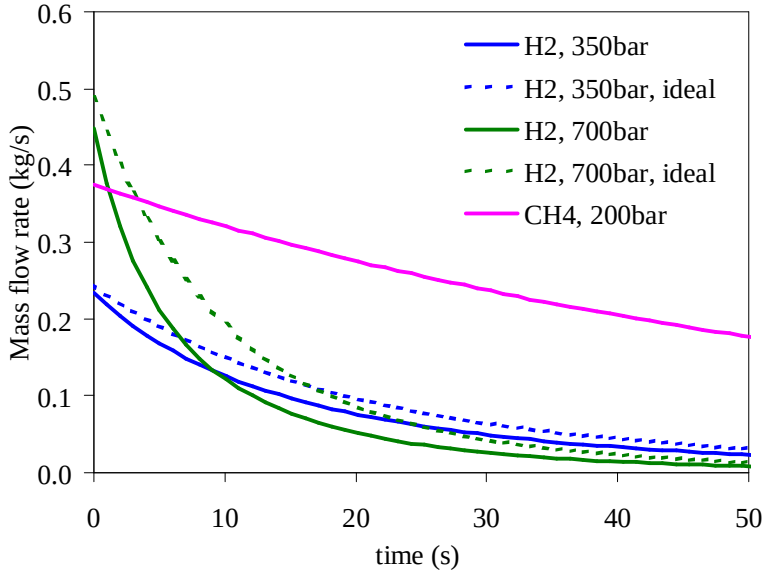

Figure 7.2.8 Release profiles for compressed hydrogen and natural compressed gas releases -including differences due to real gas effects at high pressures

Ventilation regimes

Longitudinally ventilated tunnel scenarios were studied, in which the ventilation depends on the external atmospheric conditions and the operation of impulse fans. The following longitudinal ventilation rates have been considered:

a) **0 ms^{-1}.** This is simply the limiting case of no forced or natural ventilation. It is the case studied in the EIHP-2 project. It may represent a hazardous condition for an un-ignited hydrogen release, as lack of forced airflow will result in minimal dilution of the gas. However, this case will also result in limited dispersion of the hydrogen cloud.

b) **2 ms^{-1}.** This represents a typical velocity found in naturally ventilated tunnels.

c) **3 ms^{-1}.** This represents a typical value required to control the movement of heat and smoke from a vehicle fire inside a tunnel, i.e. to eliminate the presence of back-layering so that the fire products are all forced in the direction of air flow, allowing egress in the opposite direction and easy access for the emergency services.

d) **5 m^{-1}.** This tends to be the high level of recommended air speeds inside a tunnel. It is useful to examine a higher ventilation level, as there may be benefits in terms of diluting a released hydrogen cloud so that the explosion risk is minimised. Furthermore, a high level of ventilation has been shown to be beneficial in diluting smoke and toxic gases following a fire or other incident (but conversely may promote fire spread and rapid smoke transport).

7.3 Description of the 'Bridge' Accident Scenarios selected for CFD Analysis

In order to address some of the questions left unanswered by the CFD simulations for the main tunnel scenarios, additional simulations have been performed for a wide bridge scenario where realistic ceilings have been used instead of the smooth ceiling assumption used in the tunnel studies. This was expected to have a significant influence on the results as hydrogen gas could be expected to collect between beams and other support structures and fittings. These structures may also act as 'turbulizers' and contribute to flame acceleration and higher overpressures.

The scenario considered is a hydrogen release from a bus travelling in an underpass below a highway. No other vehicles are assumed to be present except the hydrogen bus. It is also assumed that the bus remains upright after the incident. Ambient Conditions of 15 °C temperature and 1 bar pressure are assumed. Quiescent atmospheric conditions (no wind) are assumed and no mechanical/background ventilation is present.

The geometry was defined as follows (note that the origin 0, 0, 0 is at the tunnel corner) and illustrated in Figure 7.3.1:

a) Underpass length (Y) = 42m, width (X) = 15m and height (Z) = 6m;

b) 0.8m (Z) deep I-beams located every 3m in the Y direction (1cm (Y) thick web with 50cm (Y) ends) (shown in red);

c) Stiffeners on each beam on both sides of web at cross-bracing positions and mid-way between braces (shown in blue);

d) Cross bracing at supports, mid-span, and quarter-span (shown in blue);

e) Bus is at position 8m (X), 10m (Y), 0m (Z) with width of 2.55m (X), length of 12m (Y) and height to top of the tanks of 3.2m (Z). The spacing under the bus is 30cm (the wheels are 80cm diameter and 40cm long (X);

f) Light armature: 4m (Y) x 0.4m (X) x 0.2m (Z) located at a height of 5m (shown in yellow);

g) Armature units located every 2.5m in the width (X) direction (with first one at 2.3m) and every 8m in the length (Y) direction (with first one at 3m).

More details on stiffeners and bracings are presented in Figure 7.3.2.

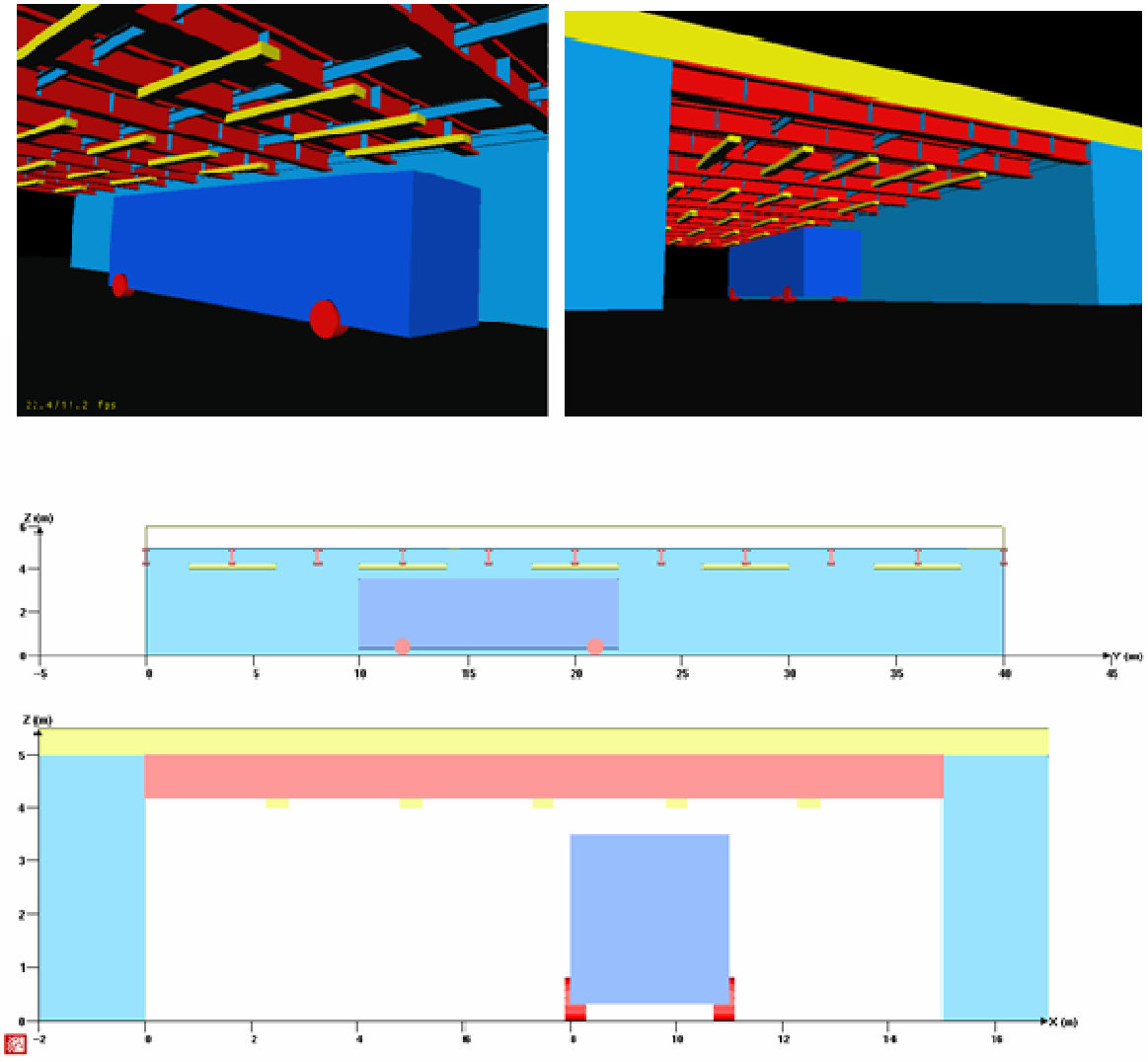

Figure 7.3.1 Snapshots of the bridge geometry

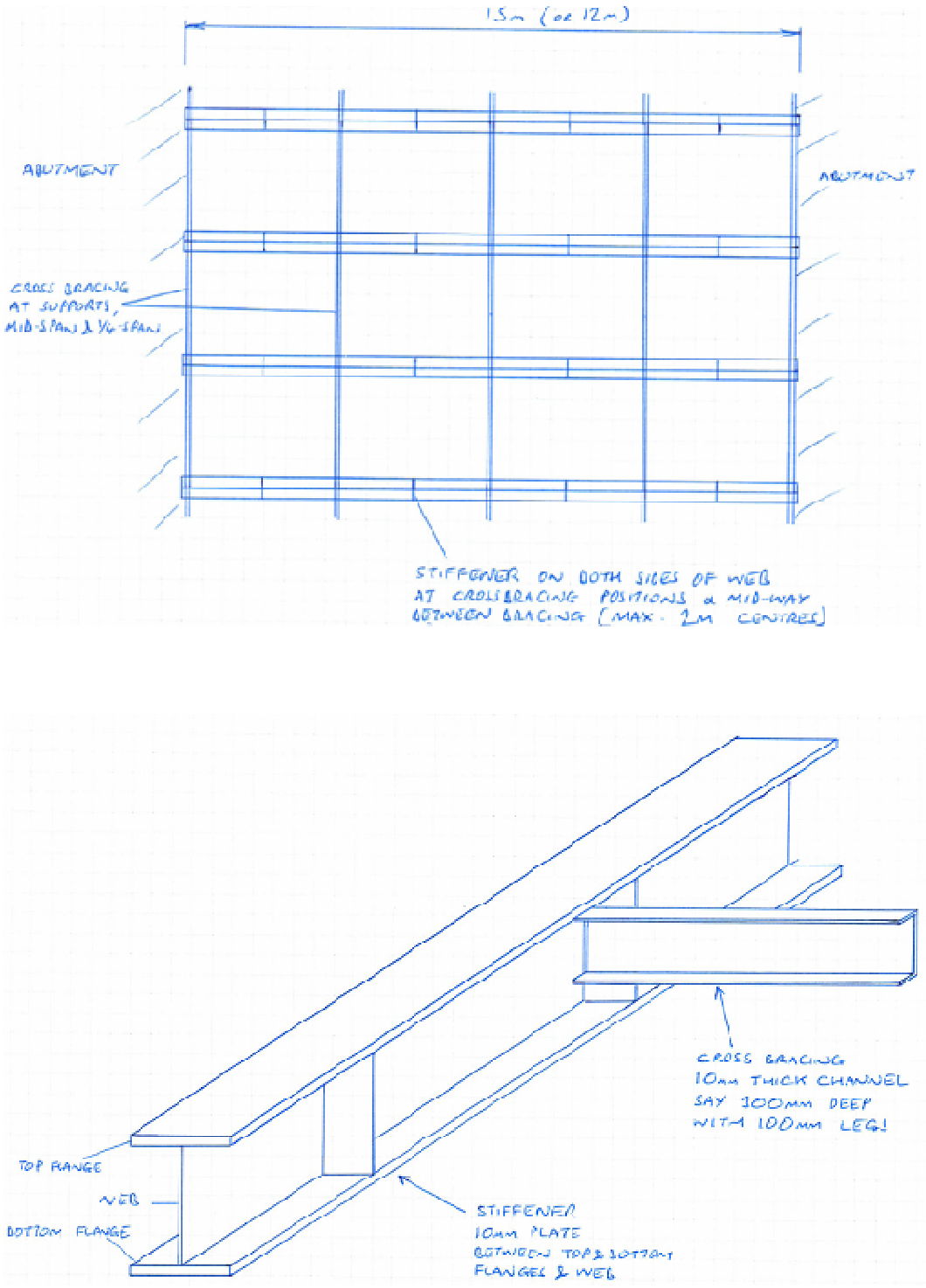

Figure 7.3.2 Stiffeners and bracings for the bridge geometry

Dispersion modelling scenarios

A mass of 20 kg of hydrogen (contained in four CGH2 tanks at a pressure of 350 bar and at ambient temperature) is released from four PRDs into a 20 mm vent line as illustrated in Figure 7.3.3.

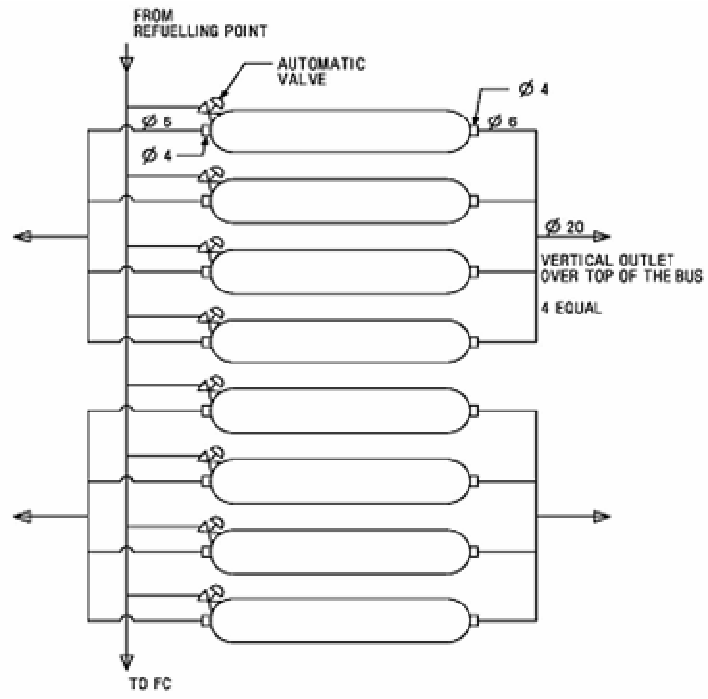

Figure 7.3.3 Hydrogen release from tanks

The release is directed upwards from a location of (9m, 20m, 3.3m). Based on the above information the diameter of the expanded jet (based on Birch notional nozzle concept) is 12 cm (6 cm for a 1 cylinder release).

Four separate cases were considered, and are listed in Table 7.3.1 The base case (scenario 1) involved the release of 20 kg hydrogen upwards as described above. The first sensitivity case (scenario 2) involved moving the release position such that the jet hits a lighting armature. The second sensitivity case (scenario 3) studied the effect of changing the ceiling to one that was completely smooth. The last case (scenario 4) studied the effect of the total mass of hydrogen released (and also initial release rate) by presuming only one hydrogen tank emptied (5 kg hydrogen released).

Table 7.3.1 Dispersion scenarios and sensitivity analyses for the bridge study

#	Simulation	Type
1	20 kg released from a tank with pressure 350 bar (position 9m, 20m, 3.3m)	Base Case
2	Jet hits light armature (move release to 10m, 20m, 3.3m)	Sensitivity 1
3	Original release location Define flat ceiling at z=5m (move sensors to 4.8m)	Sensitivity 2
4	5 kg H_2 (1 tank) released Original geometry and release point	Sensitivity 3

7.4 GEXCON Study using FLACS and the appraisal of Q9 methodology by UU for risk analysis

Description of the simulation tool FLACS

All the simulations for the scenarios described above have been carried out using the CFD code FLACS. FLACS is a computational fluid dynamics (CFD) code that solves the compressible Navier-Stokes equations on a 3-D Cartesian grid. Second order schemes (Kappa schemes with weighting between 2^{nd} order upwind and 2^{nd} order central difference, delimiters for some equations) are used to solve the conservation equations for mass, impulse, enthalpy, turbulence and species/combustion. A "beta" flame model is applied in which the reaction zone becomes 3-5 grid cells thick. The burning velocity is primarily controlled by diffusion of reaction products. A flame library decides the laminar burning velocity as function of gas mixture, concentration with air, pressure, temperature, oxygen concentration in air and more. Initial "quasi-laminar" flame wrinkling will increase the burning velocity with distance. With increasing turbulence a turbulent burning velocity will replace the quasi-laminar. All flame wrinkling at scales less than the grid size is represented by sub-grid models, which is important for flame interaction with objects smaller than the grid size. FLACS uses a standard k-ε model for turbulence. However, some modifications are implemented, the most important being a model for generation of turbulence behind sub-grid objects and turbulent wall functions.

Q8 and Q9 methodologies for risk analysis

The work performed by GexCon not only involved CFD calculations to evaluate the consequences of a potential incident, but also determination of an associated risk with hydrogen vehicles in tunnels. In order to illustrate the risk analysis, methodologies to calculate the equivalent stoichiometric gas cloud (Q8 and Q9) were used. These methodologies [81] were originally developed in the oil and natural gas industry for carrying out quantitative risk assessment (QRA) by estimating an equivalent stoichiometric gas cloud volume with comparable dispersion and explosion consequences. The size of the equivalent stoichiometric cloud at the time of ignition is calculated as the amount of gas in the flammable range, weighted by the concentration dependency of the flame speed and expansion.

For a scenario of high confinement, or a scenario where very high flame speeds (faster than speed of sound in cold air) are expected (either large clouds or very congested situations), only expansion based weighting is used, *Q*8 equivalent cloud volume is defined as:

$$Q8 = \sum V \times E \,/\, E_{\text{stoich}},$$

where, V is the flammable volume, E is volume expansion caused by burning at constant pressure in air, and the summation is over all control volumes.

For most situations lower flame speeds are expected and the conservatism can be reduced. Consequently, the Q8 methodology is modified to include a weighting of reactivity and expansion, which is referred to as *Q*9 methodology. The expression for the Q9 equivalent cloud volume is of the form:

$$Q9 = \sum V \times \mathrm{BV} \times E \,/\, (\mathrm{BV} \times E)_{\text{stoich}},$$

where, BV is the laminar burning velocity (corrected for flame wrinkling/Lewis number effects). Thus, *Q*9 cloud is a scaling of the non-homogeneous gas cloud to a smaller stoichiometric gas cloud that is expected to give similar explosion loads as the original cloud (provided conservative shape and position of cloud, and conservative ignition point). As a practical guideline, it is recommended to choose the shape of the cloud that will give maximum travel distance from ignition to end of cloud for smaller clouds. For large r clouds, end ignition scenarios with longer flame travel should also be investigated.

This concept is useful for QRA studies with several simulations, and has been found to work reasonably well for safety studies involving natural gas releases [82]. This concept has also been applied to hydrogen systems for the FZK workshop experiments [72] and has been found to give reasonably good predictions.

The application of the Q9 methodology for the quantitative risk assessment of hydrogen cloud for the dispersion and explosion scenarios described earlier is presented below.

Verbecke and Molkov [80] have undertaken appraisal of Q9 methodology [81]. They have first compared the performance of Q9 methodology against the experimental data on jet explosions [76, 77]. Then, they have questioned the applicability of such methodology for such high-momentum hydrogen jet explosions.

Their comparison of overpressures for several full-scale experiments obtained by exploding a non-uniform hydrogen-air cloud and its stoichiometric equivalent volume (Q9 methodology) show that a discrepancy between the two methodology falls into the range –32 % to +92%, thereby emphasizing that Q9 methodology may appear "conservative" in some cases or "not conservative" in other cases (see Figure 7.4.1 for illustration). Q9 methodology was also applied to hydrogen systems for the FZK workshop experiments [77]. By comparing simulated and Q9-based overpressures, Q9 methodology under predicts by up to -38%, whereas in other cases it over-predicts by up to 92%. However, according to GexCon, this methodology is not expected to bound every single scenario but provide representative results overall.

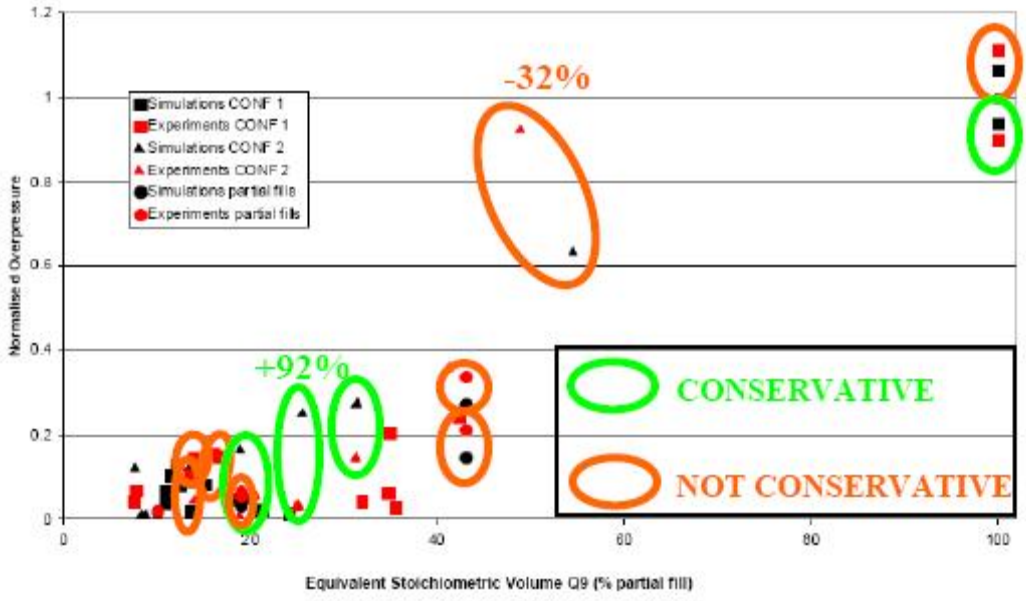

Figure 7.4.1 Comparison of FLACS predicted overpressures as a function of equivalent cloud size with HSL large-scale experiments (Phase 3B project)

Pre-ignition turbulence is also seen to have a large effect. This is confirmed by results obtained by Tanaka et al. [83] and Takeno et al. [84] which indicate that, for high-momentum hydrogen jet explosions, the turbulence on ignition has a greater pressure effect than does the total amount of fuel released or the volume of the dispersed cloud. For example, experimental data obtained by Takeno et al. [84] for a hydrogen jet released through 10 mm diameter orifice release at 400 bar constant pressure show that by increasing the ignition delay from 0.85 s to 5.2 s (ignition source was located at distance 4 m from the nozzle) the maximum explosion overpressures in the near field (about 2 m) decrease from 90 kPa to 15 kPa, i.e., a factor of 6 difference in pressure.

Recent experimental results of unconfined jet explosion released through a 6.4 mm diameter orifice at 200 bar pressure carried out by HSL during HYPER project confirm the previous findings [85]. Figure 7.4.2 shows that the maximum experimental overpressure reaches 20 kPa when the jet is ignited at 600

ms, a factor 1.65 lower at 1 s and about a factor 2 lower (10 kPa) at 2 s (blue curve). The increase of the equivalent stoichiometric cloud with time (see red line in Figure 3) suggests that higher maximum overpressures are expected at 1 s than at 0.6 s. Therefore, it appears essential to consider pre-ignition turbulence when calculating overpressure based on equivalent stoichiometric, otherwise, Q9 methodology would give opposite to observed physical phenomena: overpressure would increase with ignition delay from 0.5 s to 1 s. The pre-ignition turbulence can be easily included while applying Q9 methodology..

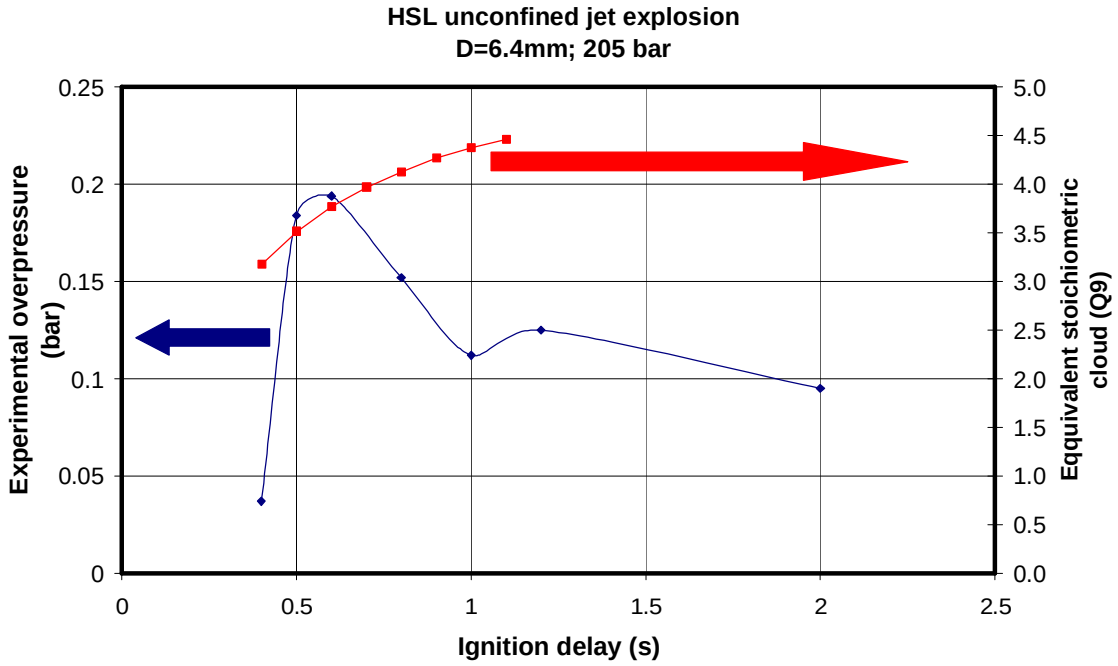

Figure 7.4.2: HSL unconfined jet explosion with nozzle diameter D=6.4 mm under 205 bar pressure ignited at 2 m form the release source [86].The blue curve represents the maximum experimental overpressures (Y-axis on the left) as a function of ignition delay. The red curve represents the evolution of the equivalent stoichiometric cloud (Y-axis on the right) with time calculated from RANS simulations by UU [79].

The effect of jet turbulence is also confirmed in the tests carried out by Shell. Shirvill et al. [86] compared the overpressure and impulse of the explosion of a premixed deflagration of uniform near-stoichiometric hydrogen-air mixture with the explosion of highly turbulent hydrogen jet in a same mock-up refuelling station. In the jet trial, the nozzle pressure on sparking was equal to 27.91 MPa and the orifice diameter was 8 mm. The time of sparking after the initiation of the hydrogen release was set to 0.7 s. It was estimated that the total mass of hydrogen present at ignition was 0.7 kg, about 3 times less than in the premixed stoichiometric gas cloud. Despite three times less total mass of hydrogen present at ignition, the local overpressures for the jet explosion trials were found to be up to a factor of 6 higher compared to the explosion of a near-stoichiometric uniform cloud.

For example, 180 kPa overpressures were measured under the car for the jet explosion whereas 35 kPa were achieved at the same locations for the premixed trial. At the bottom part of the wall, the overpressure reached the value of 87 kPa in the jet release trial, compared to 30 kPa in the premixed test. At the top of the 4 m high wall, the overpressure reached 37 kPa, compared to 18.2 kPa.

Q9 should be further tested against recent experimental data of large-scale turbulent hydrogen jet explosions, such as given in [83-86], in order to prove its capability to predict hydrogen jet explosion overpressures. The use of such simplistic approach for risk assessment is questionable taken into complexity of explosion phenomena [83-86], particularly in complex/obstructed environment such as in tunnels.

Advanced modelling methodologies such as CFD have a potential to predict pressure effects of non-uniform hydrogen-air deflagrations, including complex and obstructed geometries without application of the Q9 methodology. Thus, the use of the Q9 methodology should be considered in the light of the limitations highlighted above.

However, the Q9 methodology is directly validated in the tunnel simulations (See below) and found to work well for the worst-case when similar pressure loads were predicted. FLACS is capable of modelling deflagrations of non-uniform mixtures and this methodology was primarily used to demonstrate a risk analysis approach, since no other approaches are available for the case of several simulations.

Summary of the simulations (and risk analysis) for the main tunnel scenario

Some of the key results obtained in the study are presented here. Both dispersion and explosion simulations were carried out based on the geometrical and scenario parameters described above in Section 7.2.

First, explosion simulations were performed assuming stoichiometric gas clouds of different sizes in order to obtain an estimate of the reference overpressures. Based on the tunnel size and inventory, the worst-case possible stoichiometric cloud sizes were of the order 200-400 m^3 (4-8 m longitudinal distance) except for the larger bus release scenario. For this case, the maximum possible cloud size was about 1000 m^3 (20 m longitudinal distance). Based on this information, explosions in a range of gas cloud sizes from 5 m^3 to 1000 m^3 were simulated. The proposed cloud sizes are roughly 5 m^3 (0.1 m tunnel length), 25 m^3 (0.5 m), 50 m^3 (1 m), 125 m^3 (2.5 m), 250 m^3 (5 m), 500 m^3 (10 m) and 1000 m^3 (20 m). The smaller clouds are assumed to be rectangular boxes with aspect ratios 2:2:1. The main ignition location is at the roof exactly in the middle of the tunnel. End ignition scenarios are also simulated and represent half of the probability for the given cloud size. The main reported parameter is the maximum explosion overpressure near the tunnel ceiling. The following sensitivities were considered (included when calculating risk):

- Long cloud only filling upper 50% of tunnel cross-section versus cloud filling full cross-section (default); this only makes a difference for the three largest gas clouds

- The effect of including typical pre-ignition turbulence from a jet flow.

The results are presented in Table 7.4.1. The table presents overpressures for both tunnel cross-sections (rectangular and horseshoe), both fuels (hydrogen and CNG), and two different ignition positions – centre (C) and edge (E).

If expected values of initial turbulence are also considered (caused by the hydrogen or CNG jet), the overpressures are expected to be somewhat higher (these calculations were only performed for centre ignition). The results are presented in Table 7.4.2. It can be seen from this table that, in general, the pressures resulting from hydrogen explosions can be very high, except for small clouds. The main findings from this exercise are as follows:

- The predicted overpressures resulting from hydrogen explosions can be very high, except for small clouds.
- The highest pressure seen was almost 12 barg for a 1000 m^3 gas cloud.
- The overpressures are significantly reduced as the gas cloud size is reduced from 1000 m^3 to 250 m^3 (factor of 4-10) but the consequences are still significant.
- The overpressures are much lower for CNG explosions, and the maximum overpressure observed in this case was 0.6 barg.
- For the largest clouds, edge ignition led to higher pressures (due to longer flame path) in most cases, but the overpressures resulting from centre ignition were generally higher for smaller clouds. However, some deviations from the general trend are seen, which are due to the placement of gas cloud with respect to the vehicles in the tunnels and the effect it has on the turbulence field.
- If initial turbulence is considered, the pressures go up by a factor of 2 for the case of larger clouds for hydrogen explosions, but the effect is much larger for smaller clouds.

- For CNG explosions, the change in overpressures caused by consideration of initial turbulence is generally much more pronounced.
- For the largest cloud (1000 m^3), the maximum predicted overpressure was seen to change by a factor of 4.

Overall, these consequences are certainly severe and further analysis was deemed necessary in order to estimate the gas cloud size and concentration that can be realistically expected. For the risk assessment study, the frequency for *Q*9 cloud sizes is applied. Explosion simulations with and without pre-ignition turbulence are assumed to be equally likely.

Table 7.4.1 Summary of overpressures as a function of gas cloud size for stoichiometric explosion calculation in the two tunnel geometries for centre and end ignition (quiescent scenarios)

Ignited gas cloud volume * Overpressures (barg)	5 m^3	25 m^3	50 m^3	125 m^3	250 m^3		500 m^3		1000 m^3	
					Long	2:2:1	Long	2:2:1	Long	2:2:1
H_2 incident C	0.05	0.11	0.17	0.29	0.50	1.01	1.29	3.22	2.66	6.52
Horseshoe E	0.03	0.07	0.11	0.19	0.52	0.38	0.77	2.96	4.28	9.97
CNG incident C	0.01	0.01	0.01	0.02	0.05	0.05	0.14	0.09	0.54	0.41
Horseshoe E	0.005	0.01	0.01	0.02	0.04	0.03	0.08	0.06	0.37	0.40
H_2 incident C	0.05	0.11	0.19	0.37	2.45	1.59	2.90	3.28	9.46	5.57
Rectangular E	0.03	0.08	0.11	0.74	3.48	2.08	4.28	4.79	7.99	11.71
CNG incident C	0.005	0.01	0.02	0.03	0.06	0.05	0.21	0.14	0.67	0.60
Rectangular E	0.005	0.01	0.01	0.03	0.04	0.04	0.08	0.12	0.39	0.41

* 1 m^3 stoichiometric H_2 cloud contains 0.024 kg H_2 and 1 m^3 stoichiometric CNG cloud contains about 0.067 kg CNG

Table 7.4.2 Summary of overpressures as a function of gas cloud size for stoichiometric explosion calculation in the two tunnel geometries for centre ignition (initial turbulence included)

Ignited gas cloud volume * Overpressures (barg)	5 m^3	25 m^3	50 m^3	125 m^3	250 m^3		500 m^3		1000 m^3	
					Long	2:2:1	Long	2:2:1	Long	2:2:1
H_2 incident C Horseshoe	0.10	0.26	0.47	1.22	2.60	2.96	3.79	8.28	10.60	9.52
CNG incident C Horseshoe	0.01	0.06	0.13	0.29	0.47	0.60	0.64	1.05	0.86	1.82
H_2 incident C Rectangular	0.08	0.34	0.56	1.40	2.86	3.51	8.85	6.13	8.77	12.90
CNG incident C Rectangular	0.01	0.07	0.13	0.30	0.51	0.59	0.72	1.14	0.82	2.26

* 1 m^3 stoichiometric H_2 cloud contains 0.024 kg H_2 and 1 m^3 stoichiometric CNG cloud contains about 0.067 kg CNG

For that purpose, the release and subsequent dispersion from various hydrogen (or natural gas) release incidents were modelled. For the dispersion scenarios, the main parameter for the risk assessment is the size of the flammable gas cloud. The release and subsequent dispersion from various hydrogen (or natural gas) release incidents were modelled. The actual calculated cloud sizes are presented in Table 7.4.3. It can be seen from this table that

- LH_2 release generally results in very small clouds in both tunnel geometries.
- The releases of 5 kg of hydrogen from a car powered by CGH_2 (as well as the CGH_2 bus with small release inventory) result in a larger accumulation of combustible fuel than LH_2 release, and the flammable cloud sizes are found to be of the order of 200-300 m^3.
- Quite significant gas clouds (1500-2500 m^3) are seen for the scenario involving CGH_2 release from 4 cylinders on a bus (20 kg of hydrogen).
- Gas clouds resulting from CNG releases were found to be mostly insignificant compared to those obtained from CGH_2 releases, except for the larger bus release in a rectangular tunnel.

- There seems to be a lesser hazard associated with horseshoe shape, due to the fact that there is 50% longer distance from PRD to the ceiling, which allows further dilution prior to impingement, and also less momentum for the jet to get recirculated back towards the floor. In general, these accumulated gas clouds were quite lean.

In general, these accumulated gas clouds were quite lean. Table 7.4.3 also presents the equivalent stoichiometric gas cloud sizes for the same scenarios and for all cases. It can be seen that:

- The equivalent stoichiometric gas clouds were found to be insignificant, indicating that the accumulated fuel does not present a very large danger.
- Even for the hydrogen incidents involving gas release from 4 cylinders in a bus, the equivalent stoichiometric gas cloud was only about 25-30 m^3.
- The largest equivalent stoichiometric gas cloud was found for a CNG bus incident in a rectangular tunnel.
- The CNG study showed that a reduction of tunnel cross-section and an increase in the release rate could result in a significant increase of the hazard.

In general, the results indicate that the overpressures obtained from explosion calculations described above are likely far too conservative, and much smaller overpressures can be expected than those obtained from the large gas clouds.

Table 7.4.3 Summary of maximum flammable gas cloud sizes for all vehicle/inventory scenarios considered in the study in the two tunnel geometries

Vehicle/Release Characteristics	Inventory (kg)	Maximum flammable gas cloud size m^3 (& kg)		Maximum equivalent stoichiometric flammable gas cloud size m^3 (& kg)	
		Horseshoe tunnel	Rectangular tunnel	Horseshoe tunnel	Rectangular tunnel
Car LH_2	10 kg	1.4 (0.007)	1.8 (0.009)	0.02 (0.003)	0.02 (0.004)
Car CGH_2 700 bar (vent up)	5 kg	281 (1.14)	273 (1.21)	4.42 (0.07)	4.31 (0.09)
Car CGH_2 700 bar (vent down)	5 kg	268 (1.33)	308 (1.39)	17.75 (0.29)	8.77 (0.18)
Bus CGH_2 350 bar	5 kg	213 (0.89)	190 (0.81)	2.16 (0.04)	1.94 (0.04)
Bus CGH_2 350 bar	20 kg	1795 (7.46)	3037 (13.97)	27.46 (0.45)	24.67 (0.49)
Bus CNG 200 bar	26 kg	3.4 (0.15)	4.6 (0.19)	1.15 (0.08)	1.18 (0.08)
Bus CNG 200 bar	104 kg	45 (2.01)	647 (26.0)	13.47 (0.90)	113.48 (7.60)
Car CNG 200 bar (vent up)	26 kg	2.1 (0.10)	3.4 (0.15)	0.85 (0.06)	1.03 (0.07)
Car CNG 200 bar (vent down)	26 kg	17 (0.78)	15 (0.65)	6.31 (0.42)	5.25 (0.35)

The expected overpressures based on the equivalent stoichiometric gas clouds resulting from the various release scenarios are presented in Table 7.4.3. The maximum expected overpressures are 0.1-0.3 barg in the case of the explosion of 27.5 m^3 stoichiometric uniform hydrogen cloud (20kg of hydrogen). Although this value is somewhat lower than first expected, it is likely to be realistic because the results obtained from many other explosion and dispersion scenarios simulated by FLACS have been found to correlate well with available experiments (for both H_2 and CNG).

Table 7.4.3 Summary of maximum overpressures based on a) the entire flammable gas cloud at stoichiometric concentration and b) the equivalent stoichiometric gas cloud size for all vehicle/inventory scenarios considered in the study

Vehicle/Release Characteristics	Inventory (kg)	Maximum pressure for max. equivalent cloud *Q*9 Quiescent / Pre-ignition turb.	
		Maximum *Q*9 equivalent volume (m^3)	Maximum overpressure (barg)
Car LH_2	10 kg	0.02	< 0.05 / 0.1
Car CGH_2 700 bar (vent up)	5 kg	4.42	0.05 / 0.10
Car CGH_2 700 bar (vent down)	5 kg	17.8	0.11 / 0.34
Bus CGH_2 350 bar	5 kg	2.16	0.05 / 0.10
Bus CGH_2 350 bar	20 kg	27.5	0.11 / 0.34
Bus CNG 200 bar	26 kg	1.18	0.01 / 0.01
Bus CNG 200 bar	104 kg	113	0.03 / 0.30
Car CNG 200 bar (vent up)	26 kg	1.03	0.01 / 0.01
Car CNG 200 bar (vent down)	26 kg	6.31	0.01 / 0.07

For quality assurance purposes overpressures obtained from the ignition of the above homogenous hydrogen clouds are compared with those resulting from ignition of realistic releases (with comparable gas cloud sizes). This is done in order to ensure that the above results do not underestimate the consequences and to evaluate the uncertainty in the equivalent stoichiometric gas cloud formulation. Studies were performed by igniting the (likely) most dangerous release scenario (large H_2 release from a bus) inside the jet (two different ignition positions) at different times after the beginning of the release. Contour plots of the gas cloud concentration between 15 and 40% hydrogen at two different times (5 s and 15 s after beginning of release) are shown in Figure 7.4.3. Even for this case, the gas cloud concentration is significant only near the jet axis. The gas cloud extent with concentration above 4% (LFL) is presented in the middle part of the same figure.

It can be seen that the flammable hydrogen cloud is quite large, but most of this gas is fairly dilute and expected to lead to minimal overpressures when ignited. For comparison, similar plots for the smaller bus release are also shown. It can be seen that the gas cloud with significant concentrations resulting from this scenario is even smaller. The worst-case cloud was further ignited within the jet at a position 2.8 m (near the ceiling) from the release location on the jet axis. The flame development as a function of time is shown in Figure 7.4.4. Maximum overpressures of around 0.25 barg are seen on the pressure sensors. Local pressures will exceed 0.25 barg due to reflections on and under vehicles. Thus, the values of overpressures obtained using the equivalent stoichiometric gas cloud concept can be expected to be reasonable for all cases.

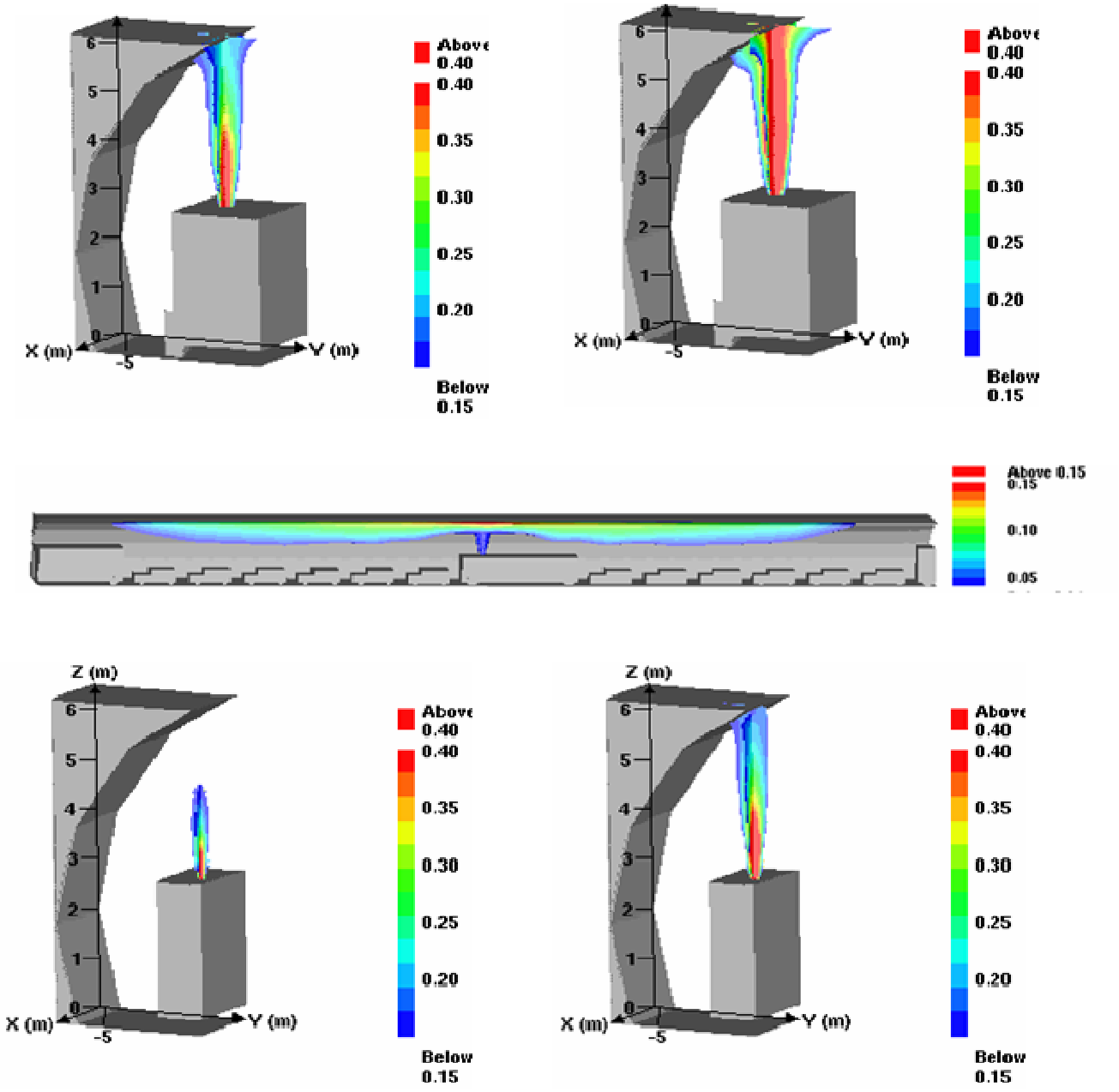

Figure 7.4.3 Hydrogen concentration contours for two different times (5 and 15 s after beginning of release) for two different release scenarios: 20 kg (top) and 5 kg (bottom) bus incident. The gas cloud extent for concentrations above 4 % (LFL) for the 20 kg bus release is shown in the middle.

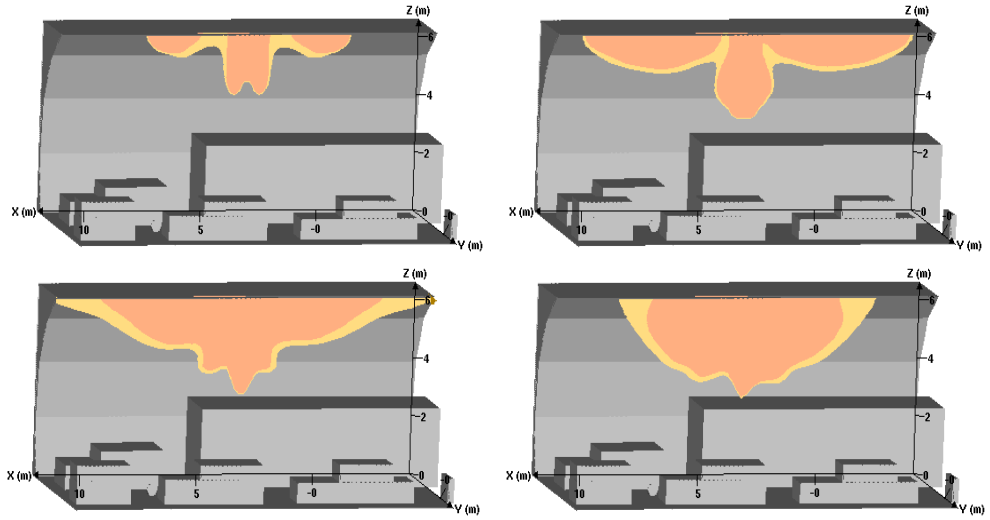

Figure 7.4.4 Flame development for the large H2 bus release upon early ignition within the jet near the ceiling

The effect of ventilation is illustrated next for the "worst-case" 4 cylinder release from a hydrogen bus. If no ventilation is present, the maximum flammable gas cloud size was found to be 1800 $m^{3.}$ With 2 ms^{-1} ventilation velocity, the maximum flammable gas cloud size was reduced to 1500 m^3. However, the maximum equivalent stoichiometric gas cloud size increased slightly to 30 m^3. For the case of 5 ms^{-1} ventilation velocity, the respective values of flammable gas cloud size and equivalent stoichiometric gas cloud size were 1000 and 25 m^3. Thus, the ventilation did not have any significant impact on equivalent stoichiometric gas cloud sizes. It can be concluded that ventilation is only important if more significant volumes of reactive clouds are seen. With the high momentum releases considered here, the momentum from jet dominates the dilution process. However, there is a possibility that lower momentum and "trapping" of gas cloud can lead to more dangerous results. The very significant buoyancy certainly precludes the "trapping" process, but more investigation is required.

A probabilistic risk assessment study is undertaken next. For this purpose, the ignition likelihood needs to be established. The probability for ignition of releases is probably very different for CNG and H_2, since there is one order of magnitude difference in necessary spark energy at stoichiometry (the ignition energy is nonetheless very similar near the LFL). Early spontaneous ignition is frequently seen in large-scale H_2 experiments (e.g. [73]), but this is seldom reported with CNG. For studies in offshore platforms with natural gas, the ignition probabilities are generally low, so there has been no need to consider detailed statistical treatment on conditionality. If ignition probability gets high, this may be needed.

Care must be taken that the total ignition probability contribution for one release scenario does not exceed one, i.e. potentially large gas clouds filling large parts of the tunnel should not contribute to risk if ignition probabilities have indicated that gas cloud will ignite much earlier. As a coarse, but realistic, assumption for this study, the following ignition probabilities/intensities were assumed:

1. Constant ignition sources ~ 0.25 [10^{-4} per m^3 volume flammable first time]
2. Intermittent ignition sources ~ 0.25 [10^{-5} per m^3 flammable volume and second]
3. Spontaneous ignition = 0.5 [constant 0.1/s first 5 seconds]

More experience and accident data is needed to refine these estimates. These values imply that the approximate probability of ignition from constant ignition sources for a given incident is about 0.25, which is reached once 2500 m^3 has been exposed to flammable gas. Similarly, the assumed maximum contribution from intermittent ignition sources is filled up if 1000 m^3 of the tunnel sees flammable gas for 25 s, or 2500 m^3 for 10 s. The spontaneous ignition probability will always be 50%, but the relative weight of the other two can vary, with the maximum total contribution being 50%.

Based on the calculations above, exposure times for a given cloud size and the associated ignition likelihoods are established. More details are given in Hansen and Middha [72]. In the end, the frequency of exceedance curves of a given pressure load for a hydrogen (or CNG) incident can be estimated. To include the effects of jet-induced turbulence simulations with pre-ignition turbulence were also included. The maximum expected overpressures are of the order of 0.35 barg (cloud assuming pre-ignition turbulence), but the estimated likelihood to ignite a cloud with that size and severity is estimated to 5%. From the study it is found that typically, pressure loads around 0.1-0.2 barg can be expected for a hydrogen incident. If the initial release rate for the large bus release is limited to maximum 234 g/s, a sensitivity study showed that the likelihood of obtaining pressure loads higher than 0.1 barg is significantly reduced. For a CNG incident, the expected pressure loads are generally of the order 0.01 barg.The sensitivity of the results for cases involving only low ventilation velocities (0 and 2 ms^{-1}) and involving only high ventilation velocities (3 and 5 ms^{-1}) was studied. It was found that the effect of ventilation is small. For the scenarios involving ignition within the jet, the maximum overpressures for both geometries and all different ignition times were found to be of the order of 0.11-0.25 barg, and hence were not significantly different from those obtained by the ignition of quiescent stoichiometric clouds of the appropriate size.

Thus, the hazards arising from the use of hydrogen vehicles in a tunnel has been estimated. The worst-case screening approach indicated the potential for very high overpressures. However, by performing a dispersion study those values were found to be far too conservative, and the explosion loads found when igniting the dispersed clouds were not too significant. In the end, a probabilistic study has been carried out which suggests that the hydrogen vehicles do not present a very significant explosion risk in a tunnel, and can be used in a safe manner. It can be concluded that larger and "taller" tunnels are even safer, as horseshoe tunnel was found to present a smaller danger in terms of the flammable cloud concentrations than a rectangular tunnel due to possibility of larger mixing and hence dilution.

Summary of the simulations for the 'bridge scenario'

In the study it has been assumed that the tunnel ceiling is smooth and that there are no obstructions near the ceiling. If the ceiling design is such that gas can be trapped and the momentum of impinging releases significantly reduced, this could reduce the mixing and change the conclusions. The presence of significant congestion elements (light armatures or fans) near the ceiling could also add some turbulence to flame propagation and make explosions slightly more severe. This is investigated here by establishing the "wide bridge scenario" described above.

The maximum flammable gas cloud is around 2200 m^3 for the base case scenario (scenario 1) and occurs around 60 seconds after the start of the release. The corresponding value for the equivalent stoichiometric gas cloud is only 120 m^3 occurring much earlier (10-15 seconds after the start of the release). This shows that the cloud is fairly dilute. The size of the gas cloud is somewhat reduced (by around 20 %) if the release is shifted to impinge on the armature. In this case, the corresponding values for the total flammable gas cloud and the equivalent stoichiometric gas cloud are 1800 m^3 and 100 m^3 respectively. This is due to the decrease in the effective height of the tunnel before the hydrogen jet impinges on a surface. As expected, the use of a flat ceiling reduces the gas cloud sizes significantly as the gas cannot get collected between the various support structures. In this case, the corresponding values for the total flammable gas cloud and the equivalent stoichiometric gas cloud are 1300 m^3 and 30 m^3 respectively. This means that the gas cloud is also significantly less reactive than that obtained for a "rough" ceiling. If it is assumed that only 5 kg of hydrogen is released (scenario 4), then the flammable gas cloud is clearly smaller (425 m^3 and 7 m^3 respectively).

The ceiling structure, release mass, and release position each have a significant effect on the size and reactivity of the gas cloud. Also, it was seen that the steady state concentrations are fairly dilute. It was seen that the equivalent stoichiometric gas cloud size is only about 100 m^3 for scenarios 1 and 2, while it is even smaller for scenario 3. This suggests that the danger of these clouds is not very high.

The gas clouds obtained as a result of dispersion calculations have also been ignited in order to obtain an estimate of the resulting overpressures. Sensitivity to ignition locations and times has been

investigated. In this case, two scenarios were considered: 20 kg hydrogen released for the case of "rough" and smooth ceiling. The maximum overpressure obtained for the rough ceiling scenario was found to be around 0.7-0.75 barg. For the case of smooth ceiling, the maximum overpressure was found to be 0.1 - 0.15 barg. Thus, the turbulence generating objects in the ceiling increase the overpressure by a factor of 5-6. The overpressure obtained for the smooth ceiling case compares well with the value reported in part 1 of the CFD simulation study where a max. pressure of the order of 0.1-0.3 barg was reported. Thus, it may be deduced that if a rough ceiling were present in those calculations, a pressure of 0.6 - 1 barg could be expected.

7.5 WUT Study using ANSYS-CFX/FLUENT

Simulated cases

Two scenarios are considered: vehicle tanks of liquid and compressed gas hydrogen. Liquid hydrogen is used only in passenger cars. The release of liquid hydrogen is simulated from the hole of 20 mm in diameter, from the upper surface of the car, with constant flow rate equal to 11 g/s. The time of release is 900 s.

Two limiting cases of hydrogen temperature will be considered: 20 K and 200 K. The 20 K refers to the temperature of liquid hydrogen. In the second case the heating of hydrogen is assumed during flow from the tank and release.

The simulation of hydrogen release will be considered from the hole of 120 mm in diameter. Due to the high pressures and possible high gas velocities, the outflow diameter was assumed not to exceed the velocity of Mach 0.3 to exclude the wave effects due to compressibility (the uncompressible fluid model was used in the simulations).

The working pressure of the tank for passenger car is 700 bar, and for busses it is 350 bar. The time of release is 84 and 147 s, respectively, with variable flow rate and temperature. The change of mass flow rate and temperature vs. time of release is show in Figures 7.5.1 and 7.5.2. After 50 s of release the constant values of mass flow rate and temperature were assumed. For the 350 bar tank it was assumed 0.01 kg/s and 110 K. For the 700 bar tank it was assumed 0.005 kg/s and 65 K.

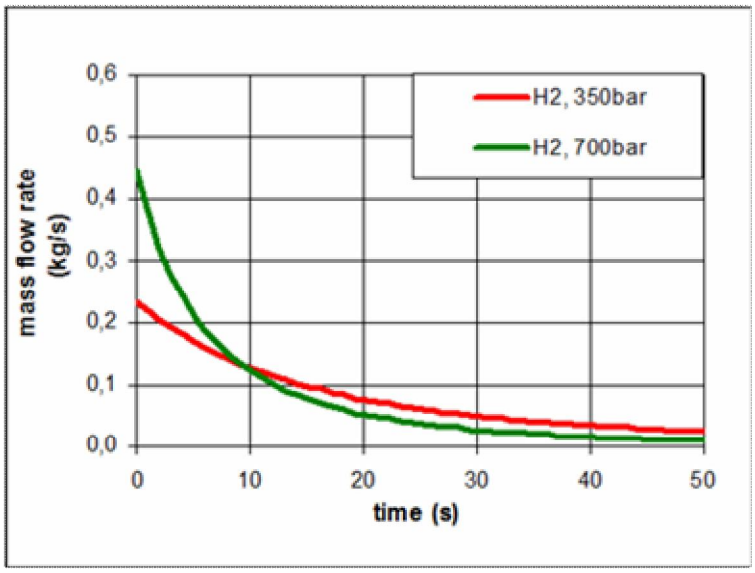

Figure 7.5.1 Hydrogen mass flow rate

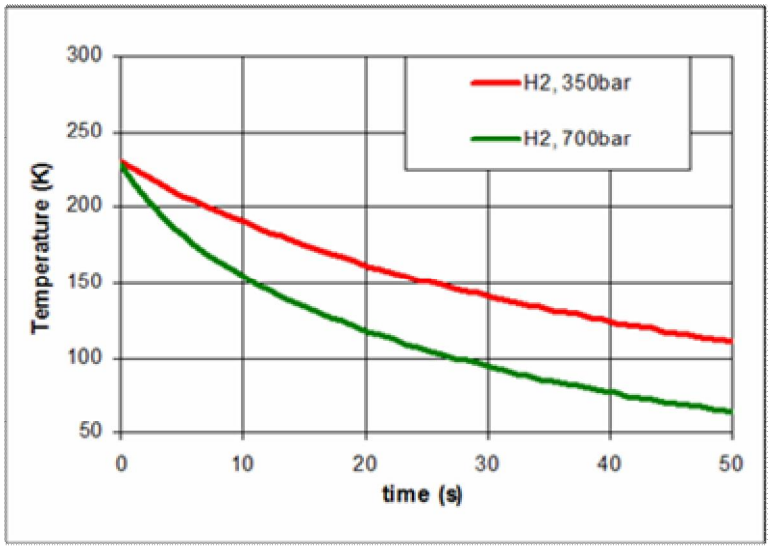

Figure 7.5.2 Temperature profile

The total number of simulations was: 2 (tunnel geometries) × 5 (ventilation cases) × 4 (release cases) = 40. Table 7.5.1 shows all cases of simulations.

Table 7.5.1 Summary of simulation cases

Type of vehicle	Initial mass flow rate [g/s]	Initial hydrogen temperature [K]	Time of release [s]	Diameter of release [mm]
Passenger car LH_2	11 – constant	20 – constant	900	20
Passenger car LH_2	11 – constant	200 – constant	900	20
Passenger car CGH_2 (700bar)	448 – variable	230- variable	84	120
Bus CGH_2 (350 bar)	234 – variable	230 - variable	147	120

Summary of results for the cases without ventilation

The scenarios with no longitudinal applied ventilation were modelled with FLUENT. The extent of the flammable (4 to 75%) hydrogen cloud was determined for both CGH2 and LH2 vehicles in both the rectangular and horseshoe cross-section tunnels.

Figure 7.5.3 provides an example of the CFD results, showing the flammable gas cloud 84s after the start of the release of compressed hydrogen gas (700 bar) from a hydrogen car.

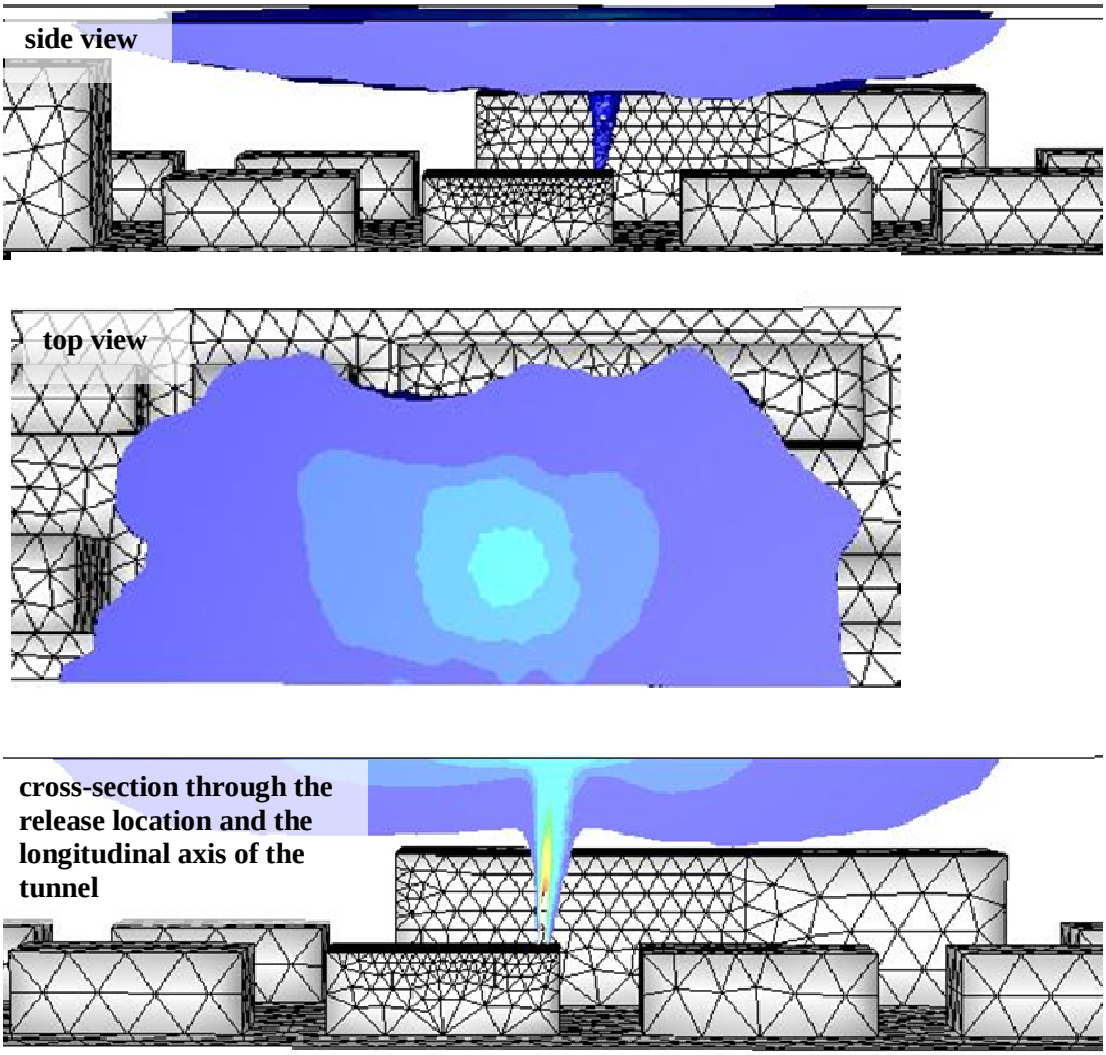

Figure 7.5.3 Hydrogen-air flammable cloud for the rectangular tunnel with no forced ventilation for CGH2 release (700 bar) from a car – at time 84s

Table 7.5.2 summarises the predicted flammable gas cloud sizes from the full set of CFD simulations.

Table 7.5.2 Comparison of flammable cloud sizes without ventilation

Type of release	Type of tunnel	Approximate flammable cloud volume [m^3]	Maximum cloud size (length × width)
CGH_2 700 bar	rectangular	245	18 m×9 m
CGH_2 350 bar	rectangular	265	18 m×10 m
LH_2 20 K	rectangular	1260	42 m×10 m
LH_2 200 K	rectangular	1125	45 m × 10 m
CGH_2 700 bar	horseshoe	185	17 m×7 m
CGH_2 350 bar	horseshoe	200	18.5 m×7 m
LH_2 20 K	horseshoe	135	27 m×5 m
LH_2 200 K	horseshoe	350	25 m×7 m

The influence of the tunnel cross-section and type of hydrogen release is explored below.

a) **Effect of tunnel cross section**

The size of flammable cloud is larger for the tunnels with rectangular cross section. This is probably due to smaller tunnel height and hydrogen accumulation under larger area of flat roof. The horseshoe cross section results in faster hydrogen diffusion and mixing with air occurs on the Langer distance to the roof. Moreover it accumulates farther up so the risk of ignitron is lower.

The horseshoe cross section tunnel is safer. The resulting flammable clouds are smaller in size and are formed higher from the probable ignition sources (vehicles, people).

b) **Effect of type of release**

For the cases with the tank of CGH2 700 bar the resulting flammable clouds for both tunnel cross sections are smaller than for the pressure 350 bar. The higher release velocity results in faster diffusion. Moreover the release of 350 bar occurs from the bus at the height of 3 m. The hydrogen reaches the roof faster where it accumulates. The release from passenger car at the height of 1.5 m gives better conditions for mixing.

In the cases of LH2 tanks the flammable Cloud are Langer than for CGH2 tanks. It is so in particular for rectangular cross section tunnels, where the difference is even fivefold. For horseshoe cross section tunnels the difference is twofold.

For LH2 release in rectangular cross section tunnel the flammable mixture covers almost whole tunnel cross section along 40 m section (both for 20K and 200K). For LH2 release at 200 K in horseshoe cross section tunnel the location, size and geometry of the flammable cloud is similar as for CGH2.

However, for LH2 release at 20 K the cloud has a different form. The flammable cloud of hydrogen-air mixture is formed above the ground. The cloud covers the whole width of the tunnel up the height of 2.5 m. The results indicate that this is due to the low initial temperature of hydrogen; cold hydrogen flows down. Additionally, hydrogen has large initial density which for the assumed constant mass flow rate results in low release velocity (1m/s). For the case of LH2 at 200K this velocity is more than 10 m/s.

The highest risk will present the release scenarios with LH_2 tanks in tunnels of rectangular cross section. In both release cases (20 K and 200 K) the flammable clouds are formed which cover the large volume of the tunnel of high probability of occurrence of ignition sources (people, vehicles). The flammable hydrogen-air cloud for the release at 20 K is about 10% Langer than for the case of 200 K. Its characteristic feature is that the hydrogen accumulates near the ground along the distance of 15m. In the case of 200 K the flammable cloud extents approximately from the roof to the height of 0.75 m above the ground.

Summary of results for the cases with ventilation

The scenarios with longitudinally applied ventilation were also modelled.

Figure 7.5.4 provides an example of the CFD results, showing for the range of longitudinal ventilation speeds the flammable gas cloud 147s after the start of the release of compressed hydrogen gas (350 bar) from a hydrogen bus. Table 7.5.3 summarises the predicted flammable gas cloud sizes from the CFD simulations.

Table 7.5.3 Comparison of flammable hydrogen-air clouds in the tunnel with ventilation

Type of tunnel	Type of tank	Velocity of ventilation (m/s)	Cloud volume (m^3)	Cloud size (length x width) (m)
Rectangular	CGH_2 700 bar	1	1,3	4,7 × 0,8
		2	0,5	4,4 × 0,6
		3	0,3	4,2 × 0,5
		5	0,1	4 × 0,4
	CGH_2 350 bar	1	5,7	6,2 × 1,3
		2	3,1	4,2 × 1,2
		3	2,2	3,7 × 1,1
		5	1,3	3,2 × 0,95
	LH_2 20K	1	6,0	5,5 × 1,4
		2	2,6	4,7 × 1,05
		3	1,5	4,7 × 0,85
		5	0,6	4,2 × 0,65
	LH_2 200K	1	3,8	4,7 × 1
		2	2,3	4,7 × 1
		3	1,0	3,7 × 0,8
		5	0,6	3,2 × 0,7
Horseshoe	CGH_2 700 bar	1	1,6	4,4 × 0,9
		2	0,8	4,4 ×0,7
		3	0,5	4,2 ×0,6
		5	0,2	3,7 × 0,5
	CGH_2 350 bar	1	4,3	4,7 × 1,3
		2	1,8	3,7 × 1
		3	1,3	3,2 × 0,95
		5	1,0	2,7 × 0,9
	LH_2 20K	1	8,1	6,7 × 1,5
		2	4,3	5,7 × 1,2
		3	0,5	4,4 × 0,6
		5	0,5	4,4 × 0,6
	LH_2 200K	1	4,1	5,4 × 1,2
		2	2,3	5,4 × 0,95
		3	1,3	4,9 × 0,8
		5	1,1	4,7 × 0,75

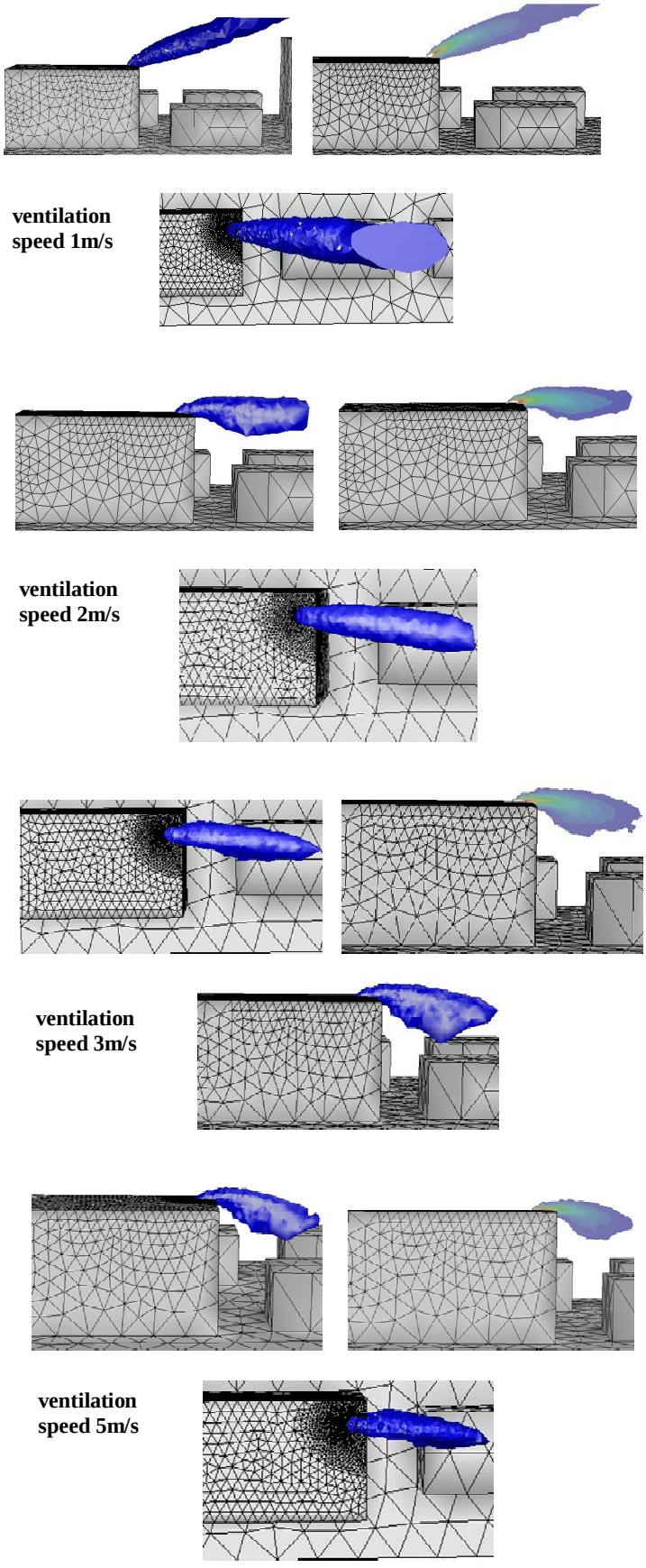

Figure 7.5.4 Hydrogen-air flammable cloud for the rectangular tunnel with forced ventilation for CGH2 release (350 bar) from a bus – at time 147s

The influence of the tunnel cross-section and type of hydrogen release is explored below.

a) **The effect of tunnel cross section**

For the CGH2 of 350 bar release the volumes of flammable hydrogen-air clouds are larger for rectangular cross section channel. However, for the CGH2 of 700 bar release the volumes are similar for both cross sections. The clouds for LH2 of 20 K and 200 K releases are smaller for rectangular cross section.

The dispersion behavior of flammable clouds for CGH2 is similar for both release pressures. In the case of LH2 releases the clouds differ substantially for both tunnel cross sections. In the rectangular cross section tunnel they have the tendency to move upward even for the maximum ventilation velocity. In the case of horseshoe cross section the flammable clouds stay close to the top surface of the vehicle.

The simulations do not show unequivocal effect of tunnel cross section on the distribution, size and range of flammable hydrogen-air clouds.

a) **The effect of ventilation velocity**

The ventilation velocity has clear effect on the size of flammable cloud. An increase of velocity causes the decrease of cloud size, shortening of its maximum range and lowering of its location. The flammable clouds reach the maximum sizes of 8.1 m^3 for the ventilation velocity of 1 and 2 m/s (the case of LH2, 20 K, 1 m/s, horseshoe). The clouds formed from the release of hydrogen from passenger car (CGH2, 700 bar + LH2, 20 K, in horseshoe tunnel) stick to the upper vehicle surface. Different results are visible for the all other cases of LH2 release where the flammable cloud is moving upwards for all ventilation velocities.

For the hydrogen release from the bus roof at the ventilation velocity of 1 m/s the flammable clouds move upwards and reach the sizes up to 5.7 m^3. When the ventilation velocity increases to 2 m/s, the clouds start to move down due to the recirculation vortex behind the vehicle and decrease their size about two times.

For the ventilation velocity of 3 and 5 m/s the clouds rarely exceed the volume of 2 m^3 (maximum of 2.2 m^3 for the CGH2, 350 bar, 3m/s, Tab. 3). For the ventilation velocity of 3 and 5 m/s for the cases of releases from passenger car all flammable Cloud stick to the upper car surface except the case of LH2, 200 K. Further shortening of cloud range and decrease of volume occurs. In the releases from the bus the increase of ventilation velocity to 3 and 5 m/s results in further decrease of the cloud size and larger recirculation downwards.

With the ventilation velocity increase from 1 to 5 m/s the size of flammable cloud decreases 4 times (CGH2, 350 bar, both tunnel cross sections), and even 16 times (LH2, 20 K, horseshoe).

An increase of ventilation velocity from 1 m/s to 3 m/s results in fast decrease of flammable cloud volume. Further velocity increase does not change the cloud size substantially.

The largest flammable hydrogen-air clouds were formed from the LH_2 releases of very low temperature of 20 K. The smallest clouds were formed from the CGH_2 of 700 bar releases.

<u>Comparison of results with the simulations of GexCon</u>

Some effort was directed to the issue of whether the same conclusions could be drawn, for a given accident scenario, by different partners using a different codes. As part of this objective WUT assessed whether it could obtain the same conclusion for various scenarios already examined by GexCon.

An agreement was reached with GexCon results in respect to the following conclusions:

a) Horseshoe cross section tunnel is safer than rectangular with regards of flammable cloud size and range; the increasing height of the tunnel improves safety.

b) The volumes of clouds from CGH2 releases reach the values of 200-250 m3; the increase of ventilation velocity decreases the cloud size and improves safety.

Contradicting results were obtained with GexCon for the LH_2 release however. In the WUT simulations the flammable clouds from LH_2 were much larger and therefore considered as presenting higher explosive risk. The results of GexCon were opposite, with smaller clouds for LH_2 than for CGH_2 and so considered as safer. This disagreement requires further study and clarification.

7.6 LES study by UU of hydrogen release from a pressure relief device of a hydrogen bus and its dispersion in a tunnel [79]

UU [79] has undertaken a study of selected scenarios akin to those described in Section 7.2 and in the previous EIHP-2 project, where the consequences of releases of compressed gaseous hydrogen from a typical city bus were examined by NSCRD.

The bus was located at the tunnel's midpoint, 100m from each exit and centrally in one lane of a two lane, bi-directional tunnel.

A CFD analysis using RANS (30 seconds) and LES (25 to 30 s and 0 to 1 second) models was carried out investigating the blowdown scenario of 5 kg of hydrogen released at initial cylinder pressure of 350 bar into a tunnel environment through a 6mm PRD orifice of the located above the roof of hydrogen powered bus. The simulation results of hydrogen dispersion within the tunnel were compared to the results published previously.

During 30 s of the blowdown process, it is found that both UU and NSCRD simulations predicted about the same total mass of hydrogen in the flammable cloud. However, there is significant difference in the distribution of hydrogen within the flammable concentration range. The UU simulations predict about 7 to 10 times greater amount of hydrogen in the most explosive concentration range of 20-60% compared to the EIHP-2 work. Therefore, it is expected that the combustion of the UU simulated cloud would generate higher overpressures than 2.3 kPa calculated previously.

Recent experiments have shown that, for high momentum hydrogen free jets released at 205 bar through a 6.4 mm diameter orifice, the overpressure reached about 20 kPa at 0.6 s ignition delay and decays to about 10 kPa at 2 s for the same ignition position located at 2 m from the nozzle (both recorded at a point x=2.8 m, z=1.5 m from the release point). In the present work, the scenario investigates the hydrogen release through an orifice of similar diameter size of 6.0 mm but at higher initial pressure of 350 bar. Therefore, it can be expected that experimental overpressures similar or greater than those mentioned could be obtained. The maximum explosion overpressure may be expected for short ignition delays i.e. of the order of a second. For long ignition delays when the maximum mass of hydrogen in its flammable concentration is achieved, the overpressures may be expected to be smaller due to less jet turbulence generated at the end of the blowdown process.

As shown by experimental data [84, 85], the use of PRD diameters smaller than 6.0 mm would significantly decrease the explosion and jet fire hazards. For example, it has been demonstrated that, for a hydrogen jet release through a 1.0 mm diameter orifice at constant 400 bar pressure and ignited at 4.0 m from the nozzle, the maximum overpressure reached 0.2 kPa at 2.0 m from the release source [84] . In [85], the combustion of hydrogen jets released through 1.5 mm diameter at constant 205 bar pressure ignited at 2.0 m from the nozzle did not produce recordable overpressure. Furthermore, it was obtained that the flame length of a free hydrogen jet fire reached 9 m when released through a 6.4 mm orifice diameter at a 205 fixed pressure compared to 3 m for a jet fire released through a 1.5 mm orifice diameter at the same initial 205 bar pressure [85].

7.7 Summary of Findings

Obviously the findings summarised below reflect the work undertaken within HyTunnel only. They should be considered in the context the wider findings from HyTunnel and other studies.

The GexCon study suggests that while the predicted flammable gas cloud sizes are large for some scenarios modelled, if the actual reactivity of the predicted clouds is taken into account, then very moderate worst-case explosion pressures result, in the region 0.1-0.2 barg.

Interestingly, the GexCon study suggests that the size of the imposed longitudinal tunnel ventilation has only a marginal impact on the predicted risk, since the momentum of the releases and buoyancy of hydrogen was observed to dominate the mixing and dilution processes.

The WUT study [78], by contrast, suggests that the introduction of even a low level of ventilation (1 m/s) causes a dramatic change in the flammable cloud size and its associated hazard. The introduction of a minimum ventilation level of 3 m/s is identified as a requirement for hydrogen vehicles to be safely accommodated in road tunnels. Another finding from this study include that horseshoe section being safer than the rectangular one as it allows for faster dispersion of the released hydrogen. It also indicated that the compressed gas hydrogen releases are safer than those form liquid hydrogen vehicles However this result requires further investigation including physical experiments.

The UU study [79] compared their results on hydrogen releases from a bus using an LES model with those generated previously under the EIHP-2 project using a RANS model. It is suggested that the explosion overpressures may be larger than previously reported. It is also suggested that the smaller PRD vent diameters may help reduce the consequential explosion hazard.

CHAPTER 8 – CONCLUDING REMARKS AND RECOMMENDATIONS

8.1 Concluding remarks

The conclusions summarised in this section are drawn from published research work and the complimentary experimental, CFD and risk assessment studies conducted within the HyTunnel project, where partners have analysed the dispersion of hydrogen released from vehicle onboard storage and the consequential fire and explosion hazards. A number of physical parameters were investigated, which included the tunnel cross-section, background longitudinal ventilation velocity (0 to 5 m/s), blockage ratio due to vehicles, duration and pressure of hydrogen release (20 MPa, 35 MPa or 70 MPa), upwards or downwards venting, single or multiple pressure relief devices (PRDs). The work also considered both compressed hydrogen gas and liquid hydrogen storage systems.

The potential hazards associated with high pressure, non-ignited (in the initial release) hydrogen jets inside a longitudinally ventilated tunnel were explored in the EIHP studies [66, 67] and the work of Mukai et al [68]. The main findings of these studies were:

- When comparing the consequence of hydrogen released inside a tunnel to that in the outside (urban) environment, it was determined to be significantly more severe and the energy available in the flammable cloud was greater and remained for a longer period.

- Releasing a large mass of hydrogen from a city bus through multiple vents was found to be more hazardous compared to when the same mass was released through a single vent. It was thus concluded that hydrogen storage systems should be designed to avoid simultaneous opening of all PRDs. Mitigating measures should be developed to avoid failure of all PRDs occurring simultaneously in a tunnel.

- While the consequence of a release from a 20 MPa natural gas system was comparable to that from a 20 MPa hydrogen system, the consequence of a similar release from a higher pressure hydrogen system was significantly more severe, in particular with respect to predicted overpressures from a subsequent explosion of the hydrogen cloud. The significant difference in the explosion hazard associated with the 20 and 35 MPa release, despite a similar energy, was attributed to the different distribution of hydrogen mass within the flammable clouds formed.

- The CFD studies highlighted that the ignition point inside the dispersed hydrogen cloud significantly affects the combustion regime. Based on the predicted overpressures, typical effects could be the damaged vehicle windows or tunnel lighting units. However, the results also indicated that fast deflagrations, or even detonations, could be produced by the most severe hydrogen releases and ignition timing from the worst case events.

- The CFD study of Mukai et al [68] has shown that a potential risk due to a hydrogen-air mixture above the lower flammability limit (4% by volume) at the exhaust fan was likely to be minimal.

The CFD modelling study of Hansen and Middha [72], conducted as part of HyTunnel, has provided insight into the risk posed by hydrogen vehicles in road tunnels, and has examined different tunnel geometries and hydrogen release scenarios, including cars and buses. As for the EIHP work, comparisons to natural gas vehicles were included. The maximum possible pressure load predicted by the simulations was in the range 0.1-0.3 barg, which represents a limited human risk due to direct injuries. It is noted that that local overpressures due to reflections from the sidewalls and/or the vehicles can be expected to be higher than those calculated in the study.

The WUT HyTunnel CFD study, also conducted as part of HyTunnel, suggests that the introduction of even a low level of ventilation (1 m/s) causes a dramatic change in the flammable cloud size and its associated hazard. The introduction of a minimum ventilation level of 3 m/s is identified as a requirement for hydrogen vehicles to be safely accommodated in road tunnels. The study indicated that

a horseshoe section is safer than a rectangular one as it allows for faster dispersion of the released hydrogen. It also indicated that the compressed gas hydrogen releases are safer than those form liquid hydrogen vehicles. However, is stressed that this requires further investigation including physical experiments.

By conducting a series of hydrogen release deflagration experiments and CFD simulations inside a reduced-scale tunnel geometry, Groethe et al [73] found that:

- The confinement of the hydrogen by the tunnel significantly raises the explosion hazard.

- The tunnel ventilation reduces the hazard dramatically, and suggested that suitable ventilation of a tunnel can significantly reduce the chance of an explosion. However, there may be the possibility that even in a well ventilated tunnel high release rate of hydrogen could produce a near homogeneous mixture at close to stoichiometric conditions, with a correspondingly increased explosion hazard.

- The complimentary computational study, covering both obstructed and unobstructed tunnel arrangements, has demonstrated the usefulness of CFD in extending the findings obtained from experiments alone, e.g. in examining explosion pressure effects in the locality of obstructions. Furthermore, it represents an important step in extending the validation of models that have previously been calibrated for hydrogen-air explosions in the open atmosphere or closed vessels.

The full-scale HSL experiments, conducted with longitudinal ventilation, indicate that

- significant levels of overpressure can be generated in confined or semi-confined spaces, by the ignition of a hydrogen-air mixture filling only a small fraction, of the order of a few percent, of the space. These could be high enough to cause damage to tunnel services, e.g. ventilation ducting.

- for larger percentage fills of hydrogen-air mixture, the possibility of DDT cannot be ruled out.

- hydrogen explosions are more prone to produce an oscillatory pressure-time profile than hydrocarbon explosions, which may have implications for the response of structures subjected to a hydrogen explosion.

The full scale FZK experiments conducted as part of HyTunnel indicated that DDT is, in principle, possible in the confined space of a tunnel. Consequently, ceiling design and mitigation measures may be important.

By undertaking LES analysis of hydrogen-air deflagrations in a short tunnel, Molkov et al. [74] have confirmed experimental observations that obstacles with a blockage ratio of 0.03, as per tested configuration, have no significant effect on maximum explosion overpressure in the tunnel beyond the immediate vicinity of the obstacles. Based on the LES analysis, it was demonstrated that side-on obstacle overpressure can increase significantly due to reflection of the shock wave formed in the tunnel during the deflagration.

Hansen & Middha [72] have argued that

- the extent of the ignited hydrogen ceiling jet poses a significant hazard compared to other (hydrocarbon) fuels. They do not, however, take into consideration the contribution of the vehicle and any carried goods, which is likely to more important than the actual fuel. The rapid development of an ignited hydrogen ceiling jet, extending some distance along the tunnel, does however warrant further investigation.

- Q9 methodoloy (based on the concept of an equivalent stoichiometric gas cloud) provides estimates of the the explosion over pressure more speedily than if the actual (computed) dispersed gas cloud is used. Although Q9 methodology is not always conservative, and is not expected to bound for all possible scenarios, it has been shown to provide similar conclusions to CFD for a large number of scenarios in non-tunnel applications (see ch. 7). It is therefore, from the point of view of the Q9 approach developer - GexCon, a useful engineering tool for optimising CFD simulations for hazard and risk analysis

8.2 Recommendations

The dispersion and explosion hazards research conducted as part of HyTunnel, together with other published work, has provided a better understanding of the potential hazards associated with hydrogen vehicles in road tunnels.

The concluding remarks drawn from the work done so far indicate that

- hydrogen-powered vehicles in tunnels are no significantly higher risk than those powered by petrol, diesel or CNG (compressed natural gas),

- the detonation in the tunnel should not be accentuated. The risk of detonation could be minimised if appropriate actions, such as ventilation, ceiling layout, PRDs design, are taken.

This suggests the possibility of the safe introduction of hydrogen powered vehicles in tunnels provided attention is given to various issues:

- Background and emergency ventilation in the tunnel. Concerning the question “what is reasonable ventilation for a given scenario?”, the limited research work done so far has indicated 3 m/s as reasonable ventilation for avoiding backlayering, but this should be supported by further research,

- Obstructions in the tunnel, particularly at the ceiling, which may influence the risk of explosion (i.e., fast deflagration or detonation).

Note that a limited number of hydrogen powered vehicles are already running safely on the roads. To ensure that the hydrogen powered vehicles run reasonably safely on the roads and in the confined space of a tunnel, we need to minimise gaps in our knowledge on important aspects such as highlighted above.

More specifically, further research is needed to gain a better understanding of the release and ignition conditions that could result in fast deflagrations or detonations, particularly in relation to obstructions caused by vehicles or ducts, light armatures, fans, etc. in the ceiling of a tunnel. Note that the obstructions in the tunnel ceiling could add some turbulence to flame propagation and make explosions more severe. Although current research has indicated that the hazard posed by hydrogen powered vehicle is not higher than conventional hydrocarbon powered vehicles, this needs confirming by further research.

Furthermore, future research should be directed to answer the following questions:

- Is forced background ventilation (> some minimum value) required to mitigate effect of hydrogen release inside tunnels? While intuition and various research indicates that this is so, we need to have wider consensus on this (currently some other researchers seem not to agree).

- How important are ceiling level obstructions in making deflagration (or even detonation) risk greater? This warrants further consideration/research.

- Do we need to design on board hydrogen systems to prevent simultaneous operation of multiple PRDs? Currently there is some evidence that this makes matters worse. Breakthrough ideas for PRDs should be developed to make releases hydrogen-air mixtures incombustible.

A detailed risk analysis would be necessary before any detailed recommendations could be made. Such an analysis would need to balance the risks associated with venting the gas as quickly as possible against those associated with restricting the energy flow from the storage system, so that the explosion risk is reduced, but with an increased risk of an uncontrolled release from a fire damaged tank.

REFERENCES

1. PIRT exercise

2. World Road Association (PIARC) (1999). *Fire and smoke control in road tunnels*. World Road Association, Paris, France.

3. *The Handbook of Tunnel Fire Safety*, ed. A Beard & R Carvel, pp 127-143, Thomas Telford, London.

4. NFPA (2004). *NFPA 502 – Standard for Road Tunnels, Bridges, and other Limited Access Highways*, (a) 2004 ed.; (b) 2008 ed. National Fire Protection Association, Quincy, Massachusetts.

5. The Highways Agency et al (1999). *Design Manual for Roads and Bridges - Volume 2, Section 2, Part 9 - BD 78/99: Design of Road Tunnels*, The (UK) Stationary Office Ltd; http://www.standardsforhighways.co.uk/dmrb/vol2/sect2/bd7899a.pdf

6. Cafaro, E. (2005). An innovative tunnel fire protection system. *Tunnel Management International*, vol. 8, issue 3, September 2005.

7. Fraser-Mitchell, J. & Charters, D. (2005). Human Behaviour in Tunnel Fire Incidents. In *Proc 8th Int. Symp. Fire Safety Science*, 18-23 September 2005, Beijing.

8. Shields, J. (2005). Human behaviour in tunnel fires. In *The Handbook of Tunnel Fire Safety*, ed. A Beard & R Carvel, pp 324-342, Thomas Telford, London.

9. Egger, M. (2005). Recommended behaviour for road tunnel users. In *The Handbook of Tunnel Fire Safety*, ed. A Beard & R Carvel, pp 343-353, Thomas Telford, London.

10. European Union (2004). *Directive 2004/54/EC of the European Parliament and of the Council on Minimum Safety Requirements for Tunnels in the Trans-European Road Network.*

11. Bendelius, A. (2005). Tunnel ventilation – state of the art. In *The Handbook of Tunnel Fire Safety*, ed. A Beard & R Carvel, pp 127-143, Thomas Telford, London.

12. Jagger, S. & Grant, G. (2005). Use of tunnel ventilation for fire safety. In *The Handbook of Tunnel Fire Safety*, ed. A Beard & R Carvel, pp 144-183, Thomas Telford, London.

13. Danziger, N.G. and Kennedy, W.D. (1982). Longitudinal ventilation analysis for the Glenwood Canyon tunnels. *Proc. 4th Int. Symp. Aerodynamics & Ventilation of Vehicle Tunnels*, pp. 169-186. BHRA Fluid Engineering.

14. Hwang, C.C. & Edwards, J.C. (2005). The critical ventilation velocity in tunnel fires – a computer simulation. *Fire Safety Journal*, vol. 40, pp. 213-244. .

15. Lemaire, T. (2003). Runehamar Tunnel Fire Tests: radiation, fire spread and back layering. Proc. Int. Symp. on Catastrophic Tunnel Fires, Boras, Sweden, Borås, Sweden, Nov 20-21 2003, pp. 105-116.

16. Wu, Y. and Baker, M.Z.A. (2000). Control of smoke flow in tunnel fires using longitudinal ventilation systems - a study of the critical velocity. *Fire Safety Journal*, vol. 35, pp. 363-390.

17. Centre d'Etudes des Tunnels (CETU) (2000). *Inter-ministry circular n°2000-63 of 25 August 2000 concerning safety in the tunnels of the national highways network.*

18. Vuilleumier, F. (2002). Safety aspects of railway and road tunnel: example of the Lötschberg railway tunnel and Mont-Blanc road tunnel. *Tunnelling and Underground Space Technology*, vol. 17, pp. 153-158.

19. World Road Association (PIARC) (2001). Report 05.11.B. *Cross Section Design for Uni-Directional Road Tunnels*.

20. World Road Association (PIARC) (2004). Report 05.12.B. *Cross Section Design for Bi-Directional Road Tunnels*.

21. *Proof of Evidence Traffic & Economic Aspects, A1 Motorway Wetherby To Walshford Section,* S. R. Pittam, The Department Of Transport, UK.

22. *Cambridge to Huntingdon Multi Modal Study (CHUMMS), Chapter 2 Problems & Issues,* DTLR (GO-East), August 2001; http://www.goeast.gov.uk/goee/docs/192025/193704/230829/230834/CHUMMS_Chapter_2_-Problems1.pdf

23. *Minimum Safety Requirements For Tunnels In The Trans-European Road network, Proposal for a directive of the European Parliament and of the Council,* COM(2002) 769 Final, Commission of the European Communities, Brussels, 30.12.2002. http://europa.eu.int/comm/transport/road/roadsafety/roadinfra/tunnels/documents/2002_0769_en.pdf http://europa.eu.int/comm/transport/road/roadsafety/roadinfra/tunnels/documents/annexes_en.pdf

24. *Hong Kong: Fire Safety, Life Safety & Ventilation In Road Tunnels,* J. Armstrong et al, June 2001 http://www.tunnels.mottmac.com/files/page/88333/188_Hong_Kong__Fire__Safety_&_Ventilation.PDF

25. *Dispersion Of CNG Fuel Releases In Naturally Ventilated Tunnels,* R. Zalosh et al, Final Report prepared for Commonwealth of Massachusetts Tunnel Safety Study Steering Committee, November 1994.

26. *Transport Statistics Great Britain 1993,* Department of Transport, HMSO, London, 1993.

27. *Recommendations Of The Group Of Experts On Safety In Road Tunnels: Final Report,* TRANS/AC.7/9, 10 December 2001, UN ECE Inland Transport Committee http://www.unece.org/trans/doc/2002/ac7/TRANS-AC7-09e.doc

28. *Studies On Norwegian Road Tunnels,* TTS 15 1997, Norwegian Public Roads Administration, 1997.

29. *Road Accidents Great Britain 1997 – The Casualty Report,* Department of the Environment, Transport and the Regions, Scottish Office, Welsh Office, HMSO, London, 1998.

30. Statistiska Centralbyrån, Statistical search, 2000.

31. *Studies On Traffic Accidents In Norwegian Tunnels,* F. H. Amundsen et al, Tunnelling & Underground Space Technology, Vol.15, No.1, pp3-11, Pergamon, 2000.

32. *Safety Aspects Of Norwegian Road Tunnels,* F. H. Amundsen, Norwegian Tunnelling Society, 1992. http://www.tunnel.no/_upl/Kap02_Safety.pdf

33. *OECD Studies In Risk Management: Norway - Tunnel Safety,* OECD, 2006 http://www.oecd.org/dataoecd/36/15/36100776.pdf

34. *Current Safety Issues In Traffic Tunnels*, A. Haack, Tunneling and Underground Space Technology, Volume 17, Number 2, pp. 117-127(11), Elsevier Science April 2002 http://www.stuva.de/de/content/doc/pdf/SIT2eng.pdf

35. *Verkehrssicherheit in Autobahn- und Autostrassentunneln des Nationalstrassennetzes*, Salvisberg, U. et al, Bfu-report no. 51, Swiss Council for Accident Prevention, BFU, Berne (with an abstract in English), 2004 http://www.bfu.ch/english/researchnews/ergebnisse/report/r_51e.pdf

36. *Questionnaire - Part A Responses*, TRANS/AC.7/2001/8, 8 January 2001, UN ECE Inland Transport Committee http://www.unece.org/trans/doc/2001/ac7/TRANS-AC7-2001-08e.doc

37. Munthe, J., Personal communication, Swedish Rescue Services Agency, 2000

38. *Methanol Fuels And Fire Safety*, Environmental Protection Agency, EPA 400-F-92-010, Fact Sheet OMS-8, USA, August 1994. http://www.epa.gov/otaq/consumer/08-fire.pdf

39. *Risk Analysis Of Hydrogen As A Vehicular Fuel*, H. Bigün, Draft version of licentiate thesis, Center for Safety Research, Dept. of Civil and Environmental Engineering, Royal Institute of Technology, Stockholm, 1999.

40. *An Analysis of Fires in Passenger Cars, Light Trucks, and Vans.* J. Tessmer, NHTSA Technical report DOT HS 808 208, National Highway Traffic Safety Administration, US Department of Transport, USA, 1994.

41. *Bilbranner, alvorlige trafikkulykker og andre hendelser i norske vegtunneler*. Amundsen, F. H. et al, Report Nr. TTS13/01, Statens vegvesen, Vegdirektoratet, Norway, 25 May 2001.

42. *Prevention And Control Of Highway Tunnel Fires*, Egilsrud, P.E., Report No. FHWA/RD-83/032, US DoT, Federal Highway Admin., May 1984. http://ntl.bts.gov/lib/2000/2400/2416/708.pdf

43. ATB Tunnel 2004, Publikation 2004:124, Vägverket, Sweden, 2004. http://www.vv.se/filer/20213/Tunnel2004_publ2004_124.pdf

45. BMW Hydrogen 7: the first premium saloon with a bivalent internal combustion engine. Fürst, S., Gräter, A., Pehr, K., 2007 JSAE Annual Spring Congress, 23 to 25 May 2007, Pacifico, Yokohama, Japan.

46. Liquid Hydrogen Storage Systems developed and manufactured for the first time for Customer Cars. Amaseder, F., Krainz, G., SAE, 3-6 Apr. 2006, Detroit, USA.

47. BMW Hydrogen 7 Series – A safe way to a clean future. Danner, S., Fürst, S., FISITA, 22-27 Oct. 2006, Yokohama, Japan.

48. Safety of Hydrogen-fueled Motor Vehicles with IC engines. Fürst, S., Dub, M., Gruber, M., Lechner, W. Müller, C., ICHS, 2005, Pisa, Italy.

49. The new 12-cylinder hydrogen engine in the 7 series: The H2 ICE age has begun. Kiesgen, G. Klüting, M., Bock, C. and Fischer, H., SAE, 3-6 Apr. 2006, Detroit, USA

50. Kennedy, W.D. et al. (2000). The development and testing of the Subway Environment Simulation version 2000. In *Proc. 10th Int. Symp. on the Aerodynamics and Ventilation of Vehicle Tunnels*, 1-3 November 2000, Boston, USA, BHR Group, pp. 259-1278.

51. Jones, W.W. et. Al. (2005). *CFAST – Consolidated Model of Fire Growth and Smoke Transport (Version 6) Technical Reference Guide*. NIST Special Publication 1026.

52. Chow, W.K. (1999). Simulation of tunnel fires using a zone model, *Tunnelling and Underground Space Technology*, vol. 11, pp. 221-236.

53. Yang, K.H. et al. (2000). Smoke management analysis of a subway station with platform screen doors. In *Proc. 10th Int. Symp. on the Aerodynamics and Ventilation of Vehicle Tunnels*, 1-3 November, Boston, USA, BHR Group, pp. 541-561.

54. Charters, D.A. et al. (1994). A computer model to assess fire hazards in tunnels (FASIT). *Fire Technology*, First Quarter, pp. 134-154.

55. Charters, D. et al. (1999). Which tunnel fire precautions are really necessary? In *Proc. 1st Int. Conf. on Tunnel Fires and Seminar on Escape from Tunnels*, 5-7 May 1999, Lyon, France, Independent Technical Conferences Ltd., pp. 147-156.

56. Salisbury, M. et al. (2001). Application and limitation of quantified fire risk assessment techniques for the design of tunnels. In *Proc.3rd Int. Conf. on Tunnel Fires and Seminar on Escape from Tunnels*, 9-11October 2001, Washington, USA, Tunnel Management International, pp. 39-47.

57. JASMINE

58. FLACS

59. FLUENT

60. STARCD

61. Versteeg and Melalsekara 1995

62. Ferziger and Pereic 1999

63. *Aerodynamics & Ventilation of Vehicle Tunnels*, Portoroz, Solvenia, 11-13 July 2006, pp. 873-881.

64. Tunnel Fires, *5th International Conference*, London, UK,Tunnel Management International, 25-27 October 2004.

65. *First International Conference on Hydrogen Safety*, 8-10 September 2005, Pisa.

66. Venetsanos, A. (2005). Review of Existing Experimental Data and CFD analysis for Hydrogen Releases in Confined Spaces. HySafe Deliverable D01_b.; Venetsanos, A.et al. (2008). CFD modelling of hydrogen release, dispersion and combustion for automotive scenarios. *Journal of Loss Prevention in the Process Industries*, vol. 21, pp. 162–184.

67. European Integrated Hydrogen Project (2000). Final Publishable Report. Joule Contract N° JOE3-CT97-0088.

68. European Integrated Hydrogen Project – Phase 2 (2004). Joint Final Technical Report – Final Publishable Version. Contract N°ENK6-CT2000-00442.

69. Mukai et al (2005). CFD Simulation on Diffusion of Leaked Hydrogen Caused by Vehicle Accident in Tunnels. In *Proc. First Int. Conf Hydrogen Safety*, 8-10 September 2005, Pisa

70. Wu, Y. (2006). Initial assessment of the implication on ventilation system of transporting hydrogen cars through existing road tunnels. In *Proc. International 12th Symp. Aerodynamics & Ventilation of Vehicle Tunnels*, Portoroz, Solvenia, 11-13 July 2006, pp. 873-881.

71. Wu, Y. (2007). Initial assessment of the impact of jet flame hazard from hydrogen cars in road tunnels and the implication on hydrogen car design. In *Proc. Second Int. Conf Hydrogen Safety*, 11-13 September 2007, San Sebastian, Spain.

72. Hansen, O.R. and Middha, P. (2007). CFD simulation study to investigate the risk from hydrogen vehicles in tunnels. In Proc. *Second Int. Conf Hydrogen Safety*, 11-13 September 2007, San Sabastian.

73. Groethe, M. et al. (2005). Large-Scale Hydrogen Deflagrations and Detonations. In *Proc. First Int. Conf Hydrogen Safety*, 8-10 September 2005, Pisa.

74. Molkov, V. et al. (2008). LES of hydrogen-air deflagrations in a 78.5-m tunnel. *Combustion Science and Technology*, vol. 180, pp. 796-808.

75. Yakhot, V. (1988). Propagation velocity of premixed turbulence flames. *Combustion Science and Technology*, vol. 60, p. 191.

76. HSL experiments

77. FZK experiments

78. WUT study

79. F. Verbecke, D. Makarov and V. Molkov, Hydrogen release from a pressure relief device of a Hydrogen-fuelled bus and its dispersion in a tunnel, Hysafe/Hytunnel Report, 2008

80. Verbecke, F., and Molkov, V., Assessment of Q9 approach for jet explosions, Hysafe/Hytunnel Report, 2009.

81. GX1 "Report on Characterization of the Risk from an Inhomogeneous Gas Cloud: Methods for Evaluating Equivalent Gas Cloud", GexCon report, September 2008.

82. NORSOK Standard Z-013. Risk and emergency preparedness analysis. Rev. 2. Sep 2001. Available from http://www.nts.no/norsok.

83. Tanaka et al., *Experimental study on hydrogen explosions in a full-scale hydrogen filling station model*, HYSAFE ICHS International Conference on Hydrogen Safety, Pisa, Italy, 8-10 September 2005.

84. K. Takeno et al., Phenomena of dispersion and explosion of high pressurized hydrogen, Proceedings of the First International Conference on Hydrogen Safety, Pisa, Italy, 8-10 September 2005.

85. HYPER, "Installation Permitting Guidance for Hydrogen and Fuel Cells Stationary Application", WP5 5.2 Report on high pressure catastrophic releases – Draft Version, European Commission Sixth Framework Programme, 2002-2006.

86. L C Shirvill, T A Roberts and M Royle, Safety studies on high-pressure hydrogen vehicle refueling stations: part 1Releases into a simulated high-pressure dispensing area, Confidential draft for HySafe.